

Electronic Thesis and Dissertation Repository

---

8-23-2021 3:00 PM

## Mathematical Modelling of Ecological Systems in Patchy Environments

Ao Li, *The University of Western Ontario*

Supervisor: Zou, Xingfu, *The University of Western Ontario*

A thesis submitted in partial fulfillment of the requirements for the Doctor of Philosophy degree in Applied Mathematics

© Ao Li 2021

Follow this and additional works at: <https://ir.lib.uwo.ca/etd>

---

### Recommended Citation

Li, Ao, "Mathematical Modelling of Ecological Systems in Patchy Environments" (2021). *Electronic Thesis and Dissertation Repository*. 8059.

<https://ir.lib.uwo.ca/etd/8059>

This Dissertation/Thesis is brought to you for free and open access by Scholarship@Western. It has been accepted for inclusion in Electronic Thesis and Dissertation Repository by an authorized administrator of Scholarship@Western. For more information, please contact [wlsadmin@uwo.ca](mailto:wlsadmin@uwo.ca).

# Abstract

In this thesis, we incorporate spatial structure into different ecological/epidemiological systems by applying the patch model. Firstly, we consider two specific costs of dispersal: (i) the period of time spent for migration; (ii) deaths during the dispersal process. Together with the delayed logistic growth, we propose a two-patch model in terms of delay differential equation with two constant time delays. The costs of dispersal, by themselves, only affect the population sizes at equilibrium and may even drive the populations to extinction. With oscillations induced by the delay in logistic growth, numerical examples are provided to illustrate the impact of loss by dispersal.

Secondly, we study a predator-prey system in a two-patch environment with indirect effect (fear) considered. When perceiving a risk from predators, a prey may respond by reducing its reproduction and decreasing or increasing (depending on the species) its mobility. The benefit of an anti-predation response is also included. We investigate the effect of anti-predation response on population dynamics by analyzing the model with a fixed response level and study the anti-predation strategies from an evolutionary perspective by applying adaptive dynamics.

Thirdly, we explore the short-term or transient dynamics of some SIR infectious disease models over a patchy environment. Employing the measurements of reactivity of equilibrium and amplification rates previously used in ecology to study the response of an ecological system to perturbations to an equilibrium, we analyze the impact of the dispersals/travels between patches and other disease-related parameters on short term dynamics of these spatially structured disease models. This contrasts with most existing works on modelling the dynamics of infectious disease which are only interested in long-term disease dynamics in terms of the basic reproduction number.

**Keywords:** dispersal, population dynamics, patch model, costs of dispersal, time delay, predator-prey, anti-predation response, adaptive dynamics, SIR disease model, amplification rate, transient dynamics

## Summary for Lay Audience

Population dynamics is an important subject that has wide applications in areas such as ecology, microbiology, epidemiology, virology, and immunology. There are millions of species in the real world, some of them interacting with each other. Among all types of interactions between species, the predator-prey type is most interesting and complicated. Moreover and importantly, the transmission mechanism of infectious diseases is also of this type, adding more weight to its significance. On the other hand, many species including ourselves are mobile. It has been widely agreed that spatial dispersion is one of the main factors responsible for biodiversity. As for the spread of disease, dispersals/travels of infected individuals play a key role. This thesis aims to address some issues on population dynamics with the above-mentioned two main features: predator-prey type interaction and dispersal in spatially heterogeneous environments. For the latter, we only deal with discrete spatial variation, meaning that we use patch models. We start from the model of one species to study the impact of costs associated with dispersal. In predator-prey systems, we consider some indirect effects in contrast to predation, including the impact on the dispersal of prey. Finally, we investigate the transmission dynamics of infectious diseases over a patchy environment.

## Co-Authorship Statement

This thesis is written by Ao Li under the supervision of Dr. Xingfu Zou. Chapter 2-4 of this thesis consist of the following papers:

Chapter 2: Ao Li and Xingfu Zou, A single species model with delay and dispersal, in preparation.

Chapter 3: Ao Li and Xingfu Zou, (2021), Evolution and adaption of anti-predation response of prey in a two-patchy environment, *Bulletin of Mathematical Biology*, 83, 59.

Chapter 4: Ao Li and Xingfu Zou, Transient dynamics of SIR models over patchy environment, in preparation.

The drafts of above papers were prepared by Ao Li and then revised by Ao Li and Dr. Xingfu Zou.

## Acknowledgements

First and foremost, I would like to express my deep gratitude to my supervisor, Dr. Xingfu Zou, for his immense knowledge, excellent guidance, continuous support, encouragement and patient. He is an incredible mentor who introduces me into this fascinating area and guides me to pursue my research interests. What I learned from him not only helps to finish this thesis but also benefits my future career.

Next, I would like to thank everyone in the Department of Applied Mathematics at Western. Special thanks go to Dr. Pei Yu and Dr. David Jeffrey who initially provided me the opportunity to study here. I am very grateful for all the advice, comments and discussions regarding my projects from other professors and fellow students. Assistance provided by the administrative staff, particularly Audrey Kager and Cinthia MacLean, is greatly appreciated.

Last but not least, I would like to thank my family, especially my husband, for their love and support. I also would like to thank my friends, Yang Wang, Tianyu Cheng and Jingjing Xu, for their companion and help. Without all of you, it would have been impossible for me to make it this far.

# Contents

<b>Abstract</b>	<b>i</b>
<b>Summary for Lay Audience</b>	<b>ii</b>
<b>Co-Authorship Statement</b>	<b>iii</b>
<b>Acknowledgements</b>	<b>iv</b>
<b>List of Figures</b>	<b>viii</b>
<b>List of Tables</b>	<b>xii</b>
<b>1 Introduction</b>	<b>1</b>
1.1 Population dynamic . . . . .	2
1.1.1 Predator-prey systems . . . . .	3
1.1.2 Transmission of infectious diseases . . . . .	4
1.2 Patch models . . . . .	7
1.3 Thesis motivations and outlines . . . . .	8
1.3.1 Cost of dispersal . . . . .	8
1.3.2 Fear effect . . . . .	9
1.3.3 Short-term epidemicity . . . . .	10
1.4 Mathematical theories and methodologies . . . . .	11
1.4.1 Stability analysis for equilibria . . . . .	11
1.4.2 Adaptive dynamics . . . . .	11
1.4.3 Reactivity . . . . .	13
Bibliography . . . . .	15

<b>2</b>	<b>A Single Species Model with Delay and Dispersal</b>	<b>21</b>
2.1	Introduction . . . . .	21
2.2	Mathematical analysis . . . . .	23
2.2.1	Equilibria . . . . .	25
2.2.2	Stability . . . . .	26
2.3	Numerical simulations . . . . .	31
2.4	Conclusion . . . . .	33
	Bibliography . . . . .	37
<b>3</b>	<b>Modelling Anti-predation Response of Prey in a Two-patchy Environment</b>	<b>39</b>
3.1	Introduction . . . . .	39
3.2	Model formulation . . . . .	43
3.3	Model analysis: without dispersal . . . . .	46
3.4	Model analysis: with dispersal . . . . .	52
3.4.1	Equilibria and stability . . . . .	52
3.4.2	Evolution of anti-predation strategy . . . . .	58
	Invasion analysis . . . . .	58
	Adaptive dynamics without time scale separation . . . . .	60
3.5	Conclusion and Discussion . . . . .	65
	Bibliography . . . . .	70
<b>4</b>	<b>Transient Dynamics of SIR Models over Patchy Environment</b>	<b>73</b>
4.1	Introduction . . . . .	73
4.2	Amplification rates and reactivity . . . . .	78
4.3	SIR epidemic patch model . . . . .	82
4.3.1	Two patches . . . . .	82
4.3.2	Estimate $\Gamma_0$ in early stage . . . . .	86
4.3.3	$n$ patches . . . . .	88
4.4	SIR endemic patch model . . . . .	89
4.4.1	Measures of dynamics . . . . .	90
4.4.2	Application to two patches . . . . .	92

4.5	Conclusion and discussion . . . . .	95
4.6	Appendix . . . . .	97
4.6.1	The dependence of $\lambda_{max}$ and $\lambda_{min}$ for SIR epidemic patch model . . . . .	97
	Bibliography . . . . .	99
<b>5</b>	<b>Conclusions and Future Work</b>	<b>103</b>
5.1	Conclusion . . . . .	103
5.2	Future work . . . . .	105
	Bibliography . . . . .	106
	<b>Curriculum Vitae</b>	<b>107</b>

# List of Figures

1.1	The solutions of the logistic equation (1.3) for different initial populations. . . . .	3
2.1	The area above the curve is where the positive equilibrium $E_*$ exists. If there is no loss during dispersal process, i.e. $m = 0$ , then $E_*$ always exists. . . . .	26
2.2	The oscillations induced by time delay $\tau_1$ of system (2.10) which is coupled by dispersal with related costs ignored, i.e. $\tau_2 = 0$ and $m = 0$ . Values of $\tau_1$ are chosen as: (a) $\tau_1 = 0.3$ ; (b) $\tau_1 = 0.5$ ; (c) $\tau_1 = 0.6$ ; (d) $\tau_1 = 1$ ; . . . . .	32
2.3	The impact of time delay $\tau_2$ due to dispersal in the case when equilibrium solutions are stable. . . . .	34
2.4	The periodic solutions of system (2.5) with different combinations of time delays.	35
3.1	Function $F(\alpha)$ has a global maximum if and only if $p/s > \max\{b_0/(c_0v), 1\}$ : (a) $F(0) > 0$ ; (b) $F(0) < 0$ but $F(\alpha^*) > 0$ . . . . .	50
3.2	Pairwise invasibility plot for model (3.10) with trait $\alpha$ . Function $F(\alpha, v)$ is in the form of (3.15) and $b_0 = 5$ , $d = 0.5$ , $c_0v = 3.5$ , $s = 1$ , $p = 3$ . The mutant can invade in the blue regions but the invader fails in the white regions. The intersection of two curves gives a convergence stable ESS $\alpha^* = 0.37$ . . . . .	51
3.3	The solid curve is implicitly defined by $F_1(\alpha, v_1)F_2(\alpha, v_2) = F_1(\alpha, v_1)m(\alpha, v_2) + F_2(\alpha, v_2)m(\alpha, v_1)$ for $F_1(\alpha, v_1) < m(\alpha, v_1)$ , below which $E_0$ is asymptotically stable. The region above this curve is where the trivial equilibrium $E_0$ is unstable which is the same region for $(F_1, F_2)$ where the positive equilibrium $E_+$ exists. . . . .	54

3.4	The effect of anti-predation response level $\alpha$ on the prey's population dynamics. (a) The curves defined by (3.22) with different values of $\alpha$ , which separate the stability region of the positive equilibrium $E_+$ from that of the trivial equilibrium $E_0$ . The red curve with arrow represents the trajectory of $[F_1(\alpha, v_1), F_2(\alpha, v_2)]$ when $\alpha$ increases from 0 to 3.5. (b) The dependence of stable population sizes on $\alpha$ , marked with the strategy values at which the populations are maximized. Other parameter values are: $b_{01} = 10$ , $b_{02} = 5$ , $d_1 = 1$ , $d_2 = 2$ , $c_0 = 0.04$ , $v_1 = 100$ , $v_2 = 200$ , $\tilde{s} = 0.01$ , $\tilde{p} = 0.03$ , $m_0 = 2$ , $\tilde{q} = 0.02$ , and $a = 1$ . . . . .	57
3.5	Pairwise invasibility plot for model (3.28) with trait $\alpha$ . The blue areas correspond to $\lambda > 0$ when the mutant can invade, and in the white areas $\lambda < 0$ implying that the mutant dies out. . . . .	60
3.6	The fitness function $F_1(\alpha, v_1)$ and $F_2(\alpha, v_2)$ and convergent dynamics of anti-predation response level $\alpha(t)$ on the two patches which are <i>not connected</i> by dispersals. . . . .	62
3.7	The fitness function is taken as the total fitness mediated by dispersals. The anti-predation response level $\alpha(t)$ converges to the point that maximizes this fitness function. . . . .	63
3.8	The fitness function is taken as the instant total growth rate of the prey on two patches given by (3.38) which also varies with time. The anti-predation response level $\alpha(t)$ converges to a different value from that in Figure 3.7(b), which maximizes the limit fitness function when populations reach steady state as shown in the left graph. . . . .	64
3.9	The dynamics of prey's population for systems (3.36), (3.37) and (3.8)-(3.39). The initial values are $[u_1(0), u_2(0), \alpha(0)] = [5, 5, 0.8]$ . . . . .	65
3.10	Population dynamics in an isolated patch for the case of a specialist predator. The parameter values are $a = 1$ , $b_0 = 5$ , $d = 0.5$ , $c_0 = 0.35$ , $\tilde{s} = 0.1$ , $\tilde{p} = 0.3$ , $\alpha_u = 0.1$ , $\alpha_w = 0.7$ , $d_v = 0.3$ , $\xi = 0.2$ ; and the initial point is $[u(0), w(0), v(0)] = [5, 5, 5]$ . . . . .	69

3.11 Population dynamics in a two-patch environment for the case of a specialist predator. The parameter values are  $a = 1$ ,  $b_{01} = 10$ ,  $b_{02} = 5$ ,  $d_1 = 0.5$ ,  $d_2 = 0.3$ ,  $c_0 = 0.4$ ,  $\tilde{s} = 0.1$ ,  $\tilde{p} = 0.3$ ,  $m_0 = 2$ ,  $\tilde{q} = 0.02$ ,  $\alpha_u = 0.1$ ,  $\alpha_w = 0.3$ ,  $d_v = 0.2$ ,  $\xi = 0.2$ ; and the initial point is  $[u_1(0), u_2(0), w_1(0), w_2(0), v_1(0), v_2(0)] = [5, 5, 5, 5, 5, 5]$ . . . . . 69

4.1 Three sample points of  $\beta_1$  are taken as: (i)  $0.2 \times 10^{-4}$ , (ii)  $0.8 \times 10^{-4}$ , and (iii)  $1.5 \times 10^{-4}$ . (a) The initial amplification rate  $\Gamma_0$  is negative for (i) and (ii), while it is positive for (iii). (b) The outbreak is mitigated with  $\beta_1$  decreasing from (iii) to (ii), and is completely under control when  $\beta_1$  further reduces to (i). (c) For the chosen value (ii), the magnitude of solution initially experiences a short-period reduction then grows to its maximal value. Set  $\beta_2 = 2 \times 10^{-5}$ ,  $\gamma_1 = 0.2$ ,  $\gamma_2 = 0.4$ ,  $d_{12}^S = 0.08$ ,  $d_{21}^S = 0.1$ ,  $d_{12}^I = 0.02$ ,  $d_{21}^I = 0.05$  and  $[S_{10}, S_{20}, I_{10}, I_{20}] = [10000, 15000, 2000, 5000]$ . . . . . 84

4.2 Three sample points of  $S_{20}$  are taken as: (i) 5000, (ii) 17000, and (iii) 30000. (a) The initial amplification rate  $\Gamma_0$  is a linear increasing function of  $S_{20}$ , whose value is negative for (i) and (ii) and is positive for (iii). (b) The dynamics of  $\|\mathbf{x}(t)\| = \|[I_1(t), I_2(t)]\|$  for different initial conditions. (c) The linear dynamics of  $\|\mathbf{x}(t)\|$  near the initial point. Set  $\beta_1 = 5 \times 10^{-5}$ ,  $\beta_2 = 2 \times 10^{-5}$ ,  $\gamma_1 = 0.2$ ,  $\gamma_2 = 0.4$ ,  $d_{12}^S = 0.08$ ,  $d_{21}^S = 0.1$ ,  $d_{12}^I = 0.02$ ,  $d_{21}^I = 0.05$  and  $[S_{10}, I_{10}, I_{20}] = [10000, 2000, 5000]$ . . . . . 85

4.3 (a–d) The contour graphs of  $\Gamma_0$  for dispersal rates of infectives. (e, f) The dynamics of  $\|\mathbf{x}(t)\|$  for the sample sets. The choices, (i)-1 and (iii)-1, (ii)-1 and (iv)-1, (i)-2 and (iii)-2, (ii)-2 and (iv)-2, yield the same  $\Gamma_0$ . Set  $\beta_1 = 5 \times 10^{-5}$ ,  $\beta_2 = 2 \times 10^{-5}$ ,  $\gamma_1 = 0.2$ ,  $d_{12}^S = 0.4$ ,  $d_{21}^S = 0.6$ , and  $\gamma_2 =$  (a, b) 0.4; (c, d) 0.2. The initial conditions for  $[S_{10}, S_{20}, I_{10}, I_{20}]$  are: (a, c, e)  $[10000, 15000, 5000, 2000]$ ; (b, d, f)  $[10000, 15000, 2000, 5000]$ . . . . . 87

4.4	Indices $\Gamma_0$ (solid line) and $\mathfrak{R}_0$ (dotted line) as functions of infection-related parameters. Except chosen to be a variable, parameter values are $b_1 = b_2 = 0.2$ , $\beta_1 = 2 \times 10^{-5}$ , $\beta_2 = 4 \times 10^{-5}$ , $\gamma_1 = 0.3$ , $\gamma_2 = 0.2$ , $d_{12}^S = 0.4$ , $d_{21}^S = 0.6$ , $d_{12}^I = 0.1$ and $d_{21}^I = 0.3$ . Set $[S_{10}, S_{20}, I_{10}, I_{20}] = [10000, 15000, 1000, 3000]$ . . . . .	93
4.5	Long-term and short-term dynamics of $\  [I_1(t), I_2(t)] \ $ . (a) is an example of (II-1a) with $\beta_1 = 10^{-5}$ and $\beta_2 = 6 \times 10^{-5}$ . (b) is an example of (II-2b) with $\beta_1 = 6 \times 10^{-5}$ and $\beta_2 = 2 \times 10^{-5}$ . Set $d_{12}^R = 0.4$ , $d_{21}^R = 0.6$ and $[S_{10}, S_{20}, I_{10}, I_{20}, R_{10}, R_{20}] = [10000, 15000, 100, 300, 0, 0]$ . Other parameter values are same as those used in Figure 4.4. . . . .	94
4.6	The contour graphs of $\Gamma_0$ and $\mathfrak{R}_0$ for dispersal rates of infectives. Other parameter values and initial conditions are same as those used in Figure 4.4. . . . .	95
4.7	The contour graphs of $\mathfrak{R}_0$ for dispersal rates of susceptibles. Set (a) $d_{12}^I = 0.2$ and $d_{21}^I = 0.8$ so that $\Gamma_0 < 0$ ; (b) $d_{12}^I = 0.9$ and $d_{21}^I = 0.1$ so that $\Gamma_0 > 0$ . Other parameter values and initial conditions are same as those used in Figure 4.4. . .	95

# List of Tables

# Chapter 1

## Introduction

Population dynamics is an important subject which has wide applications in areas such as ecology, microbiology, epidemiology, virology, immunology and so on. There are millions of species in the real world. Some of them interact with each other, affecting the population growth of every species involved. Among all types of interactions between species, predator-prey type is most interesting and complicated. This is mainly because of its ubiquity and richness on the practical side, and the challenges in mathematics it brings in. Moreover and importantly, transmission mechanism of infectious diseases is also of this type, adding more weight to its significance.

Among those species in the real world, some are very mobile, and it has been widely agreed that the spatial dispersion is one of the main factors responsible for the biodiversity. As such, it is of particular importance both in practice and mathematics to study population dynamics in spatially heterogeneous environments, particularly the population dynamics of predator-prey type interacting species including transmission dynamics of infectious diseases.

This thesis aims to address some issues on population dynamics with the above mentioned two main features: predator-prey type interaction and dispersal in spatially heterogeneous environments. For the latter, we only deal with discrete spatial variation, meaning that we will use patch models. To help the readers better understand the contexts of the main body of the thesis, in this Chapter, we first present some basic background and preparations in population dynamics, transmission dynamics of infectious diseases, predator-prey interactions and the related

fear effect, and dispersals between patches, together with a brief summary of the mathematical tools that will be used in this thesis.

## 1.1 Population dynamic

Assuming that the number of individuals  $N$  in a population varies continuously over time  $t$ , the rate of change can be expressed as the derivative with respect to  $t$ ,

$$\frac{dN}{dt} = \text{rates in} - \text{rates out.}$$

For an isolated population, the changes are resulted from births and deaths. Let  $b > 0$  be the per capita reproduction rate and  $d > 0$  be the per capita natural mortality rate. Then,

$$\frac{dN}{dt} = bN - dN = rN. \quad (1.1)$$

Given the initial population  $N(0) = N_0$ , it has solution

$$N(t) = N_0 e^{(b-d)t} = N_0 e^{rt}, \quad (1.2)$$

which is called Malthusian growth since this approach was firstly proposed by Malthus in 1798. When  $b > d$ , this exponential growth is unbounded and hence, is unrealistic.

To address this problem, Verhulst [52] modified this equation to

$$\frac{dN}{dt} = rN \left(1 - \frac{N}{K}\right) \quad (1.3)$$

by adding a quadratic term accounting for the intra-species competition. This is known as the logistic equation. Now the net per capita growth rate,  $r(1 - N/K)$ , decreases with  $N$ , and  $K > 0$  is the carrying capacity of the environment. If  $N(0) = N_0$ , the solution of (1.3) is

$$N(t) = \frac{KN_0 e^{rt}}{K + N_0(e^{rt} - 1)} \quad (1.4)$$

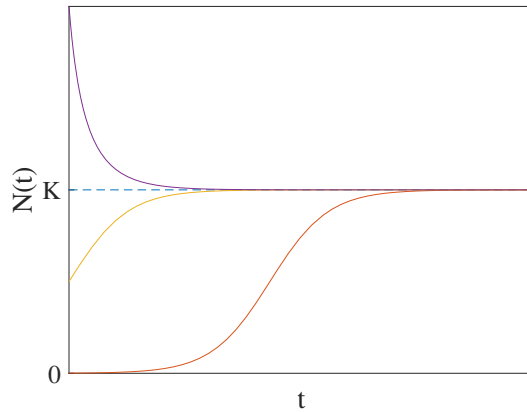


Figure 1.1: The solutions of the logistic equation (1.3) for different initial populations.

and is illustrated in Figure 1.1. One can easily verify that  $\lim_{t \rightarrow \infty} N(t) = K$ .

### 1.1.1 Predator-prey systems

When species interact, the population dynamics of those species are affected. An important type of interactions is predation, meaning that one of the species is a predator and the other is its prey. The predator has an inhibitory effect on the prey, while the prey has a beneficial effect on the predator. The earliest and probably the most well-known predator-prey model is the Lotka-Volterra equations,

$$\begin{cases} \frac{dU}{dt} = \alpha U - \beta UV, \\ \frac{dV}{dt} = -\delta V + c\beta UV, \end{cases} \quad (1.5)$$

which was proposed by Lotka [32, 33] and Volterra [53] respectively about a century ago. In this model,  $U(t)$  is the population of prey and  $V(t)$  is that of the predator. Parameters  $\alpha$ ,  $\beta$ ,  $\delta$  and  $c$  are positive constants. The assumptions made to the model are as follows.

- The population of prey is only limited by the predator, and in the absence of any predation would grow unboundedly in a Malthusian way.
- The effect of predation on prey is to reduce its per capita growth rate by a term proportional to predator population.
- In the absence of any prey for sustenance, the population of predator decays exponen-

tially.

- The consumption of prey is the only contribution to the growth of the predator population with  $c$  accounting for the conversion efficiency.

The Lotka-Volterra model helps to explain the oscillation phenomenon in nature but is structurally unstable in mathematics. Since then, there have been numerous modifications/generalizations to this model which can be represented by the following system:

$$\begin{cases} \frac{dU}{dt} = g_1(U) - p(U, V)V, \\ \frac{dV}{dt} = g_2(V) + cp(U, V)V, \end{cases} \quad (1.6)$$

where  $g_1(U)$  ( $g_2(V)$ ) represents the population dynamics of the prey (predator) in the absence of the predator (prey). The predation term is  $p(U, V)V$  and  $p(U, V)$  is referred as the functional response. One example of modifications is the Rosenzweig-MacArthur model [45] where  $g_1(U) = \alpha U(1 - U/K)$  is chosen as the logistic growth and  $g_2(V) = -\delta V$  is same as that in (1.5).

In the two models with  $g_2(V) = -\delta V$ , the predators are assumed to be specialist, whose diet is limited to that prey species (which indeed can be a very small range of species but people usually make this assumption for mathematical simplification). In the real world, there also exists a large number of generalist predators such as most omnivores that live on a wide range of food resources. Theoretical studies can be found, for examples, in [16, 48, 24] and the references therein.

### 1.1.2 Transmission of infectious diseases

Another important application of population dynamics is to model the transmission of infectious diseases, in order to explain the spread of a disease, to predict the future course of an outbreak, and to examine the likely effect of controls. One of the earliest mathematical models was proposed by Bernoulli [4] in 1760 that considered the effect of cow-pox inoculation against smallpox. However, there was little work had been done until the beginning of 20th

century. A sequence of papers by Kermack and McKendrick published in 1927, 1932, and 1933 [25, 26, 27] laid the foundations of the entire approach based on compartmental models.

We start from the special case of the model proposed by Kermack and McKendrick in 1927 which is given by the following system of ordinary differential equations:

$$\begin{cases} \frac{dS}{dt} = -\beta SI, \\ \frac{dI}{dt} = \beta SI - \gamma I, \\ \frac{dR}{dt} = \gamma I. \end{cases} \quad (1.7)$$

In this model, population is assigned to three compartments: susceptible class  $S$ —individuals who can catch the disease by contact with the infectives; infected class  $I$ —individuals who have the disease and can transmit it; and removed class  $R$ —individuals who are either recovered and immune or dead and hence play no further role in the disease. The assumptions are as follows.

- The population is closed so that immigration, emigration, births and disease-unrelated deaths are omitted.
- The infection is reflected by the term  $-\beta SI$  (analogous to the predation term in the Lotka-Volterra predator-prey system (1.5)) with the constant  $\beta > 0$  denoting the transmission rate.
- The transition rate from class  $I$  to class  $R$  is  $\gamma I$  where  $1/\gamma$  is the average of time individuals spent in the infectious state.

Given the initial population in each class,  $S(0) = S_0 > 0$ ,  $I(0) = I_0 > 0$  and  $R(0) = R_0 > 0$ , define  $\mathfrak{R}_0 = \beta S_0/\gamma$ . If  $\mathfrak{R}_0 > 1$ , then  $I(t)$  first increases up to a maximum value then decreases to zero as  $t$  goes to infinity while  $S(t)$  monotonically decreases approaching to a positive limiting value (see, e.g., [21]). This result corresponds to the scenario of an epidemic which is a sudden outbreak of a disease such as a season of influenza and the outbreak of SARS in 2002. It has also been proved that no epidemics are possible if  $\mathfrak{R}_0 \leq 1$ .

Another situation to be concerned is endemic in which a disease is always present. Because of the long time period involved, the demographic effects of births and deaths should

be incorporated into the SIR system. Consider a special case when per capital birth rates and per capital natural death rates for all compartments are equal and there are no disease-related deaths, model (1.7) is modified to

$$\begin{cases} \frac{dS}{dt} = bN - \beta SI - bS, \\ \frac{dI}{dt} = \beta SI - \gamma I - bI, \\ \frac{dR}{dt} = \gamma I - bR, \end{cases} \quad (1.8)$$

with  $R$  indicating recovered individuals with life-long immunity. The total population size  $N$  remains constant. This system has two possible steady-state solutions: disease-free equilibrium (DFE),  $\mathbf{E}_0 = [N, 0, 0]$ , and endemic equilibrium (EE),  $\mathbf{E}_+ = [S^*, I^*, R^*]$  with

$$S^* = \frac{\gamma + b}{\beta}, \quad I^* = \frac{bN}{\gamma + b} - \frac{b}{\beta}, \quad R^* = \frac{\gamma N}{\gamma + b} - \frac{\gamma}{\beta}.$$

Now define  $\mathfrak{R}_0 = \beta N / (\gamma + b)$ . The DFE is locally asymptotically stable if  $\mathfrak{R}_0 < 1$  and is unstable if  $\mathfrak{R}_0 > 1$ . The EE exists and is locally asymptotically stable as long as  $\mathfrak{R}_0 > 1$  (see, e.g., [7]).

In the extensive literature, there have been numerous variants of the SIR model regarding to different transmission mechanisms, and the threshold theorems have been extended. The threshold index  $\mathfrak{R}_0$ , called the basic reproduction number or the basic reproduction ratio, is defined as the expected number of secondary infections from a single infected individual during his or her entire period of infectiousness in a completely susceptible population. When it comes to mathematical modelling, the next generation method, which was initially introduced by Diekmann et al. [11], has been widely used to calculate  $\mathfrak{R}_0$ . Particularly in a compartmental model formulated as a system of ordinary differential equations,  $\mathfrak{R}_0$  is the spectral radius of the next generation matrix defined by Driessche and Watmough [13].

To summarize, this section gives a brief introduction to the basic mathematical models applied in ecology and epidemiology which are related to our works. The literature about mathematical modelling is now extensive and growing very fast. We refer to the book by Murray [38] and the book by Britton [7] for more detailed and systematic introductions.

## 1.2 Patch models

All the aforementioned models only treat the change of population over time despite variability in the physical environment. In other words, the habitat is assumed to be homogeneous. However, the ecological/epidemiological situation can be completely understood only if populations are considered in both time and space [41]. Spatial structure can be included in either a continuous or discrete way. If continuous space is considered, models are formulated by partial differential equations. In this work, we always assume space to be discrete and employ patch models.

Suppose the species range consists of spatially isolated local habitats. Examples can be found in nature such as coral-reefs fishes and birds living in islands. Human beings, ourselves, also live in patchy environment where each patch can be a community, city or country. On the other hand, habitat fragmentation is common nowadays for many species due to human activities and constructions.

Following the tradition of Levin [28, 29] and Vance [51], the populations in different habitats are functionally separate except through the interconnection provided by between-habitat dispersal. Consider an  $n$ -patch environment ( $n \geq 2$ ). Let  $N_i$  denote the population size in patch  $i$  and  $f_i(N_i)$  describe the population dynamics without dispersal for all  $i \in \{1, 2, \dots, n\}$ . The local dynamics are coupled to each other by dispersal terms, yielding a large system of ordinary differential equations,

$$\frac{dN_i}{dt} = f_i(N_i) + \sum_{j=1}^n (D_{ij}N_j - D_{ji}N_i), \quad 1 \leq i \leq n, \quad (1.9)$$

where  $D_{ij} \geq 0$  is the per capital dispersal rate from patch  $j$  to patch  $i$  and  $D_{ii}$  is defined as zero. More generally, written in vector notation, the model becomes

$$\frac{d\mathbf{N}}{dt} = \mathbf{F}(\mathbf{N}) + \mathbf{D}\mathbf{N} \quad (1.10)$$

where  $\mathbf{F}$  is a vector functions of growth rates and  $\mathbf{D} = [d_{ij}]_{n \times n}$  is a matrix of dispersal rates. Constant  $d_{ij}$  represents the immigration rate from patch  $j$  to patch  $i$  with  $i \neq j$ , and  $-d_{ii}$  repre-

sents the emigration rate of the population in patch  $i$ .

The theoretical study of dispersal took place after the work of Skellam [49] in which the movement of organisms was modeled as molecular diffusion. In patch models, the simplest case of dispersal is passive diffusion, in which the net exchange of the species between two patches is proportional to the difference in populations [28, 29]. Hence, matrix  $\mathbf{D}$  has the following properties as summarized by Hastings [17]:

- $\mathbf{D}$  is symmetric, that is  $d_{ij} = d_{ji}$ ;
- all diagonal entries are negative,  $d_{ii} < 0$ , and all off-diagonal entries are non-negative,  $d_{ij} \geq 0$  for  $i \neq j$ ;
- the column sums of  $\mathbf{D}$  are all zeros, that is  $-d_{ii} = \sum_{j \neq i} d_{ji}$ ;
- $\mathbf{D}$  is irreducible (see, e.g., [35, 50]).

The first three assumptions are standard for passive diffusion. If the last one is met, the  $n$  patches cannot be separated into subgroups such that no immigration is possible from one subgroup to the other. This formulation also implies that: (i) the dispersal process is instantaneous; (ii) neither births nor deaths occur during the process.

This continuous-time discrete-space model has been used in a vast literature on mathematical modelling of ecology and epidemiology. In predator-prey systems, the migration may be density-dependent (see, e.g., [30, 15, 37, 20, 34] and the references therein). For transmission of diseases, the local dynamics includes various types such as SI, SIS, SIR, SEIR and even vector-borne diseases [54, 3, 55, 1, 23, 6, 14, 2, 9].

## 1.3 Thesis motivations and outlines

### 1.3.1 Cost of dispersal

The passive diffusion, though simple in modelling and mathematical analysis, is not realistic for most cases. Bonte et al. [5] reviewed all possible costs associated with dispersal (see references therein) and classified them into four different types:

- energetic costs—metabolic energy lost in movements;
- time costs—the time invested in dispersal;
- risk costs—the mortality risks, for example, due to increased predation, and attrition costs resulted from accumulated damage or physiological changes;
- opportunity costs—loss of advantages acquired in a familiar and adapted environment.

In **Chapter 2**, we consider two specific costs of dispersal: (i) the period of time spent for migration; (ii) deaths during dispersal process. In a two-patch model, we assume that individuals moving from one patch to the other need a fixed period of time and the per capita dispersal-related mortality rate is a positive constant, which yields a system of delay differential equations. In addition, we employ the delayed logistic growth, and explore the effect of two delays in both separate and joint ways.

### 1.3.2 Fear effect

In most works on predator-prey system, the population of two species are affected by predation. However, some field observations and empirical results [47, 39, 42, 60] show that merely the presence of predator can alter ecological behaviours of prey, and thereby, influences its population size. Such effects are indirect and non-lethal compared with consumption but are of equal significance [44].

Brown et al. [8] firstly modeled the ecology of fear by conjoining the Rosenzweig-MacArthur model with a foraging theory as fear was represented by the level of vigilance. Based on the results of a field study [60], Wang et al. [57] considered fear as a cost to the prey equation which reduced the reproduction rate. Wang and Zou [59] modified the model in [57] to incorporate a benefit of the anti-predation response (reducing the chances of being caught and consumed by predator) in addition to the cost. Sasmal and Takeuchi [46] also considered both cost and benefit due to anti-predation strategies with a different functional response. The results of these mathematical works also suggest the inclusion of such indirect effects into predator-prey models.

Taking dispersal into account, prey, when perceiving a predation risk, may change their dispersal strategy to avoid encounters with the predator. In most cases, animals (such as mice) are observed to reduce their activities since moving prey are more likely to be detected by predators; usually this associates with the increased use of refuges [31]. Also, there are prey species (such as birds) that have moving advantages, which may respond to the predation risk by moving more frequently. For a spatially continuous habitat, Wang and Zou [58] presented a reaction-diffusion model with predator-taxis for the prey accounting for its intention to move away from the predator.

In **Chapter 3**, we consider the predator-prey interaction in a two-patch environment and incorporate the fear effects in three factors: reproduction, predation, and dispersion. We assume that the response functions depend on both the level of anti-predation response and the population of local predators. In order to focus on the prey's population and for mathematical simplicity, we assume the populations of predator in both patches to be constant, which approximately corresponds to a generalist predator. We investigate the effect of anti-predation response on population dynamics by analyzing the model with a fixed response level and study the anti-predation strategies from evolutionary perspective by applying adaptive dynamics.

### 1.3.3 Short-term epidemicity

In the SIR epidemic patch model which is extended from the Kermack-McKendrick system (1.7), the disease cannot persist. We are interested in the patterns by which the disease dies out. Since the system does not admit a locally asymptotically stable disease-free equilibrium, calculating the basic reproduction number  $\mathfrak{R}_0$  by the next generation matrix [13] is impossible. In **Chapter 4**, we employ the measurement of amplification rate previously used in ecology, denoted by  $\Gamma_0$ , to study the transient or short term disease dynamics. We investigate its dependence on different parameters and the effect of some common control measures. We continue to study the SIR endemic patch model with vital dynamics (births and disease-unrelated deaths) and explore the possible combinations of short-term response and long-term asymptotic behaviour in terms of the two threshold indices  $\mathfrak{R}_0$  and  $\Gamma_0$ .

The thesis ends up with a conclusion in **Chapter 5**, where I summarize the key points of all projects, and propose some possible topics for future work.

## **1.4 Mathematical theories and methodologies**

All the models presented in this work are formulated in terms of differential equations. For them to be biologically well-posed, we first show the global existence of the unique solution and make sure that the biologically meaningful state variables, such as populations, remain non-negative and are bounded. For most dynamical systems, it is hard or even impossible to obtain the solution explicitly. Thus, we apply dynamical system theory to explore the behaviour qualitatively.

### **1.4.1 Stability analysis for equilibria**

The time-independent solutions, called equilibria, expose the steady-state features of dynamical systems. An equilibrium is locally asymptotically stable if solution trajectories starting close to the equilibrium will eventually converge to it. The stability is global if the convergence occurs regardless of initial points. An equilibrium is unstable if it repels solution trajectories. For nonlinear systems, the dynamics near a hyperbolic equilibrium solution is equivalent to that of its corresponding linearization by Hartman-Grobman Theorem [43]. Hence, the local stability is determined by the eigenvalues of the Jacobian matrix evaluated at the equilibrium under consideration. The equilibrium is locally asymptotically stable if all eigenvalues have negative real part, while it is unstable if at least one eigenvalue has positive real part. Moreover, with the change of parameter values, the final state of the dynamical system may switch. Such a phenomenon is called bifurcation.

### **1.4.2 Adaptive dynamics**

In order to study the long-term evolution of phenotypes in a population, adaptive dynamics has been developed. The trait is represented by a continuous variable. Assume that the resident population is in a dynamical equilibrium which is monomorphic exhibiting trait value  $x$  and a

rare mutant with different trait value  $y$  invades. The idea of invasibility analysis [12] is to find out whether the population of mutant will grow or decay once introduced. This is associated with the local instability/stability of the boundary equilibrium of the corresponding resident-mutant competition system.

Define the invasion exponent [12] as a function of both the resident trait  $x$  and the mutant trait  $y$ , say  $\theta(x, y)$ , which measures the relative fitness of mutant in the environmental condition mediated by the resident. The sign of the selection gradient

$$\left. \frac{\partial \theta(x, y)}{\partial y} \right|_{y=x} \quad (1.11)$$

shows the direction of evolution. A higher/lower value of trait is favored when it is positive/negative. An evolutionary singular strategy  $x^*$  is a trait value at which the selection gradient vanishes. According to the criteria presented in [10, 12], if

$$\left. \frac{\partial^2 \theta(x, y)}{\partial y^2} \right|_{y=x=x^*} < 0, \quad (1.12)$$

then  $x^*$  is an evolutionary stable strategy (ESS), that is, the resident using strategy  $x^*$  can not be invaded by any mutant using other strategies. If

$$\left. \frac{\partial^2 \theta(x, y)}{\partial x^2} \right|_{y=x=x^*} > \left. \frac{\partial^2 \theta(x, y)}{\partial y^2} \right|_{y=x=x^*}, \quad (1.13)$$

then  $x^*$  is a convergence stable strategy (CSS), that is, among any pair of strategies near  $x^*$ , the one closer to  $x^*$  is always the winning strategy.

In reality, evolution dynamics is typically much slower than the population dynamics. Further assume time scale separation, in particular that the duration of the inter-strain (or inter-species) competitive interaction is much shorter than that of the mutation process. Thus, the population has always reached a steady state before the appearance of a new mutant. The population remains monomorphic if a successful invasion always ends up with the replacement of the resident strain. Repeating the trait substitution generates a sequence of trait values which converges to an optimal strategy. In addition, the pairwise invasibility plot is an important tool

which graphically illustrates the information concerning the adaptive dynamics of traits.

Without time scale separation, we assume that trait  $\alpha$  evolves continuously with time toward the direction of increasing the fitness  $\Phi$ . Then, the evolution of  $\alpha$  is governed by

$$\frac{d\alpha}{dt} = \sigma\alpha \frac{\partial\Phi}{\partial\alpha}, \quad (1.14)$$

where  $\sigma > 0$  represents the speed of evolution. This approach, though less realistic, is more tractable in mathematics.

### 1.4.3 Reactivity

Most studies of ecological models focus on asymptotic behaviour, such as finding steady states and examining their stability. The transient dynamics may differ significantly from the long-term behaviour and is also crucial for understanding ecological systems [18, 19]. Given a linear system of ordinary differential equations (or the linearization of a nonlinear system near the equilibrium under consideration) with initial conditions,

$$\frac{d\mathbf{x}}{dt} = \mathbf{A}\mathbf{x}, \quad \mathbf{x}(0) = \mathbf{x}_0, \quad (1.15)$$

Neubert and Caswell [40] defined reactivity as the maximum initial amplification rate over all possible (small) perturbations,

$$\text{reactivity} := \max_{\mathbf{x}_0 \neq \mathbf{0}} \left[ \left( \frac{1}{\|\mathbf{x}\|} \frac{d\|\mathbf{x}\|}{dt} \right) \Bigg|_{t=0} \right], \quad (1.16)$$

where  $\|\cdot\|$  denotes the Euclidean norm,

$$\|\mathbf{x}\| := \sqrt{x_1^2(t) + x_2^2(t) + \cdots + x_n^2(t)}.$$

If some perturbations initially grow (amplify), the equilibrium is called reactive. When all perturbations initially decay (attenuate), the equilibrium is called non-reactive.

By direct calculation, the authors found that,

$$\left( \frac{1}{\|\mathbf{x}\|} \frac{d\|\mathbf{x}\|}{dt} \right) \Big|_{t=0} = \frac{\mathbf{x}_0^T H(\mathbf{A}) \mathbf{x}_0}{\mathbf{x}_0^T \mathbf{x}_0}. \quad (1.17)$$

The matrix  $H(\mathbf{A}) = (\mathbf{A} + \mathbf{A}^T)/2$  is called the symmetric part or Hermitian part of  $\mathbf{A}$ . The right hand side of (1.17) is in the form known as the Rayleigh quotient (or the Rayleigh-Ritz ratio). By Rayleigh's principle (see, e.g., [22]), its maximum value is the largest eigenvalue of  $H(\mathbf{A})$  obtained at the corresponding eigenvectors. Hence,

$$\text{reactivity} = \lambda_{\max}(H(\mathbf{A})). \quad (1.18)$$

This definition has been generalized by Mari et al. [36] to  $\lambda_{\max}(H(\mathbf{C}^T \mathbf{C} \mathbf{A}))$  corresponding to a system output  $\mathbf{y}$  with an ecologically motivated linear transformation  $\mathbf{y} = \mathbf{C}\mathbf{x}$ . One application is to epidemiological models when infection-related variables are of interest. On the other hand, Wang et al. [56] has extended this concept to reaction-diffusion systems with spatial heterogeneity taken into account.

# Bibliography

- [1] Allen, L. J., Bolker, B. M., Lou, Y., & Nevai, A. L. (2007). Asymptotic profiles of the steady states for an SIS epidemic patch model. *SIAM Journal on Applied Mathematics*, 67(5), 1283-1309.
- [2] Almarashi, R. M., & McCluskey, C. C. (2019). The effect of immigration of infectives on disease-free equilibria. *Journal of Mathematical Biology*, 79(3), 1015-1028.
- [3] Arino, J., & Van den Driessche, P. (2006). Disease spread in metapopulations. *Fields Institute Communications*, 48, 1-12.
- [4] Bernoulli, D. (1760). Essai d'une nouvelle analyse de la mortalité causée par la petite vérole, et des avantages de l'inoculation pour la prévenir. *Histoire de l'Acad., Roy. Sci. (Paris) avec Mém. des Math. et Phys. and Mém.*, 1-45.
- [5] Bonte, D., Van Dyck, H., Bullock, J. M., Coulon, A., Delgado, M., Gibbs, M., ... & Schtickzelle, N. (2012). Costs of dispersal. *Biological Reviews*, 87(2), 290-312.
- [6] Brauer, F., Van den Driessche, P., & Wang, L. (2008). Oscillations in a patchy environment disease model. *Mathematical Biosciences*, 215(1), 1-10.
- [7] Britton, N. (2003). *Essential Mathematical Biology*. Springer.
- [8] Brown, J. S., Laundre, J. W. & Gurung, M. (1999). The ecology of fear: optimal foraging, game theory, and trophic interactions. *Journal of Mammalogy*, 80, 385-399.
- [9] Chen, S., Shi, J., Shuai, Z., & Wu, Y. (2020). Asymptotic profiles of the steady states for an SIS epidemic patch model with asymmetric connectivity matrix. *Journal of Mathematical Biology*, 80(7), 2327-2361.

- [10] Day, T. & Burns, J. G. (2003). A consideration of patterns of virulence arising from host–parasite coevolution. *Evolution*, 57(3), 671-676.
- [11] Diekmann, O., Heesterbeek, J. A. P., & Metz, J. A. (1990). On the definition and the computation of the basic reproduction ratio  $R_0$  in models for infectious diseases in heterogeneous populations. *Journal of Mathematical Biology*, 28, 365-382.
- [12] Diekmann, O. (2004). A beginner’s guide to adaptive dynamics, *Banach Center Publications*, 63, 47-86.
- [13] van den Driessche, P., & Watmough, J. (2002). Reproduction numbers and sub-threshold endemic equilibria for compartmental models of disease transmission. *Mathematical Biosciences*, 180, 29-48.
- [14] Eisenberg, M. C., Shuai, Z., Tien, J. H., & Van den Driessche, P. (2013). A cholera model in a patchy environment with water and human movement. *Mathematical Biosciences*, 246(1), 105-112.
- [15] El Abdllaoui, A., Auger, P., Kooi, B. W., De la Parra, R. B., & Mchich, R. (2007). Effects of density-dependent migrations on stability of a two-patch predator–prey model. *Mathematical Biosciences*, 210(1), 335-354.
- [16] Hanski, I., Hansson, L., & Henttonen, H. (1991). Specialist predators, generalist predators, and the microtine rodent cycle. *The Journal of Animal Ecology*, 353-367.
- [17] Hastings, A. (1982). Dynamics of a single species in a spatially varying environment: the stabilizing role of high dispersal rates. *Journal of Mathematical Biology*, 16, 49-55.
- [18] Hastings, A. (2004). Transients: the key to long-term ecological understanding?. *Trends in Ecology and Evolution*, 19(1), 39-45.
- [19] Hastings, A. (2010). Timescales, dynamics, and ecological understanding. *Ecology*, 91(12), 3471-3480.

- [20] Hauzy, C., Gauduchon, M., Hulot, F. D., & Loreau, M. (2010). Density-dependent dispersal and relative dispersal affect the stability of predator–prey metacommunities. *Journal of theoretical biology*, 266(3), 458-469.
- [21] Hethcote, H. W. (1976). Qualitative analyses of communicable disease models. *Mathematical Biosciences*, 28(3-4), 335-356.
- [22] Horn, R. A., & Johnson, C. R. (1985). *Matrix analysis*. Cambridge university press.
- [23] Hsieh, Y. H., Van den Driessche, P., & Wang, L. (2007). Impact of travel between patches for spatial spread of disease. *Bulletin of Mathematical Biology*, 69(4), 1355-1375.
- [24] Hsu, S. B., Ruan, S., & Yang, T. H. (2015). Analysis of three species Lotka–Volterra food web models with omnivory. *Journal of Mathematical Analysis and Applications*, 426(2), 659-687.
- [25] Kermack, W. O., & McKendrick, A. G. (1927). A contribution to the mathematical theory of epidemics. *Proceedings of the Royal Society of London. Series A*, 115(772), 700-721.
- [26] Kermack, W. O., & McKendrick, A. G. (1932). Contributions to the mathematical theory of epidemics. II.–The problem of endemicity. *Proceedings of the Royal Society of London. Series A*, 138(834), 55-83.
- [27] Kermack, W. O., & McKendrick, A. G. (1933). Contributions to the mathematical theory of epidemics. III.–Further studies of the problem of endemicity. *Proceedings of the Royal Society of London. Series A*, 141(843), 94-122.
- [28] Levin, S. A. (1974). Dispersion and population interactions. *The American Naturalist*, 108(960), 207-228.
- [29] Levin, S. A. (1976). Population dynamic models in heterogeneous environments. *Annual Review of Ecology and Systematics*, 7, 287-310.
- [30] Li, Z. Z., Gao, M., Hui, C., Han, X. Z., & Shi, H. (2005). Impact of predator pursuit and prey evasion on synchrony and spatial patterns in metapopulation. *Ecological Modelling*, 185(2), 245-254.

- [31] Lima, S. L. & Dill, L. M. (1990). Behavioral decisions made under the risk of predation: a review and prospectus. *Canadian Journal of Zoology*, 68, 619-640.
- [32] Lotka, A. J. (1920). Undamped oscillations derived from the law of mass action. *Journal of the American Chemical Society*, 42, 1595-1599.
- [33] Lotka, A. J. (1925). *Elements of Physical Biology*. Williams and Wilkins, Baltimore.
- [34] Mai, A., Sun, G., Zhang, F., & Wang, L. (2019). The joint impacts of dispersal delay and dispersal patterns on the stability of predator-prey metacommunities. *Journal of Theoretical Biology*, 462, 455-465.
- [35] Marcus, M., & Minc, H. (1964). *A Survey of Matrix Theory and Matrix Inequalities*. Allyn and Bacon.
- [36] Mari, L., Casagrandi, R., Rinaldo, A., & Gatto, M. (2017). A generalized definition of reactivity for ecological systems and the problem of transient species dynamics. *Methods in Ecology and Evolution*, 8, 1574-1584.
- [37] Mchich, R., Auger, P., & Poggiale, J. C. (2007). Effect of predator density dependent dispersal of prey on stability of a predator-prey system. *Mathematical Biosciences*, 206(2), 343-356.
- [38] Murray, J. D. (2002). *Mathematical Biology I. An Introduction*. Third edition. Springer.
- [39] Nelson, E. H., Matthews, C. E. & Rosenheim, J. A. (2004). Predators reduce prey population growth by inducing changes in prey behavior. *Ecology*, 85, 1853-1858.
- [40] Neubert, M. G., & Caswell, H. (1997). Alternatives to resilience for measuring the responses of ecological systems to perturbations. *Ecology*, 78(3), 653-665.
- [41] Okubo, A., & Levin, S. A. (2001). *Diffusion and Ecological Problems: Modern Perspectives*. Second edition. Springer.
- [42] Pangle, K. L., Peacor, S. D., & Johannsson, O. E. (2007). Large nonlethal effects of an invasive invertebrate predator on zooplankton population growth rate. *Ecology*, 88, 402-412.

- [43] Perko, L. (1991). *Differential Equations and Dynamical Systems*. Springer.
- [44] Preisser, E. L., Bolnick, D. I. & Benard, M. F. (2005). Scared To death? The effects of intimidation and consumption in predator–prey interactions. *Ecology*, 86, 501-509.
- [45] Rosenzweig, M. L., & MacArthur, R. H. (1963). Graphical representation and stability conditions of predator-prey interactions. *The American Naturalist*, 97, 209-223.
- [46] Sasmal, S. K. & Takeuchi, Y. (2020). Dynamics of a predator–prey system with fear and group defense, *Journal of Mathematical Analysis and Applications*, 481(1), 123471.
- [47] Schmitz, O. J., Beckerman, A. P., & O'Brien, K. M. (1997). Behaviorally mediated trophic cascades: effects of predation risk on food web interactions. *Ecology*, 78, 1388-1399.
- [48] Schreiber, S. J. (1997). Generalist and specialist predators that mediate permanence in ecological communities. *Journal of Mathematical Biology*, 36, 133-148.
- [49] Skellam, J. G. (1951). Random dispersal in theoretical populations. *Biometrika*, 38, 196-218.
- [50] Smith, H. L., & Waltman, P. (1995). *The Theory of the Chemostat: Dynamics of Microbial Competition*. Cambridge University.
- [51] Vance, R. R. (1984). The effect of dispersal on population stability in one-species, discrete-space population growth models. *The American Naturalist*, 123(2), 230-254.
- [52] Verhulst, P. F. (1838). Notice sur la loi que la population suit dans son accroissement. *Correspondence Mathematique et Physique*, 10, 113-126.
- [53] Volterra, V. (1926). Variazioni e fluttuazioni del numero d'individui in specie animali conviventi. *Mem. Acail. Lincei.*, 2, 31-113. Variations and fluctuations of a number of individuals in animal species living together. Translation by Chapman, R. N. (1931). In: *Animal Ecology*. pp. 409-448. McGraw Hill, New York.
- [54] Wang, W., & Zhao, X. Q. (2004). An epidemic model in a patchy environment. *Mathematical Biosciences*, 190(1), 97-112.

- [55] Wang, W., & Zhao, X. Q. (2006). An epidemic model with population dispersal and infection period. *SIAM Journal on Applied Mathematics*, 66(4), 1454-1472.
- [56] Wang, X., Efendiev, M., & Lutscher, F. (2019). How Spatial Heterogeneity Affects Transient Behavior in Reaction–Diffusion Systems for Ecological Interactions? *Bulletin of Mathematical Biology*, 81, 3889-3917.
- [57] Wang, X., Zanette, L. Y. & Zou, X. (2016). Modelling the fear effect in predator–prey interactions. *Journal of Mathematical Biology*, 73, 1179-1204.
- [58] Wang, X. & Zou, X. (2018). Pattern formation of a predator–prey model with the cost of anti-predator behaviors. *Mathematical Biosciences and Engineering*, 15, 775-805.
- [59] Wang, Y. & Zou, X. (2020). On a predator–prey system with digestion delay and anti-predation strategy. *Journal of Nonlinear Science*, 30, 1579-1605.
- [60] Zanette, L. Y., White, A. F., Allen, M. C. & Clinchy, M. (2011). Perceived predation risk reduces the number of offspring songbirds produce per year. *Science*, 334, 1398-1401.

# Chapter 2

## A Single Species Model with Delay and Dispersal

### 2.1 Introduction

In the classical population models, for example, the logistic equation [15],

$$u'(t) = ru(t) \left[ 1 - \frac{u(t)}{K} \right], \quad (2.1)$$

all the changes are assumed to be instantaneous. However, most biological activities take time. Hutchinson [6] suggested a finite time lag  $\tau > 0$  to be considered in the self-regulatory mechanism (2.1), yielding the delayed logistic equation,

$$u'(t) = ru(t) \left[ 1 - \frac{u(t - \tau)}{K} \right]. \quad (2.2)$$

An equivalent form of (2.2) is known as the Wright equation, so (2.2) is also referred as the Hutchinson-Wright equation. It has been well studied, and the following theorem concludes some well-known results (see, e.g., [5, 11] for proofs):

**Theorem 2.1.1** *The trivial solution of (2.2) is always unstable. The positive equilibrium  $u = K$  is locally asymptotically stable for  $r\tau < \pi/2$  and is unstable for  $r\tau > \pi/2$ . When  $r\tau > \pi/2$ , periodic solution occurs via Hopf bifurcation.*

In such a simple equation, the introduced time delay generates oscillated solutions. There has followed a vast body of work studying the effect of delay in different systems. Considering the variability in environment and the ability of animals to move, it becomes an increasing interest to investigate the effect of time delay on population dynamics in a spatially structured model incorporated with dispersal. In this work, we use patch model following the tradition of Levin [7, 8] and Vance [14]: assume that the species lives in discrete habitats and the populations are connected by between-habitat dispersal. To make it simple, we restrict our model to two patches. Together with the delayed logistic growth, we have the following system of delay differential equations,

$$\begin{aligned} u_1'(t) &= r_1 u_1(t) \left[ 1 - \frac{u_1(t - \tau)}{K_1} \right] + [d_{21} u_2(t) - d_{12} u_1(t)], \\ u_2'(t) &= r_2 u_2(t) \left[ 1 - \frac{u_2(t - \tau)}{K_2} \right] + [d_{12} u_1(t) - d_{21} u_2(t)], \end{aligned} \quad (2.3)$$

where  $u_i$  denotes the population in patch  $i$  and  $d_{ij} > 0$  is the per capita dispersal rate from patch  $i$  to patch  $j$ . This model allows spatial heterogeneity in the two patches in resources so that intrinsic growth rate  $r_i > 0$  and the carrying capacity  $K_i > 0$  are patch-specific. If there is no time delay and the dispersal rates between two patches are equal, the following result is obtained in Smith's book:

**Theorem 2.1.2 (Proposition 4.4.1 in [10])** *For any  $d_{12} = d_{21} = d > 0$ , system (2.3) with  $\tau = 0$  possesses a unique positive equilibrium  $\mathbf{u}^*$  which attracts all non-trivial and non-negative solutions.*

When time delay is considered, Liao and Lou [9] has analyzed the following system,

$$\begin{aligned} u_1'(t) &= \mu u_1(t) [K_1 - u_1(t - \tau)] + d[u_2(t) - u_1(t)], \\ u_2'(t) &= \mu u_2(t) [K_2 - u_2(t - \tau)] + d[u_1(t) - u_2(t)]. \end{aligned} \quad (2.4)$$

which is a special case of model (2.3) when  $r_1/K_1 = r_2/K_2 = \mu > 0$  and  $d_{12} = d_{21} = d > 0$ . This system has a unique positive equilibrium  $\mathbf{u}^*$  same as that of the corresponding system without time delay. If  $K_1 = K_2 = K$ , for any  $d > 0$ , the equilibrium  $\mathbf{u}^*$  is locally asymptotically stable for  $\tau \in [0, \tau_c)$  and is unstable for all  $\tau > \tau_c$ , where  $\tau_c = \pi/(2K\mu)$ . When  $\tau > \tau_c$ ,

periodic solutions may occur via Hopf bifurcation. It is not surprising to see that this result is equivalent to Theorem 2.1.1 since the two patches are identical and hence, the two populations can be treated as a whole. For non-homogeneous environment,  $K_1 \neq K_2$ , the authors provided a sufficient condition  $d \geq \frac{\mu}{2} \sqrt{K_1^2 + K_2^2}$  then obtained similar results. (For more details, see Theorems 1.4 and 1.5 in [9].)

In patch models with movement, random dispersal is usually presupposed, assuming that the process is instantaneous and lossless, which, however, is not realistic. Based on extensive literatures, Bonte et al. ([2]) summarized all possible costs associated with dispersal and classified them into four different types: energetic costs, time costs, risk costs and opportunity costs. In this work, we consider two specific costs of dispersal: (i) the period of time spent for migration; (ii) deaths during dispersal process. Assuming that individuals moving from one patch to the other need a fixed period  $\tau_2 > 0$  and the per capita death rate during dispersal process is  $m > 0$ , we propose the following two-patch model for a single species with delayed logistic growth and dispersal time delay,

$$\begin{aligned} u_1'(t) &= r_1 u_1(t) \left[ 1 - \frac{u_1(t - \tau_1)}{K_1} \right] + [d_{21} e^{-m\tau_2} u_2(t - \tau_2) - d_{12} u_1(t)], \\ u_2'(t) &= r_2 u_2(t) \left[ 1 - \frac{u_2(t - \tau_1)}{K_2} \right] + [d_{12} e^{-m\tau_2} u_1(t - \tau_2) - d_{21} u_2(t)]. \end{aligned} \quad (2.5)$$

In next section, we verify the well-posedness of model (2.5), then find the equilibrium solutions and analyze the stability. Some numerical simulations are provided in Section 3 to illustrate our theoretical results and further explore the effects of two time delays. A brief conclusion is given in the last section.

## 2.2 Mathematical analysis

As far as mathematical analysis is concerned, initial conditions need to be clarified at first. Let  $C = C([-\tau, 0], \mathbb{R}^2)$ , which contains all continuous functions mapping  $[-\tau, 0]$  into  $\mathbb{R}^2$ , and  $C_+ = \{\varphi \in C, \varphi(\theta) \geq 0, \theta \in [-\tau, 0]\}$ , where  $\tau = \tau_1 + \tau_2$ . The initial condition is given as below:

$$(u_1(\theta), u_2(\theta)) = (\varphi_1(\theta), \varphi_2(\theta)) := \varphi(\theta) \in C_+, \quad \theta \in [-\tau, 0], \quad (2.6)$$

where non-negativity is based on biological consideration. By using the method of steps presented in [1], we can show that system (2.5) with initial condition (2.6) has a unique solution which exists globally. To confirm this model is biologically well-posed, we need to verify the non-negativity and boundedness of its solution.

**Theorem 2.2.1** *For any  $\varphi \in C_+$ , the solution of the initial value problem (2.5)–(2.6) remains non-negative for  $t > 0$  and is bounded.*

To prove the theorem, we use the following lemma.

**Lemma 2.2.2 (Theorem 6.3.1 in [1])** *Consider the equation,*

$$x'(t) = f(t, x_t), \quad (2.7)$$

where  $f : \mathbb{R} \times D \rightarrow \mathbb{R}^n$  is continuous and  $D \subset C = C([-\tau, 0], \mathbb{R}^n)$ . Let  $C_+ = \{\varphi \in C, \varphi(\theta) \geq 0, \theta \in [-\tau, 0]\}$ . Assume that, whenever  $\varphi \in D \cap C_+$  with  $\varphi_i(0) = 0$  for some  $i \in \{1, 2, \dots, n\}$ , there holds  $f_i(t, \varphi) \geq 0$ . Then, for any  $\varphi \in D \cap C_+$ , the solution of (2.7),

$$x(t, t_0, \varphi) \geq 0, \quad \text{for all } t \geq t_0.$$

**Proof** The non-negativity of solution to (2.5)–(2.6) directly follows the above lemma. For any non-negative solution  $(u_1(t), u_2(t))$ , define  $U(t) = u_1(t) + u_2(t)$ . Then, we have

$$\begin{aligned} U'(t) &= (r_1 - d_{12})u_1(t) + (r_2 - d_{21})u_2(t) - \sum_{i=1}^2 \frac{r_i}{K_i} u_i(t)u_i(t - \tau_1) + e^{-m\tau_2} [d_{12}u_1(t - \tau_2) + d_{21}u_2(t - \tau_2)], \\ &\leq AU(t) - B \sum_{i=1}^2 u_i(t)u_i(t - \tau_1) + DU(t - \tau_2), \end{aligned}$$

where

$$A = \max\{r_1 - d_{12}, r_2 - d_{21}\}, \quad B = \min_{i=1,2}\{r_i/K_i\}, \quad D = \max\{d_{12}, d_{21}\}e^{-m\tau_2}.$$

For positive constants  $p$  and  $q > 1$ , if  $pU(t) \leq U(t + \theta) \leq qU(t)$  for  $\theta \in [-\tau, 0]$ , then

$$U'(t) \leq (A + qD)U(t) - \frac{pB}{2}U^2(t).$$

Choosing a sufficiently large  $H > 0$ , there exists a positive constant  $\omega$  such that

$$U'(t) \leq -\omega U^2(t) \leq 0 \quad \text{for} \quad U(t) \geq H.$$

Therefore,  $U(t)$  is bounded and hence,  $u_1(t)$  and  $u_2(t)$  are bounded since they are non-negative.

### 2.2.1 Equilibria

Model (2.5) admits two equilibria,  $E_0 = (0, 0)$  and  $E_* = (u_1^*, u_2^*)$  with  $u_1^*$  and  $u_2^*$  satisfying:

$$\begin{aligned} u_2^* &= \frac{e^{m\tau_2} u_1^*}{d_{21}} \left( \frac{r_1 u_1^*}{K_1} - r_1 + d_{12} \right) =: \Pi_1(u_1^*), \\ u_1^* &= \frac{e^{m\tau_2} u_2^*}{d_{12}} \left( \frac{r_2 u_2^*}{K_2} - r_2 + d_{21} \right) =: \Pi_2(u_2^*). \end{aligned}$$

Notice that the positive equilibrium  $E_*$  depends on  $\tau_2$  but is not affected by  $\tau_1$ . The first quadratic function has two roots  $u_1 = 0$  and  $u_1 = \hat{u}_1 := K_1 \left(1 - \frac{d_{12}}{r_1}\right)$ , and the second one has two roots  $u_2 = 0$  and  $u_2 = \hat{u}_2 := K_2 \left(1 - \frac{d_{21}}{r_2}\right)$ . These two parabolas intersect at the origin. When  $\hat{u}_1 \geq 0$  or  $\hat{u}_2 \geq 0$ , the two curves always have a unique intersection in the interior of the first quadrant. When both  $\hat{u}_1$  and  $\hat{u}_2$  are negative, the interior intersection in the first quadrant exists if and only if the slopes of two curves at the origin satisfy  $\Pi_1'(0) \cdot \Pi_2'(0) < 1$ , that is,  $e^{2m\tau_2}(r_1 - d_{12})(r_2 - d_{21}) < d_{12}d_{21}$ . Hence, we have the necessary and sufficient condition for the existence of positive equilibrium  $E_*$ :

**Theorem 2.2.3** *The system (2.5) has a unique positive equilibrium if and only if one of the following conditions holds:*

- (i)  $r_1 \geq d_{12}$ , or  $r_2 \geq d_{21}$ ,
- (ii)  $r_1 < d_{12}$ ,  $r_2 < d_{21}$  and  $e^{2m\tau_2}(r_1 - d_{12})(r_2 - d_{21}) < d_{12}d_{21}$ .

This can be seen more directly in Figure 2.1 in the  $r_1$ - $r_2$  plane. Condition in Theorem 2.2.3 describes the region above the solid curve, which is the graph of  $e^{2m\tau_2}(r_1 - d_{12})(r_2 - d_{21}) < d_{12}d_{21}$  for  $r_1 < d_{12}$ . This curve intersects the coordinate axes at  $(0, d_{21}(1 - e^{-2m\tau_2}))$  and  $(d_{12}(1 - e^{-2m\tau_2}), 0)$ . If no individuals die during dispersal process, i.e.  $m = 0$ , the positive equilibrium

exists for all  $r_1 > 0$  and  $r_2 > 0$ . However, when such loss is considered, i.e.  $m > 0$ , the existence region for  $E_*$  shrinks. The species requires higher growth rates to make up the loss.

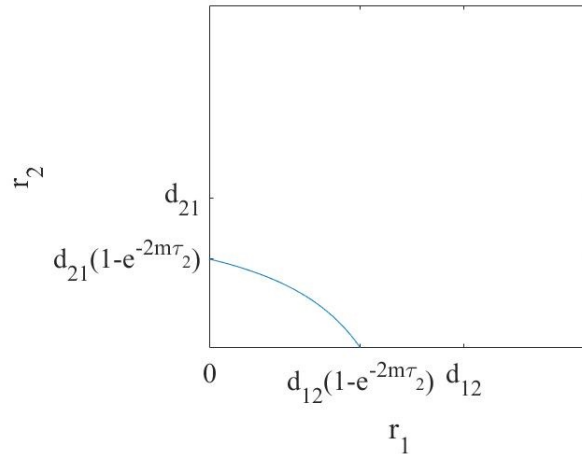


Figure 2.1: The area above the curve is where the positive equilibrium  $E_*$  exists. If there is no loss during dispersal process, i.e.  $m = 0$ , then  $E_*$  always exists.

## 2.2.2 Stability

Now we examine the stability of two equilibria.

**Case I:**  $\tau_1 = 0, \tau_2 = 0$ . We start our analysis from the associated ODE system without time delays,

$$\begin{aligned} u_1'(t) &= r_1 u_1(t) \left[ 1 - \frac{u_1(t)}{K_1} \right] + [d_{21} u_2(t) - d_{12} u_1(t)], \\ u_2'(t) &= r_2 u_2(t) \left[ 1 - \frac{u_2(t)}{K_2} \right] + [d_{12} u_1(t) - d_{21} u_2(t)]. \end{aligned} \quad (2.8)$$

The following result can be obtained in a similar way as that in [10] for Proposition 4.4.1.

**Theorem 2.2.4** *For any  $d_{21}, d_{12} > 0$ , system (2.8) possesses a unique positive equilibrium  $E_*$  which attracts all non-trivial and non-negative solutions.*

**Proof** From Figure 2.1, system (2.8) always has two equilibrium solutions, trivial equilibrium  $E_0 = (0, 0)$  and a unique positive equilibrium  $E_*$ . The Jacobian matrix of system (2.8) at  $E_0$  is

given by

$$J(E_0) = \begin{pmatrix} r_1 - d_{12} & d_{21} \\ d_{12} & r_2 - d_{21} \end{pmatrix}.$$

Let  $s(A)$  denote the maximum real part of all eigenvalues from  $A$ . Then  $s(J(E_0))$  must be positive since the trace of  $J(E_0)$  is always positive when the determinant of  $J(E_0)$  is negative. So  $E_0$  is unstable. On the other hand, since the ODE system (2.8) is positive invariant, bounded and cooperative, the unique positive equilibrium  $E_*$  attracts all non-trivial and non-negative orbits according to Theorem 4.3.3 in [10].

**Case II:**  $\tau_1 = 0, \tau_2 \neq 0$ . Next, we look at the cases when one of the time delay is vanished. First, we consider  $\tau_1 = 0$ . The system (2.5) is reduced to

$$\begin{aligned} u_1'(t) &= r_1 u_1(t) \left[ 1 - \frac{u_1(t)}{K_1} \right] + [d_{21} e^{-m\tau_2} u_2(t - \tau_2) - d_{12} u_1(t)], \\ u_2'(t) &= r_2 u_2(t) \left[ 1 - \frac{u_2(t)}{K_2} \right] + [d_{12} e^{-m\tau_2} u_1(t - \tau_2) - d_{21} u_2(t)], \end{aligned} \quad (2.9)$$

which has been well studied by Takeuchi et al. [13] in details.

**Theorem 2.2.5** *The global dynamics of system (2.9) can be concluded as follow:*

- (i) *When  $r_1 < d_{12}$ ,  $r_2 < d_{21}$  and  $\tau_2 > \frac{1}{2m} \ln \left( \frac{d_{12} d_{21}}{(r_1 - d_{12})(r_2 - d_{21})} \right)$ , system (2.9) only has a trivial equilibrium  $E_0 = (0, 0)$  and it is globally asymptotically stable.*
- (ii) *Otherwise, the trivial equilibrium  $E_0 = (0, 0)$  is unstable. There exists a unique positive equilibrium  $E_*$  and it is globally asymptotically stable.*

**Proof** Define

$$M(0) = \begin{pmatrix} r_1 - d_{12} & d_{21} e^{-m\tau_2} \\ d_{12} e^{-m\tau_2} & r_2 - d_{21} \end{pmatrix}.$$

By Theorem 2.1 in [13], when  $s(M(0)) < 0$ , the population goes extinct in each patch. Therefore,  $E_0$  is globally asymptotically stable if and only if the trace of  $M(0)$  is negative and the determinant of  $M(0)$  is positive. That is,

$$r_1 - d_{12} + r_2 - d_{21} < 0 \quad \text{and} \quad (r_1 - d_{12})(r_2 - d_{21}) - d_{12} d_{21} e^{-2m\tau_2} > 0,$$

which is equivalent to

$$r_1 < d_{12}, \quad r_2 < d_{21} \quad \text{and} \quad \tau_2 > \frac{1}{2m} \ln \left( \frac{d_{12}d_{21}}{(r_1 - d_{12})(r_2 - d_{21})} \right).$$

In addition, from Theorem 2.2.3, there is no positive equilibrium solution under this condition.

Otherwise,  $s(M(0)) > 0$ , by Takeuchi et al. [13] and Zhao and Jing [16], system (2.9) has a unique positive equilibrium and it is globally asymptotically stable.

This result shows that when the growth rates in each patch is relatively less than the dispersal rates, extinction of population may occur in both patches when the time delay due to dispersal is large (or the dispersal-related death rate is high). We also notice that if the growth rate is relatively greater than the dispersal rate in at least one patch, then any dispersal-induced delay will not change the stability of the equilibrium solution comparing to the ODE system (2.8), in which case the costs of dispersal only affect the population sizes in the steady state.

**Case III:**  $\tau_1 \neq 0, \tau_2 = 0$ . Now we consider another case when  $\tau_2 = 0$ . The system (2.5) is reduced to

$$\begin{aligned} u_1'(t) &= r_1 u_1(t) \left[ 1 - \frac{u_1(t - \tau_1)}{K_1} \right] + [d_{21}u_2(t) - d_{12}u_1(t)], \\ u_2'(t) &= r_2 u_2(t) \left[ 1 - \frac{u_2(t - \tau_1)}{K_2} \right] + [d_{12}u_1(t) - d_{21}u_2(t)]. \end{aligned} \tag{2.10}$$

As we mentioned in the introduction, a special case of this system has been investigated in [9] when random dispersal is considered (i.e., symmetric dispersal rates between patches). In system (2.10), the time delay does not affect the equilibrium solutions. Therefore, same as in system (2.8), we have a trivial equilibrium  $E_0 = (0, 0)$  and a unique positive equilibrium  $E_* = (u_1^*, u_2^*)$ . By linearization, we find the Jacobian matrix at  $E_0$  is given by

$$J(E_0) = \begin{pmatrix} r_1 - d_{12} & d_{21} \\ d_{12} & r_2 - d_{21} \end{pmatrix}.$$

From Theorem 2.2.4, the trivial equilibrium solution  $E_0$  is unstable for all  $d_{21}, d_{12} > 0$ .

Then, we study the stability of the unique positive equilibrium  $E_* = (u_1^*, u_2^*)$ . By using the transformation  $\tilde{u}_1 = u_1 - u_1^*$  and  $\tilde{u}_2 = u_2 - u_2^*$ , we obtain a translated system with the positive equilibrium being moved to the origin point. For mathematical simplicity, we drop  $\tilde{u}_1, \tilde{u}_2$  to  $u_1, u_2$  respectively. The system becomes

$$\begin{aligned} u_1'(t) &= r_1 u_1(t) \left[ 1 - \frac{u_1(t - \tau_1)}{K_1} \right] - \frac{r_1}{K_1} u_1^* (u_1(t) + u_1(t - \tau_1)) + [d_{21} u_2(t) - d_{12} u_1(t)], \\ u_2'(t) &= r_2 u_2(t) \left[ 1 - \frac{u_2(t - \tau_1)}{K_2} \right] - \frac{r_2}{K_2} u_2^* (u_2(t) + u_2(t - \tau_1)) + [d_{12} u_1(t) - d_{21} u_2(t)]. \end{aligned} \quad (2.11)$$

The linearization of (2.11) at the origin point is given by

$$\begin{aligned} u_1'(t) &= r_1 u_1(t) - \frac{r_1}{K_1} u_1^* (u_1(t) + u_1(t - \tau_1)) + [d_{21} u_2(t) - d_{12} u_1(t)], \\ u_2'(t) &= r_2 u_2(t) - \frac{r_2}{K_2} u_2^* (u_2(t) + u_2(t - \tau_1)) + [d_{12} u_1(t) - d_{21} u_2(t)]. \end{aligned}$$

Therefore, the characteristic equation can be obtained by substituting in  $(u_1(t), u_2(t)) = e^{\lambda t}(v_1, v_2)$ ,

$$\begin{aligned} D(\tau_1, \lambda) &= \det \begin{pmatrix} \lambda - (r_1 - \frac{r_1}{K_1} u_1^* - d_{12}) + \frac{r_1}{K_1} u_1^* e^{-\lambda \tau_1} & -d_{21} \\ -d_{12} & \lambda - (r_2 - \frac{r_2}{K_2} u_2^* - d_{21}) + \frac{r_2}{K_2} u_2^* e^{-\lambda \tau_1} \end{pmatrix} \\ &= \det \begin{pmatrix} \lambda + d_{21} \frac{u_2^*}{u_1^*} + \frac{r_1}{K_1} u_1^* e^{-\lambda \tau_1} & -d_{21} \\ -d_{12} & \lambda + d_{12} \frac{u_1^*}{u_2^*} + \frac{r_2}{K_2} u_2^* e^{-\lambda \tau_1} \end{pmatrix} \\ &= \lambda^2 + a\lambda + (c\lambda + d)e^{-\lambda \tau_1} + he^{-2\lambda \tau_1} \\ &= 0, \end{aligned}$$

where

$$a = \frac{d_{21} u_1^*}{u_2^*} + \frac{d_{12} u_2^*}{u_1^*}, \quad c = \frac{r_2 u_2^*}{K_2} + \frac{r_1 u_1^*}{K_1}, \quad d = \frac{d_{12} (u_1^*)^2 r_1}{K_1 u_2^*} + \frac{d_{21} (u_2^*)^2 r_2}{K_2 u_1^*} \quad \text{and} \quad h = \frac{r_1 r_2 u_1^* u_2^*}{K_1 K_2}.$$

This kind of characteristic equation has been studied by Chen et al. [4] and Liao and Lou [9]. By the framework in [4], we can find the stability of the positive equilibrium.

**Case IV:**  $\tau_1 \neq 0, \tau_2 \neq 0$ . Finally, we move to the system (2.5) where both  $\tau_1$  and  $\tau_2$  are nonzero. There is always a trivial equilibrium  $E_0 = (0, 0)$  and a unique positive equilibrium

exists when the parameters satisfy one of the conditions in Theorem 2.2.3.

We first look at the stability of the trivial equilibrium. The linearization at  $E_0 = (0, 0)$  is,

$$\begin{aligned} u_1'(t) &= (r_1 - d_{12})u_1(t) + d_{21}e^{-m\tau_2}u_2(t - \tau_2), \\ u_2'(t) &= (r_2 - d_{21})u_2(t) + d_{12}e^{-m\tau_2}u_1(t - \tau_2). \end{aligned} \quad (2.12)$$

This linear system has been studied by Takeuchi et al. [13]. Using Theorem 2.1 from [13], the origin point is globally asymptotically stable when

$$r_1 < d_{12}, \quad r_2 < d_{21} \quad \text{and} \quad \tau_2 > \frac{1}{2m} \ln \left( \frac{d_{12}d_{21}}{(r_1 - d_{12})(r_2 - d_{21})} \right). \quad (2.13)$$

Otherwise, it is unstable. Therefore, for system (2.5), the trivial equilibrium solution is locally asymptotically stable when condition (2.13) holds. Otherwise, the trivial equilibrium is unstable and there exists a unique positive equilibrium solution. Note that condition (2.13) is exactly same as that in Theorem 2.2.5 for the case when  $\tau_1 = 0$ . The time delay  $\tau_1$  in growth rate has no impact on the stability of the trivial equilibrium  $E_0$ . In other words, the extinction of the species is totally caused by the costs of dispersal.

To find the stability for the positive equilibrium  $E_* = (u_1^*, u_2^*)$ , similar to what we have done in case III, we apply the transformation  $\tilde{u}_1 = u_1 - u_1^*$  and  $\tilde{u}_2 = u_2 - u_2^*$  to move the positive equilibrium to the origin point. Again, we drop  $\tilde{u}_1, \tilde{u}_2$  to  $u_1, u_2$  respectively for simplification. Then the system can be written as

$$\begin{aligned} u_1'(t) &= r_1 u_1(t) \left[ 1 - \frac{u_1(t - \tau_1)}{K_1} \right] - \frac{r_1}{K_1} u_1^* (u_1(t) + u_1(t - \tau_1)) + [d_{21}e^{-m\tau_2}u_2(t - \tau_2) - d_{12}u_1(t)], \\ u_2'(t) &= r_2 u_2(t) \left[ 1 - \frac{u_2(t - \tau_1)}{K_2} \right] - \frac{r_2}{K_2} u_2^* (u_2(t) + u_2(t - \tau_1)) + [d_{12}e^{-m\tau_2}u_1(t - \tau_2) - d_{21}u_2(t)]. \end{aligned}$$

The linearization at the origin point now become

$$\begin{aligned} u_1'(t) &= r_1 u_1(t) - \frac{r_1}{K_1} u_1^* (u_1(t) + u_1(t - \tau_1)) + [d_{21}e^{-m\tau_2}u_2(t - \tau_2) - d_{12}u_1(t)], \\ u_2'(t) &= r_2 u_2(t) - \frac{r_2}{K_2} u_2^* (u_2(t) + u_2(t - \tau_1)) + [d_{12}e^{-m\tau_2}u_1(t - \tau_2) - d_{21}u_2(t)]. \end{aligned}$$

Therefore, the characteristic equation can be obtained by substituting in  $(u_1(t), u_2(t)) = e^{\lambda t}(v_1, v_2)$ ,

$$\begin{aligned} D(\tau_1, \tau_2, \lambda) &= \det \begin{pmatrix} \lambda - (r_1 - \frac{r_1}{K_1}u_1^* - d_{12}) + \frac{r_1}{K_1}u_1^*e^{-\lambda\tau_1} & -d_{21}e^{-m\tau_2}e^{-\lambda\tau_2} \\ -d_{12}e^{-m\tau_2}e^{-\lambda\tau_2} & \lambda - (r_2 - \frac{r_2}{K_2}u_2^* - d_{21}) + \frac{r_2}{K_2}u_2^*e^{-\lambda\tau_1} \end{pmatrix} \\ &= \lambda^2 + a\lambda + b + (c\lambda + d)e^{-\lambda\tau_1} + he^{-2\lambda\tau_1} + ke^{-2(\lambda+m)\tau_2} \\ &= 0, \end{aligned}$$

where

$$\begin{cases} a = -r_1 - r_2 + d_{12} + d_{21} + \frac{r_1}{K_1}u_1^* + \frac{r_2}{K_2}u_2^*, \\ b = (r_1 - \frac{r_1}{K_1}u_1^* - d_{12})(r_2 - \frac{r_2}{K_2}u_2^* - d_{21}), \\ c = \frac{r_1}{K_1}u_1^* + \frac{r_2}{K_2}u_2^*, \\ d = -(r_1 - \frac{r_1}{K_1}u_1^* - d_{12})\frac{r_1}{K_1}u_1^* - (r_2 - \frac{r_2}{K_2}u_2^* - d_{21})\frac{r_2}{K_2}u_2^*, \\ h = \frac{r_1r_2u_1^*u_2^*}{K_1K_2}, \\ k = -d_{12}d_{21}. \end{cases}$$

Mathematical analysis for this characteristic equation is less tractable so we use some numerical simulations to show the existence of periodic orbits bifurcated from the positive equilibrium.

## 2.3 Numerical simulations

In this section, we provide some numerical examples for system (2.5) to exhibit (i) the occurrence of periodic orbits via Hopf bifurcation; (ii) how time delays and dispersal costs influence the population dynamics. We fix the parameter values as follow,

$$r_1 = 2, \quad r_2 = 4, \quad K_1 = 40, \quad K_2 = 20, \quad d_{12} = 5, \quad d_{21} = 5, \quad m = 0.5. \quad (2.14)$$

Based on the results of theoretical analysis, oscillations can only be induced into this system by the delay in logistic growth  $\tau_1$ . Without dispersal, i.e.  $d_{12} = d_{21} = 0$ , the population dynamics on each patch follows the delayed logistic equation as described in Theorem 2.1.1:

the solutions converge to the positive equilibrium for  $r_i\tau_1 < \pi/2$  and periodic orbits occur when  $r_i\tau_1 > \pi/2$  for  $i = 1, 2$ . When the two patches are connected by dispersal with related costs ignored, i.e.  $\tau_2 = 0$  and  $m = 0$ , Figure 2.2 presents the solutions of the coupled system (2.10) with different local dynamics. If  $r_1\tau_1 < \pi/2$  and  $r_2\tau_1 < \pi/2$ , the local dynamics in both patches represent the stability of positive equilibria, which is still true for the coupled system, as is shown in Figure 2.2(a). If one patch allows oscillations while the other does not, the coupled system may have stable positive equilibrium (as in Figure 2.2(b)) or stable periodic orbits (as in Figure 2.2(c)). When  $r_1\tau_1 > \pi/2$  and  $r_2\tau_1 > \pi/2$ , oscillations are presented as in Figure 2.2(d).

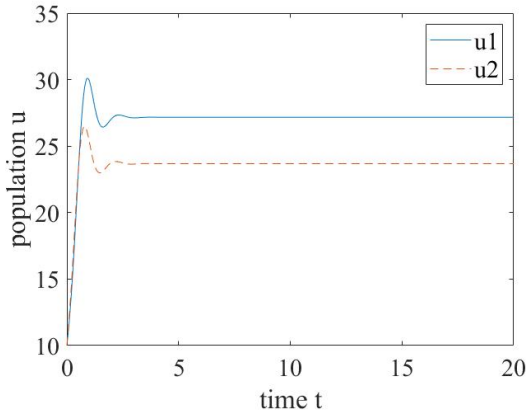
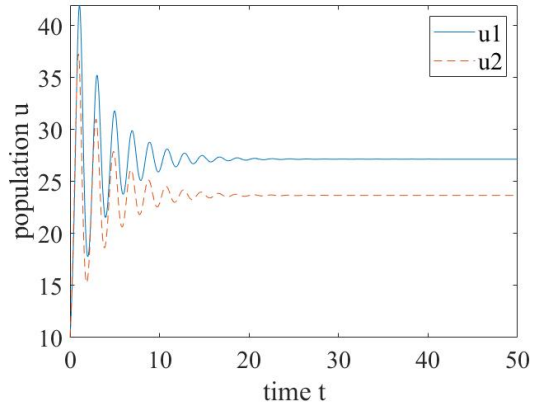
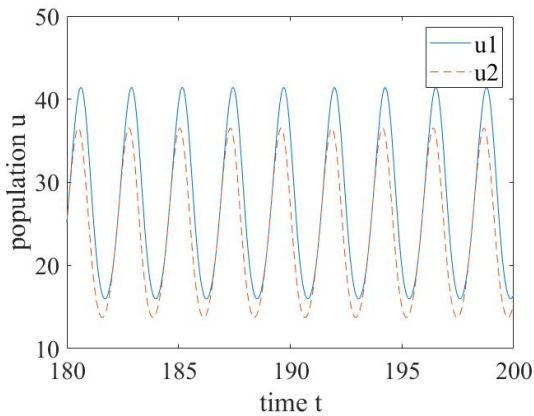
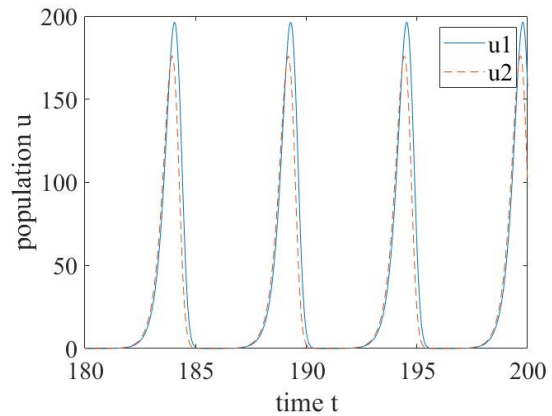
(a)  $r_1\tau_1 < \pi/2, r_2\tau_1 < \pi/2$ (b)  $r_1\tau_1 < \pi/2, r_2\tau_1 > \pi/2$ (c)  $r_1\tau_1 < \pi/2, r_2\tau_1 > \pi/2$ (d)  $r_1\tau_1 > \pi/2, r_2\tau_1 > \pi/2$ 

Figure 2.2: The oscillations induced by time delay  $\tau_1$  of system (2.10) which is coupled by dispersal with related costs ignored, i.e.  $\tau_2 = 0$  and  $m = 0$ . Values of  $\tau_1$  are chosen as: (a)  $\tau_1 = 0.3$ ; (b)  $\tau_1 = 0.5$ ; (c)  $\tau_1 = 0.6$ ; (d)  $\tau_1 = 1$ ;

Next, we explore the impact of dispersal-induced delay  $\tau_2$ . Figure 2.2 suggests that system (2.5) does not admit periodic solutions when  $\tau_1$  is small. As displayed in Figure 2.3, equilibrium solutions are stable. When there are no time delays, as in Figure 2.3(a), the positive equilibrium is globally asymptotically stable by Theorem 2.2.4. When  $\tau_1 = 0$  and  $\tau_2 \neq 0$ , this corresponds to system (2.9) with the global dynamics presented by Theorem 2.2.5. With the fixed parameter values, we have  $r_1 < d_{12}$  and  $r_2 < d_{21}$ . Thus, the positive equilibrium attracts all non-trivial and non-negative solutions for small  $\tau_2$  (as in Figure 2.3(c)), while the populations in both patches go to extinction for large  $\tau_2$  (as in Figure 2.3(e)). We also do the simulations with a small  $\tau_1$ . Comparing the plots from different lines in Figure 2.3, it is clear that the loss due to dispersal leads to the reduction in population sizes.

Figure 2.4 exhibits some periodic solutions of system (2.5). Under the joint effects of two time delays, the oscillations vary in amplitude and period. We have also observed stable equilibrium solutions when some particular combinations of delay values are chosen.

## 2.4 Conclusion

In this project, we proposed and studied a two-patch model for a single species with dispersal, assuming that the movement takes time and deaths occur during the process. Together with the delayed logistic growth, the model is given by a system of delay differential equations with two constant time delays. Our model admits asymmetric dispersal and spacial heterogeneity, by letting  $d_{12}$  and  $d_{21}$ ,  $r_1$  and  $r_2$ ,  $K_1$  and  $K_2$  be distinct.

We have investigated the impact of two time delays on the dynamics of population. The results reveal that the delay in logistic growth induces oscillations as it does in an isolated population; and the dispersal delay that related to a loss affects the population sizes. If there is no delay in local dynamics, i.e  $\tau_1 = 0$ , the positive equilibrium of system (2.5) is globally asymptotically stable when  $\tau_2 = 0$ . With costs of dispersal considered, i.e  $\tau_2 > 0$  and  $m > 0$ , extinction becomes possible for this species when such a loss is relatively large.

Even though we have already known the separate effect of two time delays, their joint impact on population dynamics is much more complex, as is demonstrated by some numer-

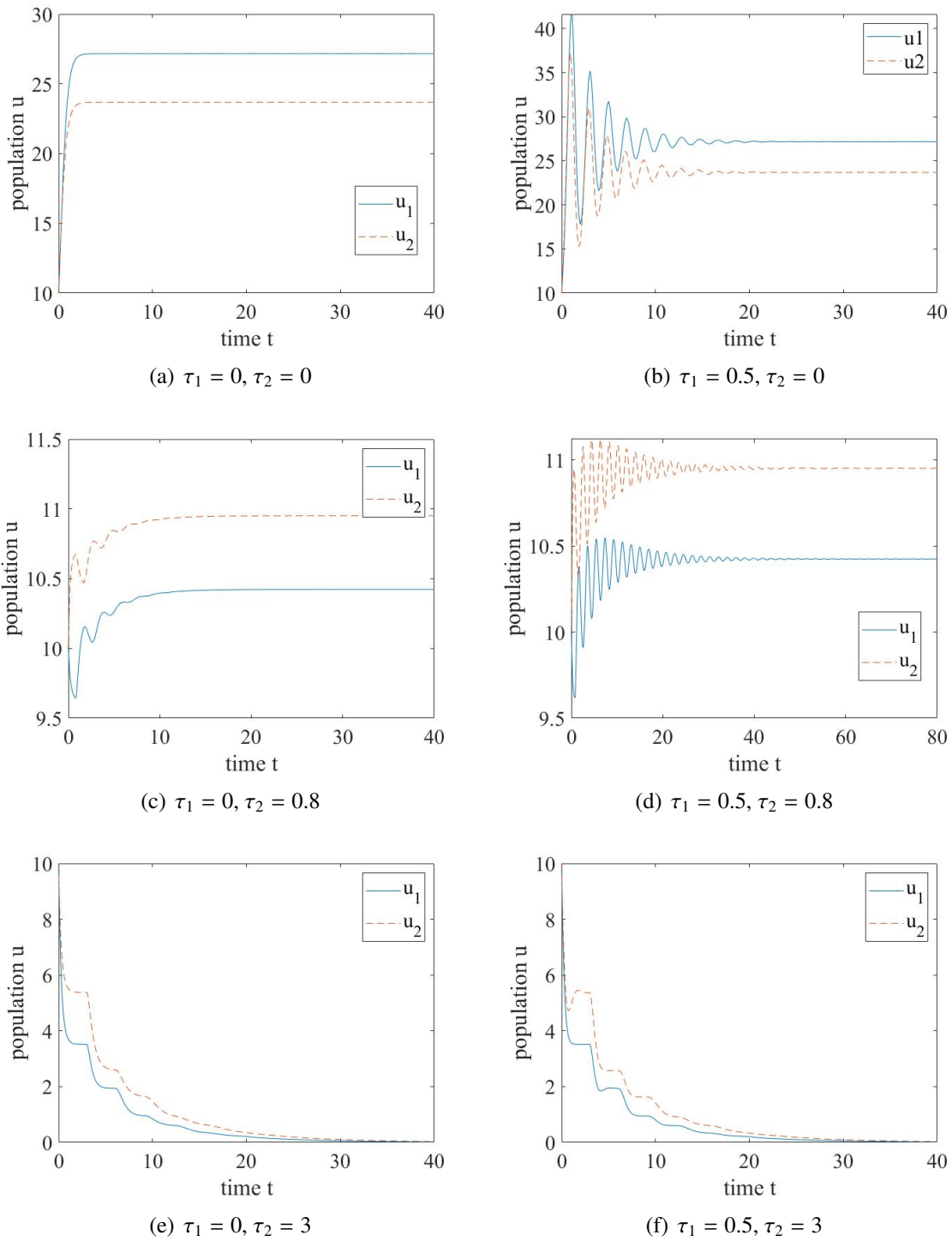


Figure 2.3: The impact of time delay  $\tau_2$  due to dispersal in the case when equilibrium solutions are stable.

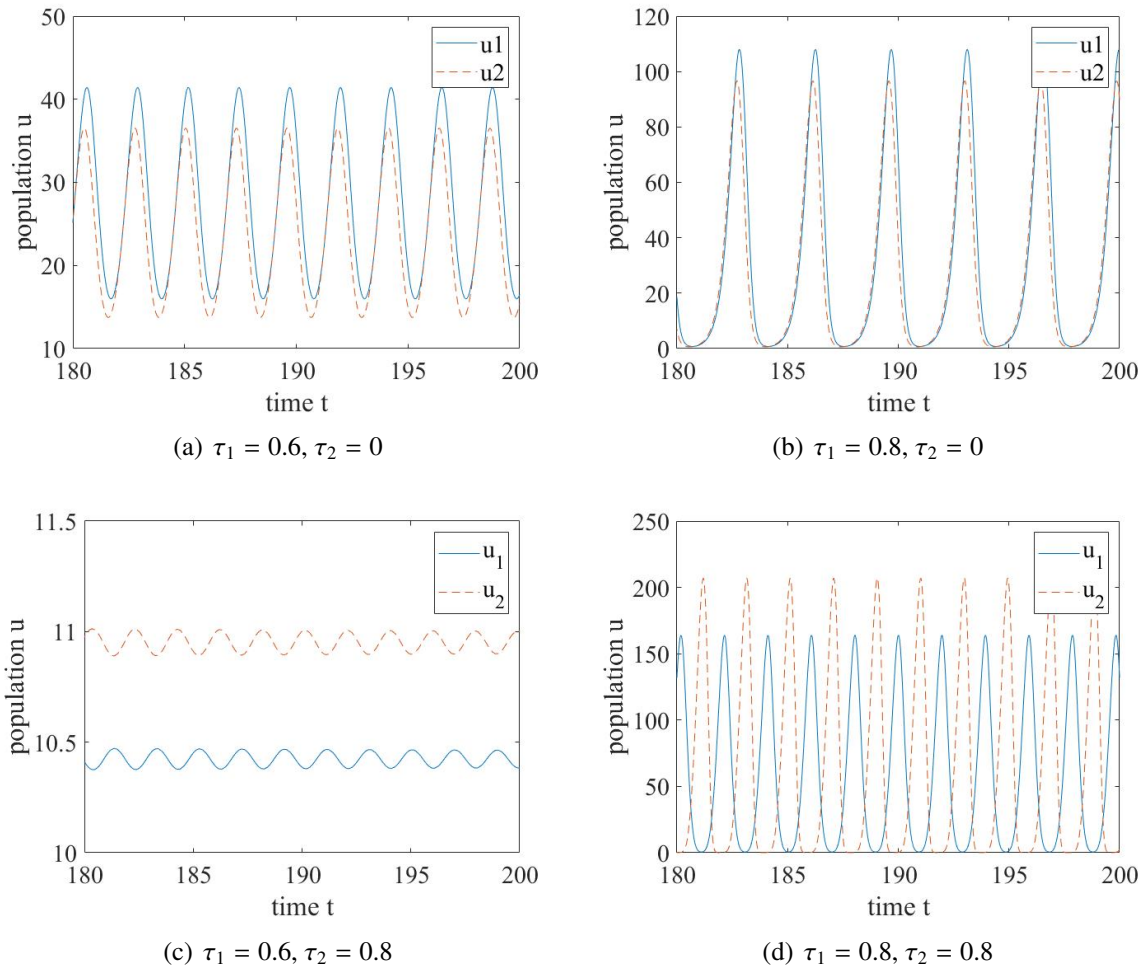


Figure 2.4: The periodic solutions of system (2.5) with different combinations of time delays.

ical examples. When periodic solutions occur via Hopf bifurcation, the oscillations vary in amplitude and frequency which is not only caused by  $\tau_1$  but also affected by  $\tau_2$ . Due to the complexity of our model, it is hard to do mathematical analysis for Hopf bifurcation. We leave this for future works.

# Bibliography

- [1] AM9512, Lecture notes, UWO-AM9512, 2017.
- [2] Bonte, D., Van Dyck, H., Bullock, J. M., Coulon, A., Delgado, M., Gibbs, M., ... & Schtickzelle, N. (2012). Costs of dispersal. *Biological Reviews*, 87(2), 290-312.
- [3] Brauer, F. (1987). Absolute stability in delay equations. *Journal of Differential Equations*, 69(2), 185-191.
- [4] Chen, S., Shi, J., & Wei, J. (2013). Time delay-induced instabilities and Hopf bifurcations in general reaction–diffusion systems. *Journal of Nonlinear Science*, 23, 1-38.
- [5] Hayes, N. (1950). Roots of the transcendental equation associated with a certain difference-differential equation. *Journal of the London Mathematical Society*, 25, 226-232.
- [6] Hutchinson, G. E. (1948). Circular causal systems in ecology. *Annals of the New York Academy of Science*, 50, 221-246.
- [7] Levin, S. A. (1974). Dispersion and population interactions. *The American Naturalist*, 108(960), 207-228.
- [8] Levin, S. A. (1976). Population dynamic models in heterogeneous environments. *Annual Review of Ecology and Systematics*, 7, 287-310.
- [9] Liao, K. L. & Lou, Y. (2014). The effect of time delay in a two-patch model with random dispersal. *Bulletin of Mathematical Biology*, 76(2), 335-376.

- [10] Smith, H. L. (1996). *Monotone Dynamical System: an Introduction to the Theory of Competitive and Cooperative systems*. Rhode Island: American Mathematical Society.
- [11] Smith, H. L. (2011). *An Introduction to Delay Differential Equations with Applications to the Life Sciences*. New York: Springer.
- [12] Takeuchi, Y., Cui, J. A., Miyazaki, R. & Saito, Y. (2006). Permanence of delayed population model with dispersal loss. *Mathematical Biosciences*, 201(1), 143-156.
- [13] Takeuchi, Y., Wang, W. & Saito, Y. (2006). Global stability of population models with patch structure. *Nonlinear Analysis: Real World Applications*, 7(2), 235-247.
- [14] Vance, R. R. (1984). The effect of dispersal on population stability in one-species, discrete-space population growth models. *The American Naturalist*, 123(2), 230-254.
- [15] Verhulst, P. F. (1838). Notice sur la loi que la population suit dans son accroissement. *Correspondence Mathematique et Physique*, 10, 113-126.
- [16] Zhao, X. Q., & Jing, Z. J. (1996). Global asymptotic behavior in some cooperative systems of functional differential equations. *Canadian Applied Mathematics Quarterly*, 4(4), 421-444.

# Chapter 3

## Modelling Anti-predation Response of Prey in a Two-patchy Environment

### 3.1 Introduction

Interactions between predator and prey species are typically very complicated, in comparison with competitions and mutualism. This is mainly because a dynamical system model that describes predator-prey interaction is non-monotone, and hence, can allow very rich dynamics.

The most classic predator-prey system was proposed by Lotka and Volterra respectively in 1920s, and is of the following form:

$$\begin{cases} \frac{du}{dt} = \alpha u - \beta uv, \\ \frac{dv}{dt} = -\delta v + \gamma uv, \end{cases} \quad (3.1)$$

where  $u(t)$  and  $v(t)$  are the populations of the prey and predator respectively at time  $t$ . This model allows a family of periodic orbits and is structurally unstable. Since then, there have been numerous modifications/generalizations on (3.1), which can be represented by the following more general form:

$$\begin{cases} \frac{du}{dt} = g_1(u) - p(u, v)v, \\ \frac{dv}{dt} = g_2(v) + cp(u, v)v, \end{cases} \quad (3.2)$$

where  $g_1(u)$  ( $g_2(v)$ ) represents the population dynamics of the prey (predator) in the absence of the predator (prey). Here the predation term  $p(u, v)v$  accounts for catching/consumption rate of prey by predator, and is a *direct effect* of the predator on prey. The positive constant  $c$  explains the efficiency of biomass transfer from prey to predator after catching and consumption, and the function  $p(u, v)$  is referred to as the functional response. To the authors' knowledge, almost all efforts in modifying and generalizing (3.1) lie in proposing various forms for  $p(u, v)$  depending on the nature of predation which is species specific. For example, for  $p(u, v)$  depending on  $u$  only, there are Holling types I, II and III; for  $p(u, v)$  truly depending on both  $u$  and  $v$ , there are Beddington-DeAngelis functional response  $p(u, v) = \frac{au}{1+bu+cv}$  and ratio dependent functional response  $p(u, v) = \frac{a(u/v)}{c+b(u/v)} = \frac{au}{bu+cv}$ . Therefore, such efforts are all along the line of the *direct effect*.

On the other hand, recent field observations and empirical results show that merely the presence of predator can alter ecological behaviours of prey, and thereby, influence its population size. For feeding animals, they may change their foraging periods and locations to avoid hunting predators ([15]). Such effects are *indirect* and non-lethal as they are not through predation and consumption. Usually, defensive actions, including avoidance, vigilance, alarm calls, grouping and even defences against predators ([5]) can diminish direct mortality from predation temporally, but will decrease lifetime fitness as well through, for example, reduced growth rate and fecundity due to less intake and mating opportunities.

To study how significant such a fear effect can be, some experiments have been designed and conducted by limiting lethal consumption. For example, Nelson *et al.* ([17]) surgically shortened the mouthparts of damsel bugs, so that they were unable to consume pea aphids but could still disturb them. The growth of aphid population was reduced by 30%. Zanette *et al.* ([29]) conducted a field experiment on song sparrows. They protected the birds from direct predation by using electric fences and broadcasted playbacks of the calls and sounds of their predators. They found that number of the bird's offspring per year was reduced by 40%. Preisser *et al.* ([19]) estimated the sizes of direct and indirect effects in 166 studies from 49 published works, and their result showed that the indirect effect size on average was similar to (more precisely it was only slightly weaker than) the direct effect size.

The aforementioned field experimental results clearly indicate that fear effect is indeed

an important factor in predator-prey interactions. As far as mathematically modelling fear effect is concerned, Brown *et al.* ([3]) firstly modelled the ecology of fear by conjoining the Rosenzweig-MacArthur model ([20]):

$$\begin{cases} \frac{du}{dt} = ru \left(1 - \frac{u}{K}\right) - g(u)v, \\ \frac{dv}{dt} = -mv + eg(u)v, \end{cases} \quad (3.3)$$

with a foraging theory in 1999, where fear was represented by the level of vigilance. In a recent work, based on the field study in [29], Wang *et al.* ([25]) incorporated the fear effect on reducing the reproduction rate of the prey in the Rosenzweig-MacArthur model with Holling Types I and II functional responses. In [26], Wang and Zou further discussed different effects of fear on juvenile and adult stages of the prey by a model with age structure, in the form of a system of delayed differential equations. Note that in [25], only a cost of the anti-predation response was considered. More recently, Wang and Zou ([28]) modified the model in [25] by (i) incorporating both cost (reducing reproduction rate) and benefit (reducing the chances of being caught and consumed by predator) to the prey equation, and (ii) introducing a time lag that accounts for the time needed for the transfer of prey biomass to predator biomass. The analysis in [28] has not only shown that there is a critical response level, but also revealed how such a critical level is affected by the digestion delay. Sasmal and Takeuchi [22] also considered both cost and benefit due to anti-predation response with the functional response  $g(u)$  being Holling Type IV, and explored the rich dynamics of the resulting ODE system. Sasmal [21] explored multiple Allee effect induced by fear effect. From the aforementioned works, it seems that the fear effect had been largely neglected in predator-prey models, and the recent results mentioned above suggests that many existing models deserve a revisit by incorporating the fear effect and various factors induced by such an indirect effect in predator-prey interactions.

Besides the factors mentioned above (age structure, types of the functional responses, digestion delay), there is also the important factor of spatial structure. Considering the ability of species moving around, many works have already been done for both *discrete* and *continuum* habitats by using random dispersal or diffusion to model the movement of individuals (for example, see [10], [14], [12], [18] and the references therein). In most existing works, dispersal

rates were postulated to be constants, independent of time, location and population densities. However, in predator-prey interactions, some prey perceiving a predation risk from the predator may accordingly change their dispersal strategy to avoid encounters with predators. In most cases, animals (such as mice) are observed to reduce their activities because moving prey are more likely to be detected by predators; usually this corresponds to the increased use of refuges ([15]). There are also biological species, such as birds which, upon perceiving a risk from the predators, in addition to reducing the reproduction rate, may respond to the risk by moving more frequently and in more advantageous direction(s). For a spatially *continuum* habitat, Wang and Zou proposed and analyzed a reaction-diffusion model in [27] with predator-taxis for the prey accounting for the prey's intention of moving away from the predator. Through the model, the role of fear effect in pattern formation is explored in conjunction with various types of functional responses.

Compared to partial differential equation models for populations in a spatially continuous habitat, patch models for discrete habitats are sometimes more practical since habitat fragmentation is common. For human beings, we live in cities and towns; for animals, the land is often separated by geographical factors and human constructions. With the above considerations, it is interesting and desirable to explore how the fear effect reflected not only in reproduction rate but also in dispersal rate of the prey will affect the population dynamics in predator-prey interactions. To this end, parallel to [27], we propose in this work a predator-prey model in the form of system of ordinary differential equations over two patches. In Section 3.2, we will formulate and explain our model; and in subsequent sections 3.3 and 3.4, we will analyze the model to gain some biological insights on the role of fear effect in conjunction with the dispersals. We begin in Section 3.3 by considering the case without dispersal; this will allow us to obtain some preliminary results on the fear effect on local population dynamics and the evolution of anti-predation response level. Then in Section 3.4, we further explore the case when the two patches are connected through dispersals with dispersal rates also affected by fear. Some numerical simulations are presented. We complete the paper by Section 3.5, summarizing the main results and discussing the biological implications and significance of the results, as well as some possible related future research projects.

## 3.2 Model formulation

The logistic growth of prey population in the Rosenzweig-MacArthur model (3.3) is a result of constant per capita birth rate  $b_0$  together with a density independent per capita death rate (nature death rate)  $d_1$  and a density dependent death rate  $d_2u$ :  $u'(t) = b_0u - d_1u - (d_2u)u = (b_0 - d_1)u[1 - \frac{u}{(b_0-d_1)/d_2}]$ . Based on this and the field experiment of [29] where predation was artificially prevented, Wang *et al.* ([25]) proposed the following predator-prey model:

$$\begin{cases} \frac{du}{dt} = b_0f(\alpha, v)u - d_1u - d_2u^2 - g(u)v, \\ \frac{dv}{dt} = -mu + cg(u)v, \end{cases} \quad (3.4)$$

where a specialist predator was considered and Holling Types I and II for the functional response function  $g(u)$  were adopted in respective analysis. Here  $v$  denotes the population of predators reflecting the level of risk, and  $\alpha$  is a non-negative parameter reflecting the anti-predation response level of the prey and hence, the decreasing properties of  $f(\alpha, v)$  in  $\alpha$  and  $v$  posed in [25] account for the effect of the prey's fear on reducing the prey's reproduction rate.

Note that the demographic equation in (3.4) for the prey population assumes a constant per capita birth rate, which has neglected the Allee effect for the prey species. Allee effect reflects the fact that for some two-sex species, the per capita birth rate is also density dependent due to the need in group defense and/or mating opportunities. A simple dependence is  $b(u) = b_0 + b_1u$ , reflecting the scenario that larger the population size is, more mating opportunities there will be and hence, more births there will be. This simple  $b(u)$  will also lead to a logistic growth for the prey in the absence of the predator, with the carrying capacity modified accordingly. There have been many research on modelling Allee effect using various density dependent birth rate function; see Terry [24] and the references therein for more details on this topic. We also point out that there are also two-sex species for which a matured individual only mates with a fixed partner. Considering this fact and in order to avoid making things too complicated, we will not consider Allee effect but just follow the line of (3.4).

With the same consideration for the prey population as in (3.4), we consider a prey species that lives on two patches and is able to move between the two patches. Let  $u_i$  and  $v_i$  denote the populations of prey and predators on patch  $i$  ( $i = 1, 2$ ), respectively. We then propose the

following model system:

$$\begin{cases} \frac{du_1}{dt} = b_1(\alpha, v_1)u_1 - d_1u_1 - au_1^2 - c(\alpha, v_1)u_1v_1 + m(\alpha, v_2)u_2 - m(\alpha, v_1)u_1, \\ \frac{du_2}{dt} = b_2(\alpha, v_2)u_2 - d_2u_2 - au_2^2 - c(\alpha, v_2)u_2v_2 + m(\alpha, v_1)u_1 - m(\alpha, v_2)u_2. \end{cases} \quad (3.5)$$

Here the Holling Type I functional response is adopted for predation interactions, and the birth rate functions  $b_i(\alpha, v_i)$ , predation rate functions  $c(\alpha, v_i)$  and dispersal rate functions  $m(\alpha, v_i)$  are assumed to depend on the perceived predation risk (represented by the quantity of predators  $v_i$ ) and vigilance level  $\alpha \in (0, \infty)$  (considered as an anti-predation strategy) of the prey, for  $i = 1, 2$ . We allow *spatial heterogeneity* in the two patches in resources and this leads to the adoption of patch specific birth rate functions. On the other hand, considering that we are dealing with the *same prey species* living in two different patches *predated by the same predator species*, we have assumed the same predation rate function and dispersal rate function in the two patches, both depending on predator population in the patch though. In order to focus on the prey's population and for simplicity, we assume that the predator has a constant population on each patch, meaning that  $v_1$  and  $v_2$  are positive constants. This approximately corresponds to a scenario that the predator is a generalist species living on a wide range of food resources and only having this prey species as a minor food resource.

According to the discussion in the introduction, prey reduce reproduction in response to the perceived predation risk, and being more alert gives them higher chances to survive through predation. To capture these biological meanings, functions  $b_i(\alpha, v_i)$  and  $c(\alpha, v_i)$  are assumed to satisfy the following properties which are similar to those in [25]:

$$\begin{cases} b_i(0, v_i) = b_i(\alpha, 0) = b_{0i}, & \lim_{\alpha \rightarrow \infty} b_i(\alpha, v_i) = \lim_{v_i \rightarrow \infty} b_i(\alpha, v_i) = 0, \\ c(0, v_i) = c(\alpha, 0) = c_0, & \lim_{\alpha \rightarrow \infty} c(\alpha, v_i) = \lim_{v_i \rightarrow \infty} c(\alpha, v_i) = 0, & i = 1, 2. \\ \frac{\partial b_i(\alpha, v_i)}{\partial \alpha} \leq 0, & \frac{\partial b_i(\alpha, v_i)}{\partial v_i} \leq 0, & \frac{\partial c(\alpha, v_i)}{\partial \alpha} \leq 0, & \frac{\partial c(\alpha, v_i)}{\partial v_i} \leq 0, \end{cases} \quad (3.6)$$

In [25], the authors presented three examples of such function satisfying the above conditions:

$$h_1(\alpha, v) = a_1 e^{-b_1 \alpha v}, \quad h_2(\alpha, v) = \frac{a_2}{1 + b_2 \alpha v} \quad \text{and} \quad h_3(\alpha, v) = \frac{a_3}{1 + b_3 \alpha v + c_3 (\alpha v)^2}.$$

As for the dispersal rate function  $m(\alpha, v_i)$ , it is species specific: when perceiving predation risk, some species may tend to move more frequently (e.g., birds), while the others may reduce their movement to avoid being captured (e.g., mice which typically have refuges). We consider the latter in this work by assuming that the dispersal rate function is decreasing with respect to  $\alpha$  and  $v_i$ :

$$\begin{cases} m(0, v_i) = m(\alpha, 0) = m_0, & \lim_{\alpha \rightarrow \infty} m(\alpha, v_i) = \lim_{v_i \rightarrow \infty} m(\alpha, v_i) = 0, \\ \frac{\partial m(\alpha, v_i)}{\partial \alpha} \leq 0, & \frac{\partial m(\alpha, v_i)}{\partial v_i} \leq 0. \end{cases} \quad (3.7)$$

Let  $F_i(\alpha, v_i) = b_i(\alpha, v_i) - d_i - c(\alpha, v_i)v_i$  for  $i = 1, 2$ . Note that  $F_i(\alpha, v_i)$  can be used as a measure of fitness for the species on patch  $i$ . Then the model (3.5) is rewritten as:

$$\begin{cases} \frac{du_1}{dt} = u_1 [F_1(\alpha, v_1) - au_1] + m(\alpha, v_2)u_2 - m(\alpha, v_1)u_1, \\ \frac{du_2}{dt} = u_2 [F_2(\alpha, v_2) - au_2] + m(\alpha, v_1)u_1 - m(\alpha, v_2)u_2. \end{cases} \quad (3.8)$$

According to the basic theory of ordinary differential equations, there exists a unique solution to system (3.8) for any given initial values  $u_1(0)$  and  $u_2(0)$ . Using the proposition given by Chepyzhov and Vishik in their book [4, proposition 1.1], one can easily check that  $\mathbb{R}_+^2$  is invariant for (3.8). Moreover, setting  $\bar{F} = \max\{F_1(\alpha, v_1), F_2(\alpha, v_2) : \alpha \geq 0, v_1 \geq 0, v_2 \geq 0\}$ , we have

$$\frac{d}{dt}(u_1 + u_2) \leq (u_1 + u_2) \left[ \bar{F} - \frac{a}{2}(u_1 + u_2) \right].$$

By a comparison argument, we then conclude that

$$\limsup_{t \rightarrow \infty} (u_1 + u_2) \leq \frac{2\bar{F}}{a},$$

indicating that the total population  $(u_1 + u_2)$  is bounded. By the non-negativity of  $u_1$  and  $u_2$ , both of them must be bounded. Furthermore, if  $\bar{F}$  is non-positive, then the total population  $(u_1 + u_2)$  converges to zero.

Summarizing the above, we have obtained the following result of well-posedness for the model.

**Lemma 3.2.1** *For any initial point  $[u_1(0), u_2(0)] \in \mathbb{R}_+^2$ , there exists a unique solution to sys-*

tem (3.8) which is non-negative and bounded.

### 3.3 Model analysis: without dispersal

We begin our analysis of the model for local population dynamics by considering the case *without dispersal*:  $m(\alpha, v_1) = m(\alpha, v_2) = 0$ . Then the model (3.8) reduces to a decoupled pair of ordinary differential equations (ODEs) with each having the same form of

$$\frac{du}{dt} = u [F(\alpha, v) - au], \quad (3.9)$$

where  $F(\alpha, v) := b(\alpha, v) - d - c(\alpha, v)v$ . This is a scalar logistic ODE in terms of the variable  $u$  and its dynamics is completely well known:

**Lemma 3.3.1** *If  $F(\alpha, v) \leq 0$ , then every solution of (3.9) with  $u(0) \geq 0$  converges to 0; if  $F(\alpha, v) > 0$ , then every solution of (3.9) with  $u(0) > 0$  satisfies*

$$\lim_{t \rightarrow \infty} u(t) = \frac{F(\alpha, v)}{a}$$

Before moving on to the patch model *with dispersal*, we want to gain some insights on the anti-predation strategy of prey from evolutionary perspective by using the method of adaptive dynamics. To this end, we take the vigilance level parameter  $\alpha$  as the trait. Assume that a resident prey with population size  $u$  uses the strategy  $\alpha_u$  and a mutant (or invading) prey with relatively small population size  $w$  ( $w \ll u$ ) adopts a different strategy  $\alpha_w \neq \alpha_u$ , and the resident and mutant strains are ecologically equivalent in all other aspects. Then model (3.9) is naturally extended to the following system of equations:

$$\begin{cases} \frac{du}{dt} = u[F(\alpha_u, v) - a(u + w)] =: g^u(u, w), \\ \frac{dw}{dt} = w[F(\alpha_w, v) - a(u + w)] =: g^w(u, w). \end{cases} \quad (3.10)$$

Suppose that the population of resident prey has already settled at the steady state  $u^*(\alpha_u, v) = \frac{F(\alpha_u, v)}{a} =: P(\alpha_u, v)$  (assuming  $F(\alpha_u, v) > 0$ ) if there is no invading (mutant) prey competing with

it. The idea of invasibility analysis (see [8] for more details) is to find out whether the population of mutant prey will grow or decay once introduced. This corresponds to the local instability/stability of the boundary equilibrium  $(P(\alpha_u, v), 0)$  of (3.10). Notice that (3.10) is a Lotka-Volterra competition model with the equal competition weight, and hence, the competition exclusion is the generic consequence in the following sense:

- (i) if  $F(\alpha_w, v) > F(\alpha_u, v)$ , then equilibrium  $E_w := (0, P(\alpha_w, v))$  is globally asymptotically stable for (3.10);
- (ii) if  $F(\alpha_w, v) < F(\alpha_u, v)$ , then equilibrium  $E_u := (P(\alpha_u, v), 0)$  is globally asymptotically stable for (3.10).

Following [8], we introduce the invasion exponent  $\theta(\alpha_u, \alpha_w)$  for the mutant prey by

$$\theta(\alpha_u, \alpha_w) = \left. \frac{\partial g^w(u, w)}{\partial w} \right|_{w=0} = F(\alpha_w, v) - au^*(\alpha_u, v) = F(\alpha_w, v) - F(\alpha_u, v),$$

which is the relative fitness of the mutant in the environmental condition mediated by the residents. Then the above competition exclusion results can be restated in terms of the sign of this invasion exponent  $\theta(\alpha_u, \alpha_w)$ : the mutant prey will invade and replace the resident prey if  $\theta(\alpha_u, \alpha_w) > 0$ ; and the mutant prey can not invade (establish) if  $\theta(\alpha_u, \alpha_w) < 0$ .

Next we explore the existence of evolutionary stable strategy (ESS) and convergence stable strategy (CSS) with respect to the fitness function  $F(\alpha, v)$ . An evolutionary singular strategy  $\alpha_u = \alpha^*$  is a trait value at which the selection gradient vanishes,

$$\left. \frac{\partial \theta(\alpha_u, \alpha_w)}{\partial \alpha_w} \right|_{\alpha_w = \alpha_u} = \left. \frac{\partial F(\alpha_w, v)}{\partial \alpha_w} \right|_{\alpha_w = \alpha^*} = 0. \quad (3.11)$$

If the resident prey using strategy  $\alpha^*$  can not be invaded by any mutant prey using other strategies, then  $\alpha^*$  is an ESS. By [6, 8], this is implied by

$$\left. \frac{\partial^2 \theta(\alpha_u, \alpha_w)}{\partial \alpha_w^2} \right|_{\alpha_w = \alpha_u = \alpha^*} = \left. \frac{\partial^2 F(\alpha_w, v)}{\partial \alpha_w^2} \right|_{\alpha_w = \alpha^*} < 0. \quad (3.12)$$

The singular point  $\alpha^*$  is a CSS if among any pair of strategies near  $\alpha^*$ , the one closer to  $\alpha^*$  is

always the winning strategy. By [6, 8], this is implied by

$$\frac{d}{d\alpha_u} \left[ \frac{\partial \theta(\alpha_u, \alpha_w)}{\partial \alpha_w} \Big|_{\alpha_w=\alpha_u} \Big|_{\alpha_u=\alpha^*} \right] = \frac{\partial^2 F(\alpha_w, v)}{\partial \alpha_w^2} \Big|_{\alpha_w=\alpha^*} < 0. \quad (3.13)$$

By condition (3.12), a local maximum of function  $F(\alpha_w, v)$  is a local ESS. Moreover, conditions (3.12) and (3.13) are equivalent for model (3.10), implying that the ESS must be convergence stable when exists.

For a general discussion on definition and biological meanings of ESS and CSS, readers are referred to [8, 9]. Here in this paper, the abbreviation CSS is used to denote a convergence stable strategy, but in some works it denotes a continuously stable strategy, which is by definition a convergence stable ESS. For convenience of associating the notions of ESS and CSS with the stability/instability, we adopt the definitions of ESS and CSS used by De Leenheer *et al.* in [7] for a setting without dispersal as below.

**Definition 3.3.1 (Definition 3.1 in [7])** *The anti-predation strategy  $\alpha^* \in [0, \infty)$  is an ESS if the boundary equilibrium  $(u^*(\alpha^*, v), 0)$  of system (3.10) is locally asymptotically stable for all  $\alpha_w \neq \alpha^*$  in some neighbourhood of  $\alpha^*$ .*

**Definition 3.3.2 (Definition 3.2 in [7])** *The anti-predation strategy  $\alpha^* \in [0, \infty)$  is a CSS if there is a neighbourhood  $N$  of  $\alpha^*$  such that the boundary equilibrium  $(u^*(\alpha_u, v), 0)$  of system (3.10) is locally asymptotically stable for all  $\alpha_u, \alpha_w \in N$  that satisfy  $\alpha_w < \alpha_u < \alpha^*$  or  $\alpha_w > \alpha_u > \alpha^*$  but is not locally asymptotically stable when  $\alpha_u < \alpha_w < \alpha^*$  or  $\alpha_u > \alpha_w > \alpha^*$ .*

To proceed further to explore the possible ESS and CSS, we choose some particular forms for the functions  $b(\alpha, v)$  and  $c(\alpha, v)$  as below:

$$b(\alpha, v) = b_0 e^{-\tilde{s}\alpha v}; \quad c(\alpha, v) = c_0 e^{-\tilde{p}\alpha v}. \quad (3.14)$$

Absorbing the positive constant  $v$  by letting  $s = \tilde{s}v$  and  $p = \tilde{p}v$ , the fitness function  $F(\alpha, v)$  is a single variable function,

$$F(\alpha, v) = F(\alpha) = b_0 e^{-s\alpha} - d - c_0 v e^{-p\alpha}. \quad (3.15)$$

Analysis on  $F(\alpha)$  distinguishes two cases: (i)  $p > s$ ; and (ii)  $p < s$ , with their respective consequences summarized below.

(i) Assume  $p/s > 1$ , then

(i)-1 if  $\frac{p}{s} < \frac{b_0}{c_0v}$ , then  $F'(\alpha) < 0$  for all  $\alpha > 0$  and there is no critical point for  $F(\alpha)$ ;

(i)-2 if  $\frac{p}{s} > \frac{b_0}{c_0v}$ , then  $F(\alpha)$  has a unique critical point  $\alpha^* > 0$  at which  $F(\alpha)$  attains a maximum;

(ii) Assume  $p/s < 1$ , then

(ii)-1 if  $\frac{p}{s} < \frac{b_0}{c_0v}$ , then  $F(\alpha)$  has a unique critical point  $\alpha^* > 0$  at which  $F(\alpha)$  attains a minimum;

(ii)-2 if  $\frac{p}{s} > \frac{b_0}{c_0v}$ , then  $F'(\alpha) > 0$  for all  $\alpha > 0$  (hence,  $F(0) < F(\alpha) < F(\infty) = -d < 0$  for all  $\alpha > 0$ , which should be excluded).

From the above, we can see that only (i)-2 (i.e.,  $p/s > \max\{b_0/(c_0v), 1\}$ ) offers the scenario of local interior value  $\alpha^*$  given by

$$\alpha^* = \frac{1}{p-s} \ln\left(\frac{pc_0v}{sb_0}\right) \quad (3.16)$$

at which the fitness function  $F(\alpha)$  attains its global maximum. By the definition of ESS and CSS, it is easy to see that such strategy  $\alpha^*$  is an ESS which is convergence stable. One can also check that both conditions (3.12) and (3.13) are satisfied. Lemma 3.3.1 implies that the persistence of prey's population requires  $F(\alpha)$  to be positive. If  $F(0) = b_0 - d - c_0v > 0$ , then the maximum  $F(\alpha^*) > 0$ ; and even if  $F(0) = b_0 - d - c_0v < 0$  meaning that the prey will go to extinction without any anti-predation response, it is possible to have  $F(\alpha^*) > 0$  which shows that an anti-predation response can help the prey survive. See the figures in Figure 3.1(a) and 3.1(b) for a demonstration.

We can interpret the above mathematical results from biological point of view. Note that the ratio  $p/s$  measures the relative effect of the anti-predation response on surviving the predation (benefit) as opposed to that on reducing the reproduction (cost). Thus, when  $p/s$  is small (large  $s$  and small  $p$ ), the effect of reducing the predation is not as significant as the effect of reducing

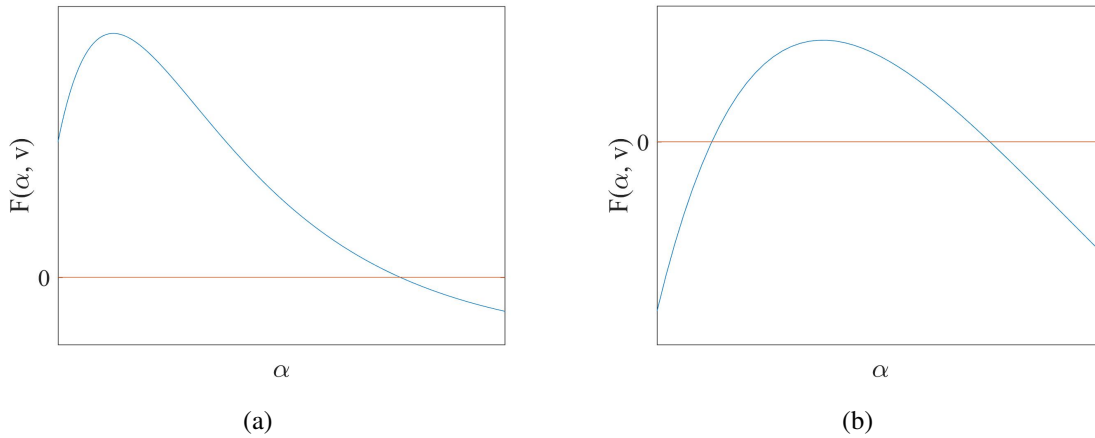


Figure 3.1: Function  $F(\alpha)$  has a global maximum if and only if  $p/s > \max\{b_0/(c_0v), 1\}$ : (a)  $F(0) > 0$ ; (b)  $F(0) < 0$  but  $F(\alpha^*) > 0$

the reproduction, and hence, it seems to be preferable for the prey to take less response; this corresponds to the cases (i)-1 and (ii)-1 in which the maximum of  $F(\alpha)$  is attained at  $\alpha = 0$ . When  $p/s$  is sufficiently large (i.e.,  $p/s > \max\{b_0/(c_0v), 1\}$ ), the effect of reducing the predation is more significant than the effect of reducing the reproduction, and hence, a positive and relatively larger response level should be favoured, and this corresponds to the cases (i)-2 and (ii)-2. Moreover, when the population grows to the steady state  $F(\alpha^*)/a$  after the prey strain with the ESS/CSS  $\alpha^*$  having occupied the patch, it is also the maximal population size the species can reach.

Apparently, the value  $b_0/(c_0v)$  plays an important role in determining the population dynamics of prey, which is the ratio of per capita birth rate to per capita death rate due to predation without anti-predation response. When the ratio is smaller than one, the existence of positive convergence stable ESS only requires  $p/s > 1$ . When the ratio is greater than one, the condition becomes  $p/s > b_0/(c_0v) > 1$ . If a species population is able to produce more offspring (meaning larger  $b_0$ ), anti-predation behaviours are less likely to be developed. Moreover, the ratio  $b_0/(c_0v)$  depends on the population of predator, while  $p/s = (\tilde{p}v)/(\tilde{s}v) = \tilde{p}/\tilde{s}$  is only related to the prey species. When the number of predators is sufficiently small, indicating that the existence of predators does not threaten the survival of prey, such fear will not change the behaviours of prey. If there are too many predators meaning that predation risk is relatively high, the prey species will be driven/forced to develop some anti-predation strategies.

In this model, co-existence is impossible since  $\theta(\alpha_w, \alpha_u)$  and  $\theta(\alpha_u, \alpha_w)$  can not be positive simultaneously. A successful invasion of mutant prey always leads to the extinction of resident prey and the mutant prey becomes new resident prey. This means that trait substitution occurs. In reality, evolution dynamics is typically much slower than the population dynamics. Thus, we further assume that the duration of the inter-strain (or inter-species) competitive interaction is much shorter than the mutation process, so that the population has approached a steady state before the appearance of new mutant. Repeating the trait substitution generates a sequence of trait values which converges to the ESS/CSS. Biologically speaking, an optimal anti-predation strategy is developed by mutation and natural selection.

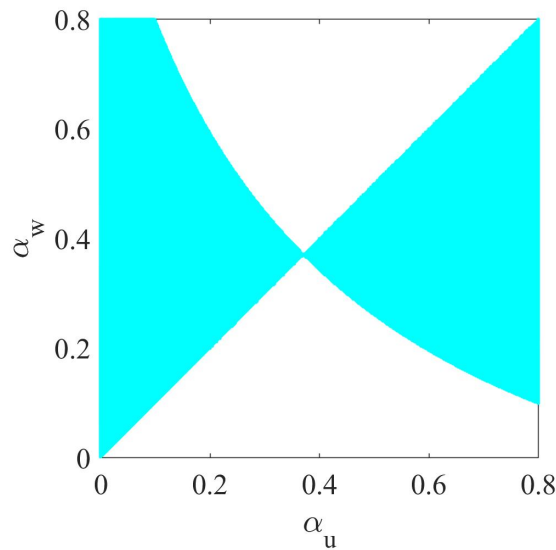


Figure 3.2: Pairwise invasibility plot for model (3.10) with trait  $\alpha$ . Function  $F(\alpha, v)$  is in the form of (3.15) and  $b_0 = 5$ ,  $d = 0.5$ ,  $c_0v = 3.5$ ,  $s = 1$ ,  $p = 3$ . The mutant can invade in the blue regions but the invader fails in the white regions. The intersection of two curves gives a convergence stable ESS  $\alpha^* = 0.37$ .

The information concerning the adaptive dynamics of anti-predation strategy  $\alpha$  can be illustrated graphically in the pairwise invasibility plot (PIP). See Figure 3.2 for an example when a positive convergence stable ESS exists with the chosen parameter values satisfying  $p/s > b_0/(c_0v) > 1$ . The  $\alpha_u - \alpha_w$  plane is divided by the curves where  $\theta(\alpha_u, \alpha_w) = 0$ . In the blue regions  $\theta(\alpha_u, \alpha_w)$  is positive, corresponding to successful invasion by mutant, whereas in the white regions the invader fails since  $\theta(\alpha_u, \alpha_w)$  is negative. The point where two curves intersect is consistent with the value given by (3.16). Such a strategy is both an ESS and a CSS.

### 3.4 Model analysis: with dispersal

In this section, we consider the full model (3.8) with dispersals which are also affected by fear.

#### 3.4.1 Equilibria and stability

Firstly, we consider the trait  $\alpha$  as a constant. System (3.8) admits only two equilibria:  $E_0 = (0, 0)$  and  $E_+ = (u_1^*, u_2^*)$ , with  $u_1^*$  and  $u_2^*$  satisfying:

$$\begin{aligned} u_1^* &= \frac{au_2^*}{m(\alpha, v_1)} \left[ u_2^* - \frac{F_2(\alpha, v_2) - m(\alpha, v_2)}{a} \right] =: \Pi_1(u_2^*), \\ u_2^* &= \frac{au_1^*}{m(\alpha, v_2)} \left[ u_1^* - \frac{F_1(\alpha, v_1) - m(\alpha, v_1)}{a} \right] =: \Pi_2(u_1^*). \end{aligned} \quad (3.17)$$

The first quadratic function  $\Pi_1$  has two roots

$$u_2 = 0 \quad \text{and} \quad u_2 = \frac{F_2(\alpha, v_2) - m(\alpha, v_2)}{a} =: \hat{u}_2,$$

and the second function  $\Pi_2$  also has two roots

$$u_1 = 0 \quad \text{and} \quad u_1 = \frac{F_1(\alpha, v_1) - m(\alpha, v_1)}{a} =: \hat{u}_1.$$

These two parabolas intersect at the origin. Moreover, when  $\hat{u}_1 \geq 0$  or  $\hat{u}_2 \geq 0$ , the two curves always have a unique intersection in the interior of the first quadrant. When  $\hat{u}_1 < 0$  and  $\hat{u}_2 < 0$ , there is an interior intersection in the first quadrant if and only if the slopes of two curves at the origin satisfy  $\Pi_1'(0) \cdot \Pi_2'(0) < 1$ , which is equivalent to  $F_1(\alpha, v_1)F_2(\alpha, v_2) < F_1(\alpha, v_1)m(\alpha, v_2) + F_2(\alpha, v_2)m(\alpha, v_1)$ . Hence, we have the following result on the existence of co-persistence equilibrium.

**Theorem 3.4.1** *The system (3.8) has a unique positive equilibrium if and only if one of the following conditions holds:*

(i)  $F_1(\alpha, v_1) \geq m(\alpha, v_1)$ ,

(ii)  $F_2(\alpha, v_2) \geq m(\alpha, v_2)$ ,

(iii)  $F_1(\alpha, v_1) < m(\alpha, v_1)$ ,  $F_2(\alpha, v_2) < m(\alpha, v_2)$ , and  $F_1(\alpha, v_1)F_2(\alpha, v_2) < F_1(\alpha, v_1)m(\alpha, v_2) + F_2(\alpha, v_2)m(\alpha, v_1)$ .

The Jacobian matrix for system (3.8) is given by

$$\mathbf{J} = \begin{pmatrix} F_1(\alpha, v_1) - m(\alpha, v_1) - 2au_1 & m(\alpha, v_2) \\ m(\alpha, v_1) & F_2(\alpha, v_2) - m(\alpha, v_2) - 2av_2 \end{pmatrix}. \quad (3.18)$$

At the trivial equilibrium  $E_0$ , it becomes

$$\mathbf{J}(E_0) = \begin{pmatrix} F_1(\alpha, v_1) - m(\alpha, v_1) & m(\alpha, v_2) \\ m(\alpha, v_1) & F_2(\alpha, v_2) - m(\alpha, v_2) \end{pmatrix}. \quad (3.19)$$

Thus, the trivial equilibrium  $E_0$  is locally asymptotically stable if

$$\begin{aligned} \text{tr}(\mathbf{J}(E_0)) &= F_1(\alpha, v_1) - m(\alpha, v_1) + F_2(\alpha, v_2) - m(\alpha, v_2) < 0, \\ \det(\mathbf{J}(E_0)) &= F_1(\alpha, v_1)F_2(\alpha, v_2) - F_1(\alpha, v_1)m(\alpha, v_2) - F_2(\alpha, v_2)m(\alpha, v_1) > 0. \end{aligned} \quad (3.20)$$

As is shown graphically in Figure 3.3, this condition represents the region under the solid curve defined by the equation

$$F_1(\alpha, v_1)F_2(\alpha, v_2) = F_1(\alpha, v_1)m(\alpha, v_2) + F_2(\alpha, v_2)m(\alpha, v_1), \quad (3.21)$$

or written in the explicit form,

$$F_2(\alpha, v_2) = \frac{m(\alpha, v_1)m(\alpha, v_2)}{F_1(\alpha, v_1) - m(\alpha, v_1)} + m(\alpha, v_2), \quad (3.22)$$

for  $F_1(\alpha, v_1) < m(\alpha, v_1)$  on the  $F_1$ - $F_2$  plane. It is not difficult to observe that conditions in (3.20) is precisely the conditions that exclude the existence of a positive equilibrium.

**Remark** Notice that the tangent line of the curve at  $(F_1(\alpha, v_1), F_2(\alpha, v_2)) = (0, 0)$  is  $F_1(\alpha, v_1)m(\alpha, v_2) + F_2(\alpha, v_2)m(\alpha, v_1) = 0$ , shown as the thick solid straight line in Figure 3.3. Hence, the condition

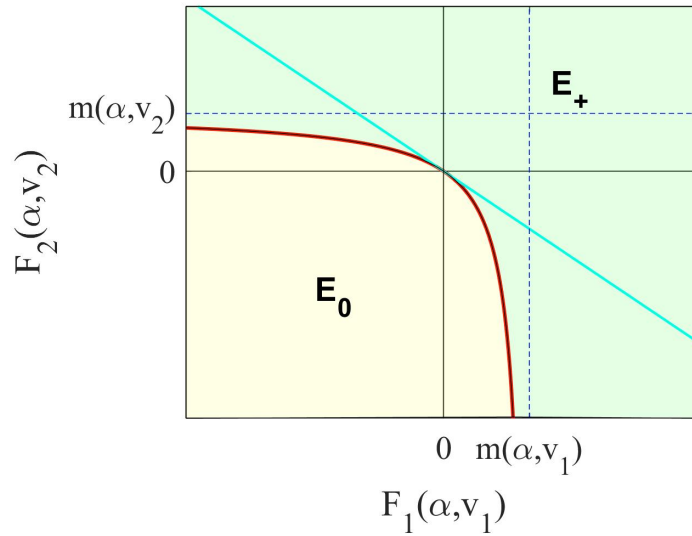


Figure 3.3: The solid curve is implicitly defined by  $F_1(\alpha, v_1)F_2(\alpha, v_2) = F_1(\alpha, v_1)m(\alpha, v_2) + F_2(\alpha, v_2)m(\alpha, v_1)$  for  $F_1(\alpha, v_1) < m(\alpha, v_1)$ , below which  $E_0$  is asymptotically stable. The region above this curve is where the trivial equilibrium  $E_0$  is unstable which is the same region for  $(F_1, F_2)$  where the positive equilibrium  $E_+$  exists.

in Theorem 3.4.1 for the existence of positive equilibrium can be equivalently stated as

$$\begin{aligned} \text{either (A)} \quad & F_1(\alpha, v_1)m(\alpha, v_2) + F_2(\alpha, v_2)m(\alpha, v_1) \geq 0, \\ \text{or (B)} \quad & 0 > F_1(\alpha, v_1)m(\alpha, v_2) + F_2(\alpha, v_2)m(\alpha, v_1) > F_1(\alpha, v_1)F_2(\alpha, v_2), \end{aligned} \tag{3.23}$$

The advantage of these equivalent statements is that they are expressed in terms of the weighted total fitness  $F_1(\alpha, v_1)m(\alpha, v_2) + F_2(\alpha, v_2)m(\alpha, v_1)$ , which is the *total of the two local fitness functions mediated by the dispersal strengths*. Such a weighted total obviously combines the local fitness and the dispersal effect, and is thus a biologically meaningful measure for the total fitness of the prey on the two patches.

As for the positive equilibrium  $E_+ = (u_1^*, u_2^*)$ , recall that  $u_1^*$  and  $u_2^*$  satisfy (3.17) which can be written as

$$\begin{aligned} \frac{m(\alpha, v_1)u_1^*}{u_2^*} &= au_2^* - (F_2(\alpha, v_2) - m(\alpha, v_2)), \\ \frac{m(\alpha, v_2)u_2^*}{u_1^*} &= au_1^* - (F_1(\alpha, v_1) - m(\alpha, v_1)). \end{aligned}$$

Using these to rewrite the diagonal entries of  $\mathbf{J}(E_+)$ , we have

$$\mathbf{J}(E_+) = \begin{pmatrix} -\frac{m(\alpha, v_2)u_2^*}{u_1^*} - au_1^* & m(\alpha, v_2) \\ m(\alpha, v_1) & -\frac{m(\alpha, v_1)u_1^*}{u_2^*} - au_2^* \end{pmatrix} \quad (3.24)$$

with

$$\begin{aligned} \text{tr}(\mathbf{J}(E_+)) &= -\frac{m(\alpha, v_2)u_2^*}{u_1^*} - au_1^* - \frac{m(\alpha, v_1)u_1^*}{u_2^*} - au_2^* < 0, \\ \det(\mathbf{J}(E_+)) &= \frac{am(\alpha, v_2)(u_2^*)^2}{u_1^*} + \frac{am(\alpha, v_1)(u_1^*)^2}{u_2^*} + a^2u_1^*u_2^* > 0. \end{aligned}$$

Hence, the positive equilibrium is always locally asymptotically stable as long as it exists.

Indeed, we can prove that for this model system (3.8), the local asymptotic stability of an equilibrium also implies the global asymptotic stability. To this end, we just need to show that there is no periodic solution of system (3.8) by using the Dulac criterion. Set  $B(u_1, u_2) = 1/(u_1u_2)$ , then we have

$$\begin{aligned} G_1(u_1, u_2) &:= B(u_1, u_2) \frac{du_1}{dt} = \frac{F_1(\alpha, v_1) - m(\alpha, v_1) - au_1}{u_2} + \frac{m(\alpha, v_2)}{u_1}, \\ G_2(u_1, u_2) &:= B(u_1, u_2) \frac{du_2}{dt} = \frac{F_2(\alpha, v_2) - m(\alpha, v_2) - au_2}{u_1} + \frac{m(\alpha, v_1)}{u_2}. \end{aligned}$$

Since

$$\frac{\partial G_1}{\partial u_1} + \frac{\partial G_2}{\partial u_2} = -\frac{a}{u_2} - \frac{m(\alpha, v_2)}{u_1^2} - \frac{a}{u_1} - \frac{m(\alpha, v_1)}{u_2^2}$$

is not identically zero and does not change sign in  $\mathbb{R}_+^2$ , there is no periodic orbit. Hence, by the Poincaré-Bendixson theory of planar dynamical systems, a locally asymptotically stable equilibrium is also globally asymptotically stable.

Summarizing the above analysis, we have obtained the following global threshold result.

**Theorem 3.4.2** *The following statements hold:*

- (i) *If condition (3.20) holds, then for any initial point  $[u_1(0), u_2(0)] \in \mathbb{R}_+^2$ , the corresponding solution of (3.8) satisfies  $\lim_{t \rightarrow \infty} u_1(t) = \lim_{t \rightarrow \infty} u_2(t) = 0$ .*
- (ii) *If condition (3.20) is violated (i.e., (3.23) holds), then the trivial equilibrium becomes*

*unstable, and there is a unique positive equilibrium  $E_+$  (representing the prey's co-persistence on both patches) which is globally asymptotically stable.*

Recall that in the absence of dispersal, the species survives in *both patches* if and only if  $F_1(\alpha, v_1) > 0$  and  $F_2(\alpha, v_2) > 0$ . However, with the dispersal, the range of  $F_1(\alpha, v_1)$  and  $F_2(\alpha, v_2)$  for co-persistence of the species in both patches has obviously been *enlarged*, as is shown in Figure 3.3. Particularly, co-existence in both patches is also possible even if *one of the fitness functions is negative*, and this clearly and explicitly shows the positive role of dispersal on maintaining the population persistence.

Although dispersal can enhance the chance to survive, it does not necessarily mean that higher dispersal rate is always better. When the dispersal rates are greater than the corresponding linear net growth rates (i.e., when  $m(\alpha, v_i) > F_i(\alpha, v_i)$  for  $i = 1, 2$ ), there are ranges for parameters within which the species will be driven to extinction. See the region under the solid curve and located in the two stripes  $F_1(\alpha, v_1) \in (0, m(\alpha, v_1))$  and  $F_2(\alpha, v_2) \in (0, m(\alpha, v_2))$  in the  $F_1$ - $F_2$  plane as shown in Figure 3.3. Or to be more explicit, we consider a special case where dispersal rate is independent of the populations of predator, denoted as  $m(\alpha)$ . Then the conditions in (3.23) for the persistence of prey on both patches are simplified to

$$\begin{aligned} \text{either (A*) } & F_1(\alpha, v_1) + F_2(\alpha, v_2) \geq 0, \\ \text{or (B*) } & F_1(\alpha, v_1) + F_2(\alpha, v_2) < 0 \text{ and } 0 < m(\alpha) < \frac{F_1(\alpha, v_1)F_2(\alpha, v_2)}{F_1(\alpha, v_1) + F_2(\alpha, v_2)}. \end{aligned} \quad (3.25)$$

In Case (B\*), there is an explicit upper bound for the dispersal strength  $m(\alpha)$ . Therefore, in such a special case, when the total fitness is positive, the species always persists on both patches even if one local fitness is negative (patch quality is very poor), as long as there is dispersal ( $m(\alpha) > 0$ ) regardless of how small and how large it is. However, if the total fitness is negative, the species will eventually die out on both patches if the dispersal rate exceeds the threshold given in (3.25), but will persist if the prey maintains a mild dispersal rate.

Combining the above results with the dependence of  $F_i(\alpha, v_i)$  and  $m(\alpha, v_i)$  on  $\alpha$  for  $i = 1, 2$ , one then can explore the effect of the anti-predation response level  $\alpha$  on the prey's population

dynamics. To illustrate possible outcomes, we choose the following particular functions,

$$F_i(\alpha, v_i) = b_{0i}e^{-\tilde{s}\alpha v_i} - d_i - c_0 v_i e^{-\tilde{p}\alpha v_i}, \quad i = 1, 2, \quad (3.26)$$

$$m(\alpha, v_i) = m_0 e^{-\tilde{q}\alpha v_i}, \quad i = 1, 2, \quad (3.27)$$

which satisfy all those assumptions proposed in Section 3.2. Figure 3.4(a) shows the variation of curve defined by (3.22) with respect to anti-predation strategy  $\alpha$ . Recall that this curve separates the stability region of the trivial equilibrium  $E_0$  from the region where the positive equilibrium  $E_+$  is globally asymptotically stable. When  $\alpha$  increases, the stability region of the positive equilibrium is enlarged, and the pair of values  $[F_1(\alpha, v_1), F_2(\alpha, v_2)]$  moves along the red curve from the stability region of  $E_+$  into the stability region of  $E_0$ . Consequently, the population on two patches converges to a positive steady state for small  $\alpha$ , but prey on both patches go to extinction when  $\alpha$  exceeds some critical point. The stable population sizes are plotted in Figure 3.4(b), marked with the strategy values when populations reach their maxima. Enhancing anti-predation response level is beneficial to population size when  $\alpha$  is small, then it becomes detrimental. Such effect is not synchronous on the two patches.

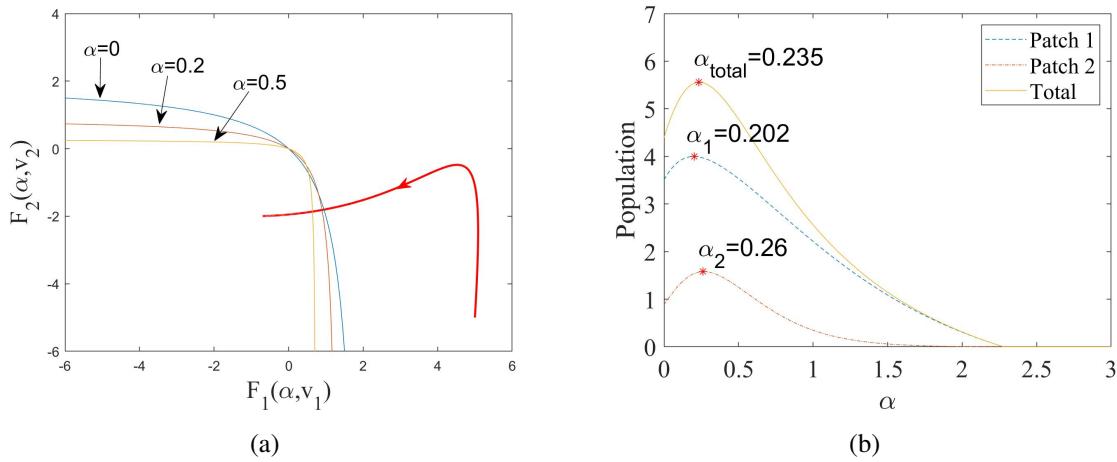


Figure 3.4: The effect of anti-predation response level  $\alpha$  on the prey's population dynamics. (a) The curves defined by (3.22) with different values of  $\alpha$ , which separate the stability region of the positive equilibrium  $E_+$  from that of the trivial equilibrium  $E_0$ . The red curve with arrow represents the trajectory of  $[F_1(\alpha, v_1), F_2(\alpha, v_2)]$  when  $\alpha$  increases from 0 to 3.5. (b) The dependence of stable population sizes on  $\alpha$ , marked with the strategy values at which the populations are maximized. Other parameter values are:  $b_{01} = 10$ ,  $b_{02} = 5$ ,  $d_1 = 1$ ,  $d_2 = 2$ ,  $c_0 = 0.04$ ,  $v_1 = 100$ ,  $v_2 = 200$ ,  $\tilde{s} = 0.01$ ,  $\tilde{p} = 0.03$ ,  $m_0 = 2$ ,  $\tilde{q} = 0.02$ , and  $a = 1$ .

### 3.4.2 Evolution of anti-predation strategy

In this subsection, we move on to study the evolution of anti-predation strategy  $\alpha$ .

#### Invasion analysis

Due to the presence of dispersal between the patches, adopting the same invasibility analysis as in Section 3 leads to a four-dimensional ODE system,

$$\begin{cases} \frac{du_1}{dt} = u_1 [F_1(\alpha_u, v_1) - a(u_1 + w_1)] + m(\alpha_u, v_2)u_2 - m(\alpha_u, v_1)u_1 \\ \frac{du_2}{dt} = u_2 [F_2(\alpha_u, v_2) - a(u_2 + w_2)] + m(\alpha_u, v_1)u_1 - m(\alpha_u, v_2)u_2 \\ \frac{dw_1}{dt} = w_1 [F_1(\alpha_w, v_1) - a(u_1 + w_1)] + m(\alpha_w, v_2)w_2 - m(\alpha_w, v_1)w_1, \\ \frac{dw_2}{dt} = w_2 [F_2(\alpha_w, v_2) - a(u_2 + w_2)] + m(\alpha_w, v_1)w_1 - m(\alpha_w, v_2)w_2. \end{cases} \quad (3.28)$$

The ability of the mutant to invade can be determined from the eigenvalues of the Jacobian matrix of the augmented system at boundary equilibrium  $(u_1^*, u_2^*, 0, 0)$  with  $u_1^*$  and  $u_2^*$  being solved from (3.17):

$$\mathbf{J} = \begin{pmatrix} \mathbf{J}_{11} & \mathbf{J}_{12} \\ \mathbf{0} & \mathbf{J}_{22} \end{pmatrix} \quad (3.29)$$

This is an upper triangular matrix, so the eigenvalues are simply those of the two  $2 \times 2$  block-diagonal elements  $\mathbf{J}_{11}$  and  $\mathbf{J}_{22}$ . The matrix  $\mathbf{J}_{11}$  is identical to the Jacobian matrix  $\mathbf{J}(E_+)$  given by (3.24). Since we are only interested in resident prey populations that are at a stable positive equilibrium, the two eigenvalues of  $\mathbf{J}_{11}$  must have negative real parts. Thus, the local stability fully depends on the dominant eigenvalue of matrix  $\mathbf{J}_{22} = \begin{pmatrix} A & B \\ C & D \end{pmatrix}$ ,

$$\lambda = \frac{1}{2} \left( A + D + \sqrt{(A - D)^2 + 4BC} \right), \quad (3.30)$$

where

$$\begin{aligned} A &= F_1(\alpha_w, v_1) - m(\alpha_w, v_1) - au_1^*, & B &= m(\alpha_w, v_2), \\ C &= m(\alpha_w, v_1), & D &= F_2(\alpha_w, v_2) - m(\alpha_w, v_2) - au_2^*. \end{aligned}$$

A mutant prey with strategy  $\alpha_w$  can invade the resident population with strategy  $\alpha_u$  provided that  $\lambda > 0$ . Hence, we choose  $\lambda$  as the invasion exponent because it directly determines whether the mutant strain, when being rare, will grow or decay (invade or not). An evolutionary singular strategy  $\alpha_u = \alpha^*$  is a solution to the equation

$$\left. \frac{\partial \lambda(\alpha_u, \alpha_w)}{\partial \alpha_w} \right|_{\alpha_w = \alpha_u} = 0. \quad (3.31)$$

This strategy is an ESS if

$$\left. \frac{\partial^2 \lambda(\alpha_u, \alpha_w)}{\partial \alpha_w^2} \right|_{\alpha_w = \alpha_u = \alpha^*} < 0; \quad (3.32)$$

and  $\alpha^*$  is convergence stable if

$$\left. \frac{\partial^2 \lambda(\alpha_u, \alpha_w)}{\partial \alpha_u^2} \right|_{\alpha_w = \alpha_u = \alpha^*} > \left. \frac{\partial^2 \lambda(\alpha_u, \alpha_w)}{\partial \alpha_w^2} \right|_{\alpha_w = \alpha_u = \alpha^*}. \quad (3.33)$$

See [8] for details. It is not easy to explore further explicitly by applying these criteria. This is because of the complexity of  $\lambda(\alpha_u, \alpha_w)$  — it depends on  $u_1^*(\alpha_u)$  and  $u_2^*(\alpha_u)$  which are determined by but cannot be explicitly solved from (3.17).

However, we can still gain some information about the adaptive dynamics of anti-predation strategy  $\alpha$  by sketching the pairwise invasibility plot numerically. An example is illustrated in Figure 3.5 using the particular functions  $F_i(\alpha, v_i)$  and  $m(\alpha, v_i)$  given by (3.26) and (3.27) and the same parameter values as in Figure 3.4. The  $\alpha_u - \alpha_w$  plane is partitioned according to the signs of invasion exponent  $\lambda$  defined by (3.30). We can easily tell that the singular point at which the two curves of neutrality intersect is an ESS. Even though the condition for mutual invasibility ([8]),

$$\left. \frac{\partial^2 \lambda(\alpha_u, \alpha_w)}{\partial \alpha_u^2} \right|_{\alpha_w = \alpha_u = \alpha^*} > - \left. \frac{\partial^2 \lambda(\alpha_u, \alpha_w)}{\partial \alpha_w^2} \right|_{\alpha_w = \alpha_u = \alpha^*}, \quad (3.34)$$

is hard to check, it seems to be impossible since the plot in Figure 3.5 is symmetric about the line  $\alpha_w = \alpha_u$ . One may expect the dynamics to be monomorphic.

We have seen there are some shortcomings of invasibility analysis. This motivates us to employ an alternative method, that is, considering an augmented system with the anti-predation response level  $\alpha$  being another variable. We explore this method in the next subsection.

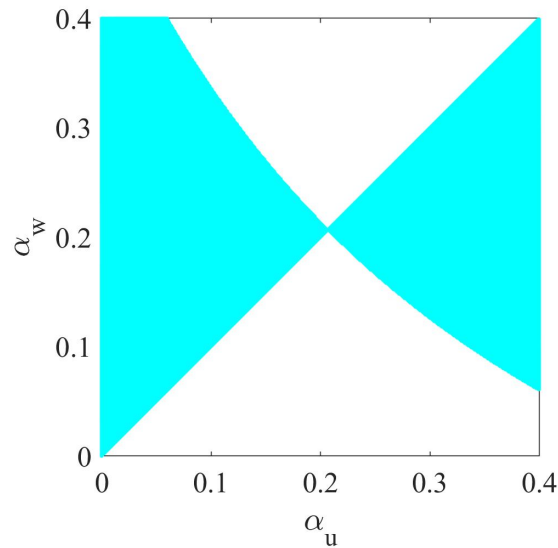


Figure 3.5: Pairwise invasibility plot for model (3.28) with trait  $\alpha$ . The blue areas correspond to  $\lambda > 0$  when the mutant can invade, and in the white areas  $\lambda < 0$  implying that the mutant dies out.

### Adaptive dynamics without time scale separation

Assume that the prey has complete knowledge about the surrounding environment and always adapts its behaviour to increase fitness. Thus the evolution of  $\alpha = \alpha(t)$  with respect to time should be toward the direction of increasing the fitness of the prey species. This can be reflected by assuming that the relative change rate of  $\alpha$  is proportional to the gradient of the fitness with respect to  $\alpha$ , that is,

$$\frac{d\alpha}{dt} = \sigma \alpha \frac{\partial \Phi}{\partial \alpha} \quad (3.35)$$

where  $\Phi$  accounts for some measure of fitness for the prey and  $\sigma > 0$  represents the speed of evolution. It is easy to see that the solution to (3.35) remains positive, given any positive initial value. We point out that here our trait variable  $\alpha$  is within  $[0, \infty)$  in comparison to some previous used replicator equations of the form  $\alpha'(t) = \sigma \alpha(1 - \alpha) \frac{\partial \Phi}{\partial \alpha}$  where  $\alpha$  is confined to  $[0, 1]$ . See, e.g. [23, 25] and some references therein.

To gain some motivation for the fitness function  $\Phi$ , let us revisit the case without dispersal discussed in Section 3, using this alternative idea of evolving strategy  $\alpha$  (rather than comparing two different constant values for  $\alpha$  as done in Section 3). Then, instead of the model (3.10)

that describes the competition between resident prey and mutants with different anti-predation response levels, we may consider following new system consisting of equation (3.9) for the population and equation (3.35) for strategy:

$$\begin{cases} \frac{du}{dt} = u [F(\alpha, v) - au], \\ \frac{d\alpha}{dt} = \sigma\alpha \frac{\partial \Phi}{\partial \alpha}, \end{cases} \quad (3.36)$$

where  $\sigma$  should be relatively small since speed of evolution is much slower than the demographic process. As discussed in Section, 3,  $F(\alpha, v)$  is a measure of fitness for the species and hence, is a natural candidate for  $\Phi$ . With this choice of  $\Phi = F(\alpha, v)$ , the second equation in (3.36) is decoupled from the first equation, and hence can be dealt with independently. Besides  $\alpha = 0$ , all singular points of  $\Phi$  such that  $\frac{\partial \Phi}{\partial \alpha} = 0$  are fixed points of the strategy equation. When  $\alpha(t)$  starting from any initial value eventually converges to one fixed point  $\alpha^*$ , the population approaches to its steady state accordingly based on the sign of  $F(\alpha^*, v)$ . If  $F(\alpha, v)$  is in the form of (3.15) for  $p/s > \max\{b_0/(c_0v), 1\}$  which is a one-hump function, then  $\alpha^*$  is the point at which  $F(\alpha, v)$  attains its maximum. This result is consistent with what we obtained in Section 3.

Now we combine the strategy equation (3.35) with the two-patch population model (3.8) with dispersals. The first and most important thing is to determine what function is appropriate to be the fitness  $\Phi$ . From the discussion in Remark 4.1, we have seen that total fitness mediated by the dispersals, that is  $F_1(\alpha, v_1)m(\alpha, v_2) + F_2(\alpha, v_2)m(\alpha, v_1)$ , is of both mathematical and biological significance. Thus, similar to the choice of  $\Phi = F(\alpha, v)$  for model (3.36), we may use the above quantity as a measure of fitness for the prey in two-patch environment. Then, we are led to consider the system given below:

$$\begin{cases} \frac{du_1}{dt} = u_1 [F_1(\alpha, v_1) - au_1] + m(\alpha, v_2)u_2 - m(\alpha, v_1)u_1, \\ \frac{du_2}{dt} = u_2 [F_2(\alpha, v_2) - au_2] + m(\alpha, v_1)u_1 - m(\alpha, v_2)u_2, \\ \frac{d\alpha}{dt} = \sigma\alpha \frac{\partial}{\partial \alpha} [F_1(\alpha, v_1)m(\alpha, v_2) + F_2(\alpha, v_2)m(\alpha, v_1)] \end{cases} \quad (3.37)$$

The strategy equation is also decoupled from the population equations, and its dynamics

depends on the choices of  $F_i(\alpha, v_i)$  and  $m(\alpha, v_i)$ ,  $i = 1, 2$ . Without specifying these functions, one can hardly obtain any conclusive results. Thus, in order to illustrate how the anti-predation response level  $\alpha$  evolves along time, we use the functions (3.26) and (3.27) again and conduct some numeric investigations with the same parameter values as those used in Section 4.1 and  $\sigma = 0.01$ .

If the two patches are *not* connected by dispersals, the prey evolves separately on each patch according to system (3.36) with different parameter values. The fitness functions  $F_1(\alpha, v_1)$  and  $F_2(\alpha, v_2)$  are of the same form as (3.15), and hence, their behaviours are also as demonstrated in Figure 3.1 with the given parameter values satisfying  $\tilde{p}/\tilde{s} > \max\{b_{0i}/(c_0v_i), 1\}$  for  $i = 1, 2$ . Their maximal values are reached at different critical points  $\alpha_1^*$  and  $\alpha_2^*$ . As is shown in Figure 3.6, the anti-predation response level  $\alpha$  in each patch evolves toward the corresponding critical points  $\alpha_1^*$  and  $\alpha_2^*$ .

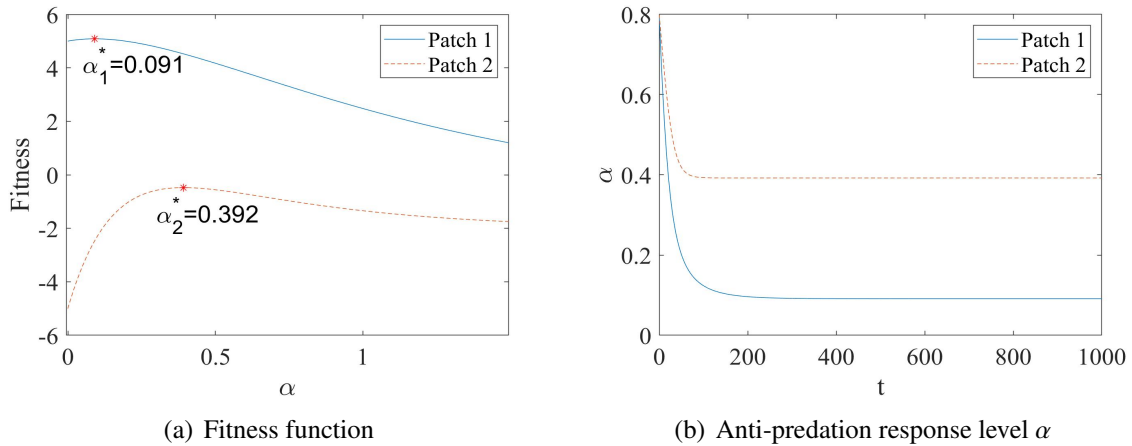


Figure 3.6: The fitness function  $F_1(\alpha, v_1)$  and  $F_2(\alpha, v_2)$  and convergent dynamics of anti-predation response level  $\alpha(t)$  on the two patches which are *not connected* by dispersals.

In the *presence of dispersals*, the weighted total fitness with the same parameter values also has a global maximum attained at point  $\alpha^{1*}$ , as plotted in Figure 3.7(a), which is in between of  $\alpha_1^*$  and  $\alpha_2^*$ . The convergence of  $\alpha(t)$  to  $\alpha^{1*}$  for some initial values near  $\alpha^{1*}$  is numerically demonstrated in Figure 3.7(b), indicating that  $\alpha^{1*}$  at least is a local attractor.

Besides the total fitness mediated by dispersals, there are other choices for the fitness function  $\Phi$ . In principle, any thing that captures that biological meaning and in the mean time, is mathematically tractable can be used to measure the fitness. For example, as was used in [26],

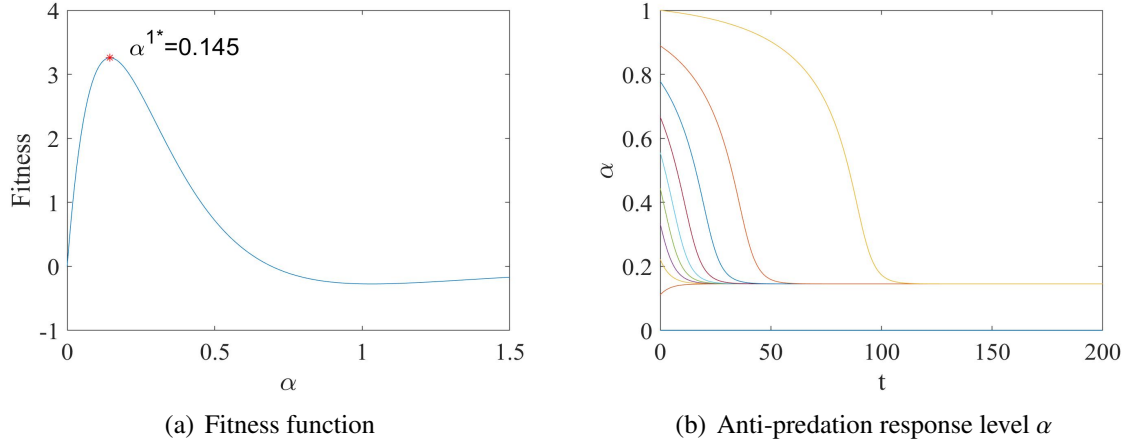


Figure 3.7: The fitness function is taken as the total fitness mediated by dispersals. The anti-predation response level  $\alpha(t)$  converges to the point that maximizes this fitness function.

the instant growth rate of the total population of the prey species,

$$\begin{aligned}\Phi &= \frac{du_1}{dt} + \frac{du_2}{dt} \\ &= u_1 [F_1(\alpha, v_1) - au_1] + u_2 [F_2(\alpha, v_2) - au_2].\end{aligned}\tag{3.38}$$

Accordingly, the equation governing the strategy's evolution becomes

$$\frac{d\alpha}{dt} = \sigma\alpha \left[ u_1 \frac{\partial F_1(\alpha, v_1)}{\partial \alpha} + u_2 \frac{\partial F_2(\alpha, v_2)}{\partial \alpha} \right].\tag{3.39}$$

Unlike in the above two examples, now we have a *coupled* system for the strategy and the populations. It becomes impossible to plot the fitness function since it also varies with time. But we can still explore the dynamics of  $\alpha(t)$  numerically. With the same function forms in (3.26) and (3.27) and the same values of the parameters involved, the adaptive dynamics of  $\alpha(t)$  are illustrated in Figure 3.8(b). We can see that the variable  $\alpha(t)$  beginning within the same range for initial values used in Figure 3.7 converges to a value  $\alpha^{2*}$  which is different from  $\alpha^{1*}$ . Additionally,  $\alpha^{2*}$  maximizes the limit fitness function when the populations reach steady state, as is shown in Figure 3.8(a). We also observe that the convergence of  $\alpha(t)$  is faster than that in previous example.

From the above numerical explorations, we have seen that for both choices of  $\Phi$ , the trait variable  $\alpha(t)$  demonstrates convergent dynamics. However, the convergence speed and the

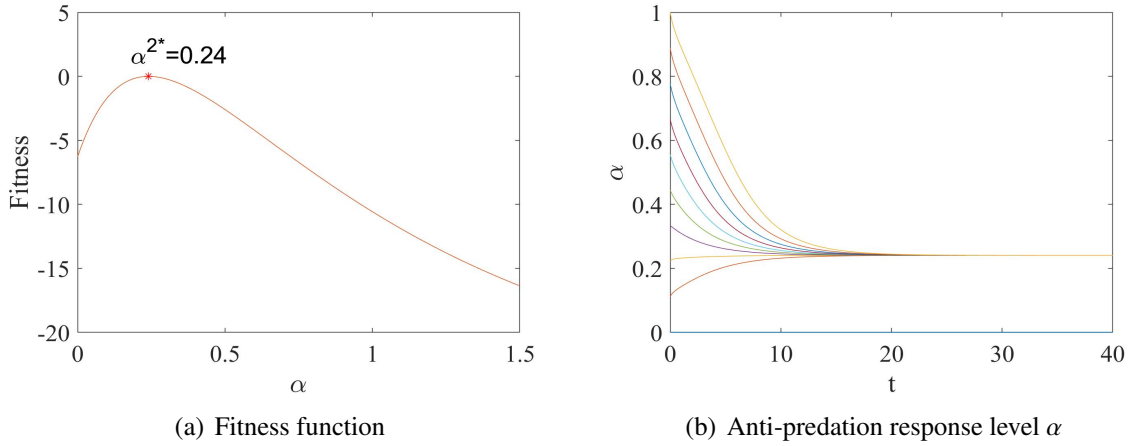


Figure 3.8: The fitness function is taken as the instant total growth rate of the prey on two patches given by (3.38) which also varies with time. The anti-predation response level  $\alpha(t)$  converges to a different value from that in Figure 3.7(b), which maximizes the limit fitness function when populations reach steady state as shown in the left graph.

destination values  $\alpha^{1*}$  and  $\alpha^{2*}$  can be different for different  $\Phi$ . This is because those fitness functions have different emphases and hence, may not be maximized uniformly. Moreover, none of the critical points matches the ESS obtained from the pairwise invasibility plot shown in Figure 3.5. We point out that the numerical results on the convergence of  $\alpha(t)$  to a critical value  $\alpha^{i*}$  demonstrated in Figure 3.7(b) and Figure 3.8(b) respectively does not depend on the initial populations.

We are also interested to the final populations of prey on both patches when optimal strategy  $\alpha^{i*}$  is reached. With the same parameter values used for Figures 3.6, 3.7 and 3.8, numerical results for the populations are displayed in Figure 3.9 which corresponds to the scenarios illustrated above: (a) no dispersals (Figure 3.6), (b) dispersal considered with total fitness mediated by dispersals (Figure 3.7), and (c) dispersal considered with fitness being the instant total growth rate (Figure 3.8). From the numerical results given in Figure 3.9, we see that when dispersals between the two patches are not allowed, the prey's population can only persist in patch 1 since  $F_1(\alpha_1^*, v_1) > 0$  and  $F_2(\alpha_2^*, v_2) < 0$ ; but if the individuals of prey are free to move between the two patches, the prey coexists on both patches with the population size in patch 1 being higher than that in patch 2. Moreover, in the presence of dispersal, the total population in the steady state is larger than that in the case without dispersals, no matter which fitness function is adopted. Comparing with the results obtained in Figure 3.4, we observe that none of the

optimal strategies maximizes the population of prey. Such a phenomenon that an optimal strategy does not necessarily maximize the total population was also observed in previous studies. For example, in Hastings [11], it was shown that the ESS dispersal strategy does not maximize the total population of the species on two patches; and in Lundberg [16], it was also observed that the maximal population deviates from the solution with an ESS migration probability.

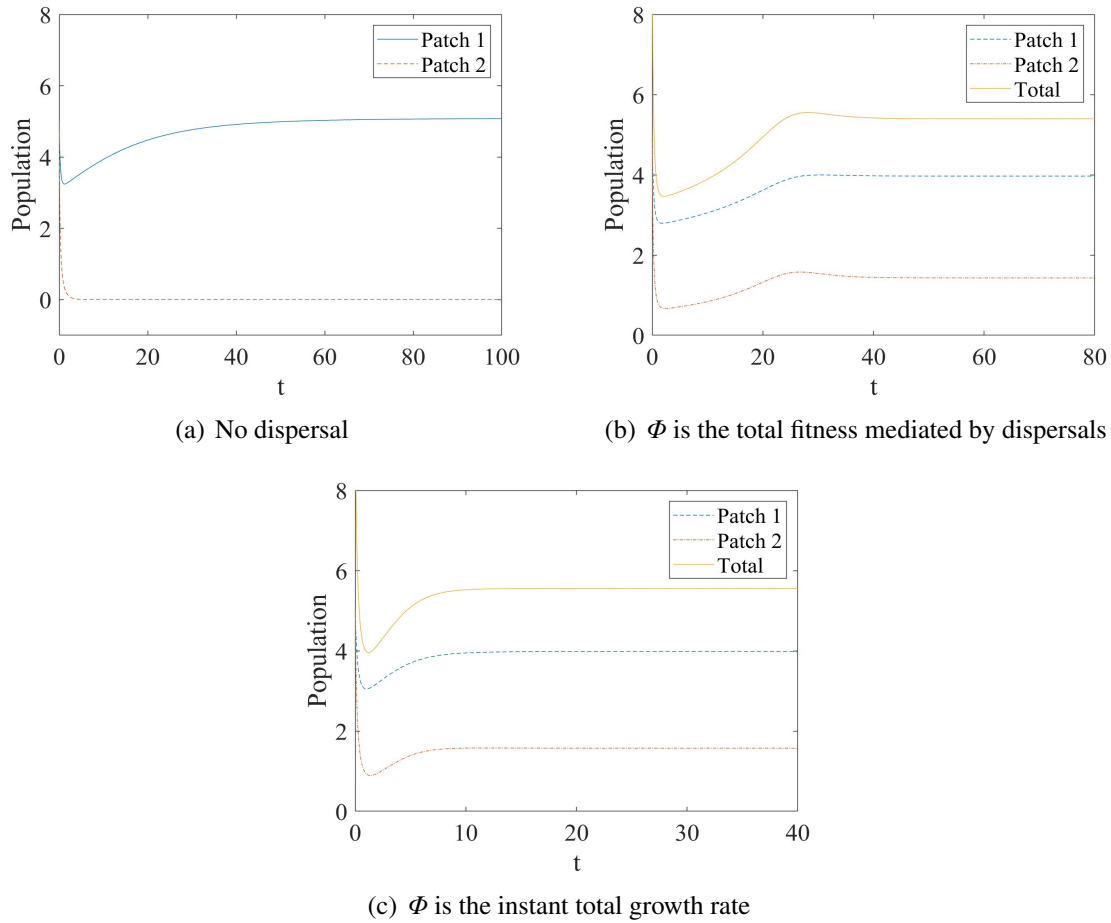


Figure 3.9: The dynamics of prey's population for systems (3.36), (3.37) and (3.8)-(3.39). The initial values are  $[u_1(0), u_2(0), \alpha(0)] = [5, 5, 0.8]$ .

### 3.5 Conclusion and Discussion

Motivated by some recent works about indirect effect on predator-prey systems, we have proposed a mathematical model to examine the impact of fear on the population dynamics of prey. Unlike in [25] where only the cost of the anti-predation response (reducing reproduction) was

considered, here we have also considered the benefit of such a response for surviving the predation. Both the cost and benefit functions depend on the anti-predation response level and the population of predator. However, in other works concerning about the evolution of predator-prey interactions, the responses are only density independent (see [1, 2, 13, 30] for examples). In addition, we also have considered the fear effect on the dispersal strategy of prey under predation risk. In other words, we have incorporated the fear effects in three factor: reproduction, predation and dispersion. To this end, we have considered a two-patch environment by assuming that the habitat of a prey consists of two discrete regions with individuals being able to disperse between the two regions. The unaffected dispersal rates are assumed to be symmetric since we are focused on the effect of fear and the anti-predation trait.

We start from a special case when there is no dispersal between the patches. Our results show that the optimal anti-predation response level  $\alpha$  depends on whether its effect on *reducing the predation* is more or less significant than its effect on *reducing the reproduction*. For the former, there is a continuously stable strategy (which is both an ESS and a CSS)  $\alpha^* > 0$  (see Figure 3.1 and 3.2), while for the latter, no response  $\alpha = 0$  should be favoured. See Section 3 for detailed discussion. For the case when the patches are connected through dispersal of the prey, our results indicate that the dispersal can enhance the co-persistence of the prey in the two patches. This is clearly and visually demonstrated in Figure 3.3 and is also discussed in details after Theorem 3.4.2 in Section 4. If a particular form of the dispersal function  $m(\alpha, v)$  is given (e.g., by (3.27) or some other functions satisfying (3.7) ), one may further explore to obtain more detailed results on how  $\alpha$  affects the co-persistence region in the  $F_1$ - $F_2$  plane. The numerical simulation displayed in Figure 3.4 is provided as an example.

We continued to study the evolution of anti-predation response level  $\alpha$  by invasibility analysis in Section 4.2.1. The criteria, however, are not practically useful. Alternatively, we let the trait  $\alpha$  be another variable evolving with respect to time, which leads to a model given by a system of three ordinary differential equations. The replicator equation governing the direction of evolution depends on a fitness function  $\Phi$ . We have considered two particular forms of this  $\Phi$ : (i) the total fitness mediated by dispersals which comes up in our analysis for the population system (see Section 4.1); (ii) the instant growth rate of the total population on both patches (motivated by [26]). However, we have only numerically explored the model to see how the

response level (as a trait variable) evolves with time, and the results at least indicate local convergence to a positive equilibrium of the full model with the response level  $\alpha(t)$  evolving toward a positive value. This implies the existence of an optimal anti-predation response level. More rigorous and thorough analysis is still needed in order to obtain more detailed (explicit) qualitative and quantitative results.

As we pointed out in the numerical examples, there are many choices for the fitness functions in the extensive literatures of adaptive dynamics and evolutionary dynamics, and we just tried two. Other quantities, like the basic reproduction ratio, life span and basic depression ratio, are also often considered by researchers. When choosing functions to measure fitness, besides the main biological feature(s), mathematical convenience is often a main consideration. We believe that the biological species as well as the biological problem under consideration should also make some difference(s). It would not be surprising to see that the strategy variable  $\alpha(t)$  would evolve to different positive values when different fitness functions are chosen.

In this paper, we have studied the evolutionary dynamics in two ways: adaptive dynamics with time scale separation (in Sections 3 and 4.2.1) and adaptive dynamics without time scale separation (in Section 4.2.2). By the former approach, the changes of trait are from mutation and natural selection and the process is graphically demonstrated by the pairwise invasibility plot. The critical strategies ESS and CSS are defined based on invasibility, associating with the stability/instability of corresponding competition system. The conditions for ESS and CSS have been proposed in previous works, but direct application may hardly provide any information due to the complexity of our model. The latter approach, however, clearly shows the direction of evolution, and the resulted system is more tractable in mathematics. Even though our results derived from the two methods are not quantitatively equivalent, we believe that there exists such a fitness function leading to the same evolutionary destination as the invasion method.

We have assumed in this paper that the fear effect decreases the mobility of the prey, reflected by the assumption (3.7) for the dispersal function  $m(\alpha, v_i)$ , and this assumption has those species that have refuges as prototypes of the prey species. On the other hand, there are prey species that have moving advantages (such as birds), for which, perceived predation risk would increase their dispersal rates (actively escaping from predators, or predator-taxis). For such

species, in contrast to (3.7), the dispersal function  $m(\alpha, v_i)$  would be an increasing function of both  $\alpha$  and  $v_i$ . We will explore this case in another work. For the spatially continuum case, a predator-taxis diffusion mechanism has been discussed in [27].

Finally, we remark that in our model in this paper, the population of predators is assumed to remain constant. Although there are numerous situations that fit in such a scenario (e.g., when the predator is a generalist), a case where the predator population is not a constant may intrigue further extensions. This will increase the dimension of the model system and consequently, increase the difficulty level of analysis. In the meanwhile, the model may present richer dynamics. Considering a specialist predator living in both patches, its populations decay exponentially in the absence of prey, governed by the following equations,

$$\begin{cases} \frac{dv_1}{dt} = \xi c(\alpha_u, v_1)u_1v_1 + \xi c(\alpha_w, v_1)w_1v_1 - d_vv_1, \\ \frac{dv_2}{dt} = \xi c(\alpha_u, v_2)u_2v_2 + \xi c(\alpha_w, v_2)w_2v_2 - d_vv_2, \end{cases} \quad (3.40)$$

where  $\xi > 0$  denotes ingestion efficiency and  $d_v > 0$  is the natural death rate. Assume that predators are not able to move between the patches. Combining these two predator equations with model system (3.28) and using the particular functions (3.26) and (3.27), numerical examples of population dynamics are shown in Figures 3.10 and 3.11, corresponding to one-patch and two-patch environment respectively. Unlike models (3.10) and (3.28) with constant predator populations showing monomorphic dynamics, co-existence of prey using different strategies is observed in the augmented model. Hence, evolutionary branching is possible. We leave this for future research projects.

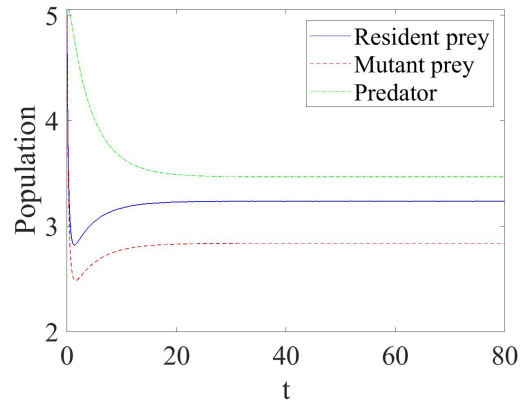


Figure 3.10: Population dynamics in an isolated patch for the case of a specialist predator. The parameter values are  $a = 1$ ,  $b_0 = 5$ ,  $d = 0.5$ ,  $c_0 = 0.35$ ,  $\tilde{s} = 0.1$ ,  $\tilde{p} = 0.3$ ,  $\alpha_u = 0.1$ ,  $\alpha_w = 0.7$ ,  $d_v = 0.3$ ,  $\xi = 0.2$ ; and the initial point is  $[u(0), w(0), v(0)] = [5, 5, 5]$ .

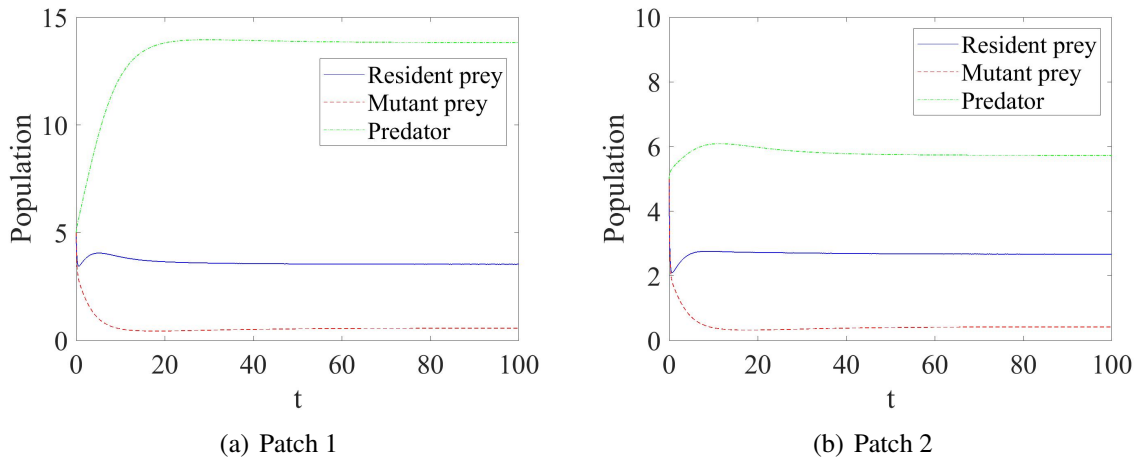


Figure 3.11: Population dynamics in a two-patch environment for the case of a specialist predator. The parameter values are  $a = 1$ ,  $b_{01} = 10$ ,  $b_{02} = 5$ ,  $d_1 = 0.5$ ,  $d_2 = 0.3$ ,  $c_0 = 0.4$ ,  $\tilde{s} = 0.1$ ,  $\tilde{p} = 0.3$ ,  $m_0 = 2$ ,  $\tilde{q} = 0.02$ ,  $\alpha_u = 0.1$ ,  $\alpha_w = 0.3$ ,  $d_v = 0.2$ ,  $\xi = 0.2$ ; and the initial point is  $[u_1(0), u_2(0), w_1(0), w_2(0), v_1(0), v_2(0)] = [5, 5, 5, 5, 5, 5]$ .

# Bibliography

- [1] Abrams, P. A., *Adaptive responses of predators to prey and prey to predators: the failure of the arms-race analogy*, *Evolution* 40.6(1986), 1229-1247.
- [2] Abrams, P.A., *The evolution of anti-predator traits in prey in response to evolutionary change in predators*, *Oikos* (1990): 147-156.
- [3] Brown, J. S., Laundre, J. W. and Gurung, M., *The ecology of fear: optimal foraging, game theory, and trophic interactions*, *Journal of Mammalogy* 80(1998), 385-399.
- [4] Chepyzhov, V. V. and Vishik, M. I., *Attractors for Equations of Mathematical Physics*, American Mathematical Society, Providence RI, 2002.
- [5] Cresswell, W., *Non-lethal effects of predation in bird*, *Ibis* 150(2008), 3-17.
- [6] Day, T. and Burns, J. G., *A consideration of patterns of virulence arising from host-parasite coevolution*, *Evolution* 57.3(2003), 671-676.
- [7] De Leenheer, P., Mohapatra, A., Ohms, H. A., Lytle, D. A. and Cushing, J. M., *The puzzle of partial migration: Adaptive dynamics and evolutionary game theory perspectives*, *J. Theor. Biol.* 412(2017), 172-185.
- [8] Diekmann, O., *A beginner's guide to adaptive dynamics*, Banach Center Publications 63(2004), 47-86.
- [9] Geritz, S. A. H., Kisdi, E., Meszena, G. and Metz, J. A. J., *Evolutionary singular strategies and the adaptive growth and branching of evolutionary tree*, *Evolutionary Ecology* 12(1998), 35-57.

- [10] Hastings, A., *Dynamics of a single species in a spatially varying environment: the stabilizing role of high dispersal rates*, J. Math. Biol. 16(1982), 49-55.
- [11] Hastings, A., *Can spatial variation along lead to selection for dispersal?* , Theoretical Population Dynamics 24(1983), 244-251.
- [12] Jansen, V. A. A., *The dynamics of two diffusively coupled predator-prey populations*, Theor. Popul. Biol. 59(2001), 119-131.
- [13] Křivan, V., *The Lotka-Volterra predator-prey model with foraging-predation risk trade-offs*, The American Naturalist 170.5(2007): 771-782.
- [14] Levin, S. A., Cohen, D. and Hastings, A., *Dispersal strategies in patchy environments*, Theor. Popul. Biol. 26(1984), 165-191.
- [15] Lima, S. L. and Dill, L. M., *Behavioral decisions made under the risk of predation: a review and prospectus*, Canadian Journal of Zoology 68(1990), 619-640.
- [16] Lundberg, P., *On the evolutionary stability of partial migration*, J. Theor. Biol. 321(2013), 36-39.
- [17] Nelson, E. H., Matthews, C. E. and Rosenheim, J. A., *Predators reduce prey population growth by inducing changes in prey behavior*, Ecology 85(2004), 1853-1858.
- [18] Okubo, A. and Levin, S. A., *Diffusion and Ecological Problems: Modern Perspectives*, Springer, New York, 2001.
- [19] Preisser, E. L., Bolnick, D. I. and Benard, M. F., *Scared To death? The effects of intimidation and consumption in predator-prey interactions*, Ecology 86(2005), 501-509.
- [20] Rosenzweig, M. L. and MacArthur, R. H., *Graphical representation and stability conditions of predator-prey interactions*, The American Naturalist 97(1963), 209-223.
- [21] Sasmal, S. K., *Population dynamics with multiple Allee effects induced by fear factors a mathematical study on prey-predator interactions*, Appl. Math. Model. 64(2018), 1-14.

- [22] Sasmal, S. K. and Takeuchi, Y., *Dynamics of a predator–prey system with fear and group defense*, J. Math. Anal. Appl. 481(2020), 12347.
- [23] Takeuchi, Y., Wang, W., Nakaoka, S. and Iwami, S., *Dynamical adaptation of parental care*, Bull. Math. Biol. 71(2009), 931-951.
- [24] Terry, A. J., *Predator–prey models with component Allee effect for predator reproduction*, J. Math. Biol. 71(2015), 1325-1352.
- [25] Wang, X., Zanette, L. Y. and Zou, X., *Modelling the fear effect in predator–prey interactions*, J. Math. Biol. 73(2016), 1179-1204.
- [26] Wang, X. and Zou, X., *Modeling the fear effect in predator–prey interactions with adaptive avoidance of predators*, Bull. Math. Biol. 79(2017), 1325-1359.
- [27] Wang, X. and Zou, X., *Pattern formation of a predator–prey model with the cost of anti-predator behaviors*, Math. Biosci. Eng. 15(2018), 775-805.
- [28] Wang, Y. and Zou, X., *On a predator–prey system with digestion delay and anti-predation strategy*, J. Nonlin. Sci. 30(2020), 1579-1605.
- [29] Zanette, L. Y., White, A. F., Allen, M. C. and Clinchy, M., *Perceived predation risk reduces the number of offspring songbirds produce per year*, Science 334(2011), 1398-1401.
- [30] Zu, J. and Takeuchi, Y., *Adaptive evolution of anti-predator ability promotes the diversity of prey species: Critical function analysis*, BioSystems 109(2012): 192-202.

# Chapter 4

## Transient Dynamics of SIR Models over Patchy Environment

### 4.1 Introduction

Mathematical modelling of transmission dynamics of infectious disease is an important tool that has been used to investigate the mechanism of how a disease spreads, to predict the future course of an outbreak, and to examine the likely outcomes of public health interventions. Among the questions one would like to explore by mathematical modelling are the following two important ones. (Q1) Long term disease dynamics: will an infectious disease eventually die out or become endemic? (Q2) Short term disease dynamics: at a given time, is the epidemic of an infectious disease getting worse/breaking out, or is it getting mitigated? To better explain these two questions, let us first look at the simplest Kermack-McKendrick model proposed and studied in [15], which is given by the following set of ordinary differential equations:

$$\begin{cases} \frac{dS}{dt} = -\beta SI, \\ \frac{dI}{dt} = \beta SI - \gamma I, \\ \frac{dR}{dt} = \gamma I. \end{cases} \quad (4.1)$$

Here the host population is divided into three compartments: susceptible class, infected class and removed class, with the respective subpopulations denoted by  $S(t)$ ,  $I(t)$  and  $R(t)$ . This model is reasonable for infectious diseases that are transmitted from human to human with  $\beta > 0$  denoting the transmission rate. Individuals leave the infected class due to recovery or death. The transition rate is proportional to the infectious population where  $\gamma > 0$  is the removal rate. Note that in (4.1), neither demography nor disease-caused deaths are considered, and hence, it is suitable only for mild infectious diseases that has relatively short epidemics (comparing to human's lifespan). This model has been well studied, and the following results have been obtained (see, e.g., [22]).

I. Given  $S(0) = S_0 > 0$ ,  $I(0) = I_0 > 0$  and  $R(0) = R_0 \geq 0$ , the following conclusions hold:

- (I-1) if  $\mathfrak{R}_0 := \beta S_0 / \gamma < 1$ , then  $I(t)$  decreases to zero as  $t \rightarrow +\infty$ ;
- (I-2) if  $\mathfrak{R}_0 > 1$ , then  $I(t)$  first increases up to a maximum value  $I_{max}$  then decreases to zero as  $t \rightarrow +\infty$ ;
- (I-3)  $S(t)$  is a decreasing function approaching to the limiting value  $S_\infty := \lim_{t \rightarrow +\infty} S(t)$ ;
- (I-4) both  $I_{max}$  and  $S_\infty$  depend on the initial populations,  $S_0$  and  $I_0$ , and the value of parameters,  $\beta$  and  $\gamma$ .

The number  $\mathfrak{R}_0 = \beta S_0 \cdot \frac{1}{\gamma}$  above is called the basic reproduction number for the model (4.1). Noting that  $\frac{1}{\gamma}$  is the average infection time for infected individuals and  $\beta$  is the transmission rate, it is clear that  $\mathfrak{R}_0$  actually measures the average number of new infections that an infected individual causes when the susceptible population is  $S_0$ . From (I-1) and (I-2), one can easily see that the value of  $\mathfrak{R}_0$  determines whether or not there will be an outbreak for the disease when initially  $I_0 > 0$  and  $S_0 > 0$ : there will be no outbreak if  $\mathfrak{R}_0 < 1$ , and there will be an outbreak if  $\mathfrak{R}_0 > 1$ . This dichotomy can also be obtained by looking at

$$I'(0) = \beta S(0)I(0) - \gamma I(0) = [\beta S_0 - \gamma]I_0 =: \Gamma_0 I_0 \quad (4.2)$$

with  $S_0 > 0$  and  $I_0 > 0$ : there will be no outbreak if  $\Gamma_0 := \beta S_0 - \gamma < 0$  (i.e.,  $I'(0) < 0$ ); and there will be an outbreak if  $\Gamma_0 > 0$  (i.e.,  $I'(0) > 0$ ). Note that  $\Gamma_0 = \beta S_0 - \gamma$  is the *related change*

rate of the subpopulation  $I(t)$  at the initial time  $t = 0$ , which measures the amplification rate of  $I(t)$  at  $t = 0$ . Here we have *two different notions*: the basic reproduction number  $\mathfrak{R}_0$  which is of *long time nature* (during infection period), and the initial amplification rate  $\Gamma_0$  which is of *short time nature* (at a particular time  $t = 0$ ). The former is supposed to predict the long time disease dynamics while the latter is supposed to predict the short time disease dynamics. However, they amazingly agree to each other in predicting the disease dynamics of (4.1), because the long term and short term disease dynamics in terms of outbreak coincide.

The SIR model (4.1) has numerous variants when different transmission mechanisms and demographics are taken into account, and the threshold theorems have been extended. Denote  $N$  as the total population,  $N(t) = S(t) + I(t) + R(t)$ . For example, if the *demographic equation* is  $N'(t) = B(N) - dN$  and a disease-related death rate  $\epsilon > 0$  is assumed, then (4.1) is naturally extended to

$$\begin{cases} \frac{dS}{dt} = B(N) - \beta SI - dS, \\ \frac{dI}{dt} = \beta SI - (\gamma + d + \epsilon)I, \\ \frac{dR}{dt} = \gamma I - dR. \end{cases} \quad (4.3)$$

Assuming  $N'(t) = B(N) - dN$  has a unique positive equilibrium  $N_+ > 0$  which is globally stable; and before the disease appears, the host population have settled at (or is close to)  $N_+$ . This implies that (4.3) has a *unique disease-free equilibrium*  $E_0 = [N_+, 0, 0]$  (as opposed to (4.1) for which there are infinitely many disease-free equilibria). By standard dynamical system approach, one can easily show that (4.3) also has the *long term* threshold dynamics in terms of its basic reproduction number  $\hat{\mathfrak{R}}_0 = \beta N_+ / (\gamma + d + \epsilon)$ : if  $\hat{\mathfrak{R}}_0 < 1$ , then  $E_0$  is asymptotically stable meaning that the disease will eventually die out provided that initial infection is not too big (i.e.,  $0 < I(0) \ll N_+$ ); if  $\hat{\mathfrak{R}}_0 > 1$ ,  $E_0$  becomes unstable and the disease becomes endemic (i.e.,  $I(t)$  is uniformly persistent). In the mean time, from

$$I'(0) = [\beta S(0) - (\gamma + d + \epsilon)]I(0) =: \hat{\Gamma}_0 I(0), \quad (4.4)$$

one knows that if  $\hat{\Gamma}_0 < 0$ , then there will be no outbreak at  $t = 0$ ; if  $\hat{\Gamma}_0 > 0$ , then there will be an outbreak at  $t = 0$ . Observe that generally  $R(0) = 0$ ,  $N(0) = N_+$  (or  $N(0)$  is close to  $N_+$ )

and  $I(0)$  is very small in reality when a disease appears. Hence,  $\hat{\Gamma}_0 = \beta S(0) - (\gamma + d + \epsilon) \approx \beta N(0) - (\gamma + d + \epsilon) = \beta N_+ - (\gamma + d + \epsilon)$ . This implies that generically,  $\hat{\mathfrak{R}}_0 - 1$  and  $\hat{\Gamma}_0$  have the same sign. Therefore, generically  $\hat{\mathfrak{R}}_0$  also determines whether or not an initial *small infection*  $I(0)$  will result in an outbreak in the coming short period of time after  $t = 0$ , the same conclusion as for (4.1).

The above results for (4.3) are for the initial time  $t = 0$  when an epidemic occurs. If, at some given time  $t_0 > 0$  during an epidemic, one wants to predict whether or not there will be an outbreak in the coming short period after this time  $t_0$ , one would have to look at  $I'(t_0) = \hat{\Gamma}(t_0)I(t_0)$  for (4.3), where  $\hat{\Gamma}(t_0) = \beta S(t_0) - (\gamma + d + \epsilon)$ . Unfortunately,  $S(t_0)$  can now be far away from  $S(0)$  (hence  $N(0)$ ), and hence, the sign of  $\hat{\mathfrak{R}}_0 - 1$  (independent of  $t_0$ ) may not agree with the sign of  $\hat{\Gamma}(t_0)$ . Thus, the value of *the long term characteristics* quantity  $\hat{\mathfrak{R}}_0$  generally *cannot predict* whether or not there will be an outbreak in the *coming short period of time* after  $t_0$ . That is, even if  $\hat{\mathfrak{R}}_0 < 1$  (hence eventually  $I(t) \rightarrow 0$ ), there can be an outbreak at some  $t_0 > 0$ ; and even if  $\hat{\mathfrak{R}}_0 > 1$ , there may be some time  $t_0 > 0$  such that  $I'(t_0) < 0$ , which can easily mislead the publics. Therefore, for a general model of infectious disease dynamics, the long term and short term behaviours often do not imply each other, and they both deserve careful analysis.

For *long term* disease dynamics, there have been a very rich literature with publications on various models. Typically the long term dynamics of a disease model is of threshold type in terms of the basic reproduction number  $\mathfrak{R}_0$ . For a model that has a unique disease-free equilibrium (DFE), the basic reproduction number  $\mathfrak{R}_0$  is still biologically defined as the expected number of secondary infections from a single infected individual during his or her entire period of infectiousness *in a completely susceptible population*. Mathematically,  $\mathfrak{R}_0$  is identified by the next generation method, which was initially introduced by Diekmann et al. [12]. In this method,  $\mathfrak{R}_0$  is defined as the spectral radius of the next generation operator. For compartmental models formulated as systems of ordinary differential equations (ODEs), van den Driessche and Watmough [13] derived an expression for the next generation matrix. The authors further demonstrated the threshold *long term* dynamics by showing that: if  $\mathfrak{R}_0 < 1$  then the DFE of the model is locally asymptotically stable meaning that the disease eventually dies out; if  $\mathfrak{R}_0 > 1$

then the DFE is unstable and the disease becomes endemic.

In contrast, there are only *very few works* in literature (see Section 2) that analytically investigate *short term or transient disease dynamics* by mathematical models, and this is mainly due to the lack of effective tools and methods. For simple models like (4.1) and (4.3), the equation governing the change rate of the infected subpopulation is conveniently related to its amplification rate that has an explicit formula. When there is some heterogeneity, for example, *spatial heterogeneity as we will discuss next*, analyzing short term or transient disease dynamics becomes much more difficult, if not impossible. On the other hand, just like short term or transient population dynamics is important in ecology as emphasized by Hastings [17, 18], short term disease dynamics is also very important because it may affect the health decisions on implementing some interventions for controlling the epidemics of an infectious disease.

Nowadays the world is highly connected, and such a high connectivity has obviously enhanced the spread of infectious diseases. The pandemic of COVID-19 is such an example. Thus, when modelling the transmission dynamics of an infectious disease, we need to consider spatial structure. Typically, patch models are used with each patch representing a country, city or some other geographic area. The dynamics of each patch is coupled by spatial dispersals or travels reflecting movement of the host population. Such couplings bring challenge to the analysis of the resulting model. Taking the Kermack-McKendrick SIR system (4.1) as an example and considering  $n \geq 2$  patches, the coupled SIR system corresponding to (4.1) is

$$\begin{cases} \frac{dS_i}{dt} = \sum_{j \in \Omega, j \neq i} d_{ji}^S S_j - \sum_{j \in \Omega, j \neq i} d_{ij}^S S_i - \beta_i S_i I_i, \\ \frac{dI_i}{dt} = \sum_{j \in \Omega, j \neq i} d_{ji}^I I_j - \sum_{j \in \Omega, j \neq i} d_{ij}^I I_i + \beta_i S_i I_i - \gamma_i I_i, \\ \frac{dR_i}{dt} = \sum_{j \in \Omega, j \neq i} d_{ji}^R R_j - \sum_{j \in \Omega, j \neq i} d_{ij}^R R_i + \gamma_i I_i, \end{cases} \quad \text{for } i \in \Omega. \quad (4.5)$$

Here  $\Omega = \{1, \dots, n\}$ . Parameters  $\beta_i > 0$  and  $\gamma_i > 0$  have the same meanings as in (4.1) but for patch  $i$ , and the constant  $d_{ij}^X \geq 0$  is a per capita rate at which individuals in class  $X$  move from patch  $i$  to patch  $j$  for  $X \in \{S, I, R\}$ ,  $i, j \in \{1, \dots, n\}$ , and  $i \neq j$ . Now due to the coupling, obtaining results similar to (I-1)-(I-4) for the non-spatial model (4.1) becomes very difficult, if not impossible. This is because (A) the computation of the basic reproduction

number  $\mathfrak{R}_0$  is harder; and (B) there may be some time moments at which  $I'_i(t)$ ,  $i = 1, \dots, n$ , have different signs, and hence the measurement of outbreak should consider all patches. To our best knowledge, there are only two studies [29, 30] that have considered the short time transient dynamics of disease transmission *over patchy environment*. For this type of disease models over patches, even when a model has a unique DFE at which the next generation method is applicable to establish the threshold long term dynamics, it is hard (if not impossible) to obtain an explicit expression for  $\mathfrak{R}_0$  as the spectral radius of a large matrix. See, e.g., [5, 6, 35, 7, 1, 21, 14, 2, 10] and the references within.

This paper is stimulated by the aforementioned need for approaches to explore short term dynamics of infectious diseases over connected patches. To this end, we borrow the notion of *reactivity* used in ecology and take advantage of the developed mathematical results for reactivity in mathematical ecology. By applying this idea to some patch models of disease transmission, we wish to provide a framework and an approach that can be used for more disease models with spatial structure.

The rest of the paper is organized as below. In Section 2, we provide the mathematical background for some related notions in mathematical ecology, including reactivity, amplification rate and resilience. We then move on to apply these notions and ideas behind them to some disease models over patches to examine the short term dynamics presented by each system. This will allow us to explore how the spatial dispersals/travels and other model parameters as well as initial values affect the short term disease dynamics at a given time during an epidemic. Two types of patch models will be examined: Section 3 deals with models without demography, and Section 4 focuses on models with demographic structure. Some numerical simulations will also be exhibited to more visually demonstrate our results. We end the paper by Section 5 in which we summarize our main conclusions and present some discussions.

## 4.2 Amplification rates and reactivity

The notion of reactivity in ecology was first introduced by Neubert and Caswell [31], as a description of the short-term response to perturbations. Specifically, it is defined as the maximum initial amplification rate over all possible small perturbations to an equilibrium. An

equilibrium with positive reactivity is said to be reactive, corresponding to the case when some perturbations can grow initially.

Consider the initial value problem of a linear system of ODEs:

$$\frac{d\mathbf{x}}{dt} = \mathbf{A}\mathbf{x}, \quad \mathbf{x}(0) = \mathbf{x}_0 \quad (4.6)$$

where  $\mathbf{x} \in \mathbb{R}^n$  and  $\mathbf{A} = [a_{ij}]_{n \times n}$  is a real matrix. Equation (4.6) can be the linearization of a population dynamics for  $n$  interacting species at an equilibrium, with  $\mathbf{x}$  being the deviation from the equilibrium. Thus, the Euclidean norm of  $\mathbf{x}(t)$ , i.e.,

$$\|\mathbf{x}(t)\| := \sqrt{x_1^2(t) + x_2^2(t) + \cdots + x_n^2(t)},$$

measures the size of vector  $\mathbf{x}(t)$ , and it also measures the distance of  $\mathbf{x}(t)$  to the origin, or equivalently measures how far away of the population vector at time  $t$  from the equilibrium. Denote by  $\Gamma(t)$  the relative rate of change of  $\|\mathbf{x}(t)\|$ , that is,

$$\Gamma(t) := \frac{1}{\|\mathbf{x}\|} \frac{d\|\mathbf{x}\|}{dt}. \quad (4.7)$$

Obviously,  $\Gamma(t)$  measures the amplification rate for  $\|\mathbf{x}(t)\|$  at time  $t$ . Particularly,  $\Gamma_0 := \Gamma(0)$  is called the initial amplification rate. If  $\mathbf{x}(t)$  is a solution to (4.6), then direct calculation gives (see [31])

$$\Gamma(t) = \frac{\mathbf{x}^T(t)H(\mathbf{A})\mathbf{x}(t)}{\|\mathbf{x}(t)\|^2} \quad \text{where} \quad H(\mathbf{A}) = \frac{\mathbf{A} + \mathbf{A}^T}{2}. \quad (4.8)$$

By the definition,  $\Gamma(t) > 0$  ( $\Gamma(t) < 0$ ) means that the size of the solution  $\|\mathbf{x}(t)\|$  to (4.6) is growing (decaying) at  $t$ . Particularly, the sign of the initial amplification rate,

$$\Gamma_0 = \frac{\mathbf{x}_0^T H(\mathbf{A}) \mathbf{x}_0}{\mathbf{x}_0^T \mathbf{x}_0}, \quad (4.9)$$

predicts whether the solution with  $\mathbf{x}_0$  will initially grow or decay. Note that  $\Gamma_0 = \Gamma(\mathbf{x}_0)$  depends on the initial value  $\mathbf{x}_0$  (so does  $\Gamma(t)$ ).

Let  $\lambda_1(\mathbf{A})$  denote the eigenvalue of  $\mathbf{A}$  that has the largest real part. Then  $-\lambda_1(\mathbf{A})$  is called

the *resilience* of (4.6), which is independent of the initial value  $\mathbf{x}_0$  and reflects the *long term dynamics* of (4.6). On the other hand,  $H(\mathbf{A})$  is a real symmetric matrix and hence all its eigenvalues are real. Let  $\lambda_{min}$  and  $\lambda_{max}$  denote the smallest and largest eigenvalues of  $H(\mathbf{A})$  respectively. Since  $\Gamma_0(\mathbf{x}_0)$  given by (4.9) is in the form called the Rayleigh quotient or the Rayleigh-Ritz ratio, it is known (see, e.g., [20]) that

$$\lambda_{min} \leq \Gamma_0(\mathbf{x}_0) = \frac{\mathbf{x}_0^T H(\mathbf{A}) \mathbf{x}_0}{\mathbf{x}_0^T \mathbf{x}_0} \leq \sup_{\mathbf{x}_0 \neq 0} \frac{\mathbf{x}_0^T H(\mathbf{A}) \mathbf{x}_0}{\mathbf{x}_0^T \mathbf{x}_0} = \max_{\|\mathbf{x}_0\|=1} \frac{\mathbf{x}_0^T H(\mathbf{A}) \mathbf{x}_0}{\mathbf{x}_0^T \mathbf{x}_0} = \lambda_{max}. \quad (4.10)$$

The *reactivity* of (4.6) is defined in [31] as the largest initial amplification rate over all initial values, that is,

$$\text{reactivity} = \sup_{\mathbf{x}_0 \neq 0} \left( \frac{1}{\|\mathbf{x}\|} \frac{d\|\mathbf{x}\|}{dt} \Big|_{t=0} \right) = \sup_{\mathbf{x}_0 \neq 0} \frac{\mathbf{x}_0^T H(\mathbf{A}) \mathbf{x}_0}{\mathbf{x}_0^T \mathbf{x}_0} = \lambda_{max}. \quad (4.11)$$

Apparently, the reactivity measures the maximal possible *initial growth* for (4.6) which is of *short term nature*. Moreover,

- if the *reactivity*  $\lambda_{max}$  of (4.6) is negative, then for any initial value  $\mathbf{x}_0$ , the solution will *initially decay in size* (norm) since  $\Gamma_0 = \Gamma(\mathbf{x}_0) < 0$ ;
- if  $\lambda_{min} > 0$ , then for any initial value  $\mathbf{x}_0$ , the solution will *initially grow in size* since  $\Gamma_0 = \Gamma(\mathbf{x}_0) > 0$ ;
- if  $\lambda_{min} < 0 < \lambda_{max}$ , then there will be initial values  $\mathbf{x}_0$  for which  $\Gamma_0 = \Gamma(\mathbf{x}_0) < 0$  and there will also be  $\mathbf{x}_0$  for which  $\Gamma_0 = \Gamma(\mathbf{x}_0) > 0$ .

We remark that there have been some extensions/generalizations of the above notions of reactivity and amplification rates in ecology. For example, Mari et al. [27] generalized *reactivity* to  $\lambda_{max}(H(\mathbf{C}^T \mathbf{C} \mathbf{A}))$  corresponding to a system output  $\mathbf{y} = \mathbf{C} \mathbf{x}$  where matrix  $\mathbf{C}$  reflects the interest in a set of state variables. Wang et al. [36] recently extended the measurements of reactivity and amplification rates to some reaction-diffusion models to explore how spatial heterogeneity affects transient dynamics. In a more recent work, Lutscher and Wang [24] explored the reactivity of *periodic orbits*. The results reveal some differences between the reactivity of a stable

equilibrium and that of a stable periodic orbit. In the *context of disease dynamics models* (a type of population models with predator-prey type interactions), reactivity has been applied to study short term disease dynamics in [37, 32]. Also, parallel to  $\mathcal{R}_0$  for long-term endemicity, Hosack et al. [23] derived a threshold index for short-term epidemicity by using the concept of reactivity at the disease-free equilibrium (DFE). The more general definition of reactivity proposed in aforementioned reference, Mari et al. [27], allows the authors to measure the initial growth rates of infection-related variables; and such a generalized reactivity has been used to some infectious disease models in [28, 29, 30], including a most recent work for the outbreak of COVID-19.

Among the above works on transient dynamics, only [29, 30] are works on short term disease dynamics considering discrete spatial variation, which is the focus of this paper. In the subsequent sections, we will use the notion of amplification rate (closely related to the notion of reactivity) to explore short term or transient dynamics represented by two types of SIR model over patchy environment, of which one type ignores demography and the other includes a simple demographic structure, as has been demonstrated in the introduction for a single patch case.

## 4.3 SIR epidemic patch model

### 4.3.1 Two patches

We start from the SIR system without demography and consider a simple case of two patches.

Then model (4.5) reduces to

$$\begin{cases} \frac{dS_1}{dt} = d_{21}^S S_2 - d_{12}^S S_1 - \beta_1 S_1 I_1, \\ \frac{dS_2}{dt} = d_{12}^S S_1 - d_{21}^S S_2 - \beta_2 S_2 I_2, \\ \frac{dI_1}{dt} = d_{21}^I I_2 - d_{12}^I I_1 + \beta_1 S_1 I_1 - \gamma_1 I_1, \\ \frac{dI_2}{dt} = d_{12}^I I_1 - d_{21}^I I_2 + \beta_2 S_2 I_2 - \gamma_2 I_2, \\ \frac{dR_1}{dt} = d_{21}^R R_2 - d_{12}^R R_1 + \gamma_1 I_1, \\ \frac{dR_2}{dt} = d_{12}^R R_1 - d_{21}^R R_2 + \gamma_2 I_2. \end{cases} \quad (4.12)$$

It is easy to verify that the total population of two patches is of constant size since there are no births and natural deaths. By Proposition 1.1 in [11], all solutions to model (4.12) with non-negative initial conditions remain non-negative for all  $t > 0$ . Let  $M(t) = S_1(t) + S_2(t) + I_1(t) + I_2(t)$ . Then,

$$M'(t) = -\gamma_1 I_1 - \gamma_2 I_2 \leq 0,$$

and hence,  $M(t)$  is a decreasing function. In addition,  $M(t)$  is non-negative, leading to the conclusion that its limit,  $\lim_{t \rightarrow \infty} M(t)$ , exists and thus,  $\lim_{t \rightarrow \infty} M'(t) = 0$ . Together with the non-negativity of  $I_i(t)$  for  $i \in \{1, 2\}$ , we have

$$I_1(t) \rightarrow 0 \quad \text{and} \quad I_2(t) \rightarrow 0 \quad \text{as} \quad t \rightarrow \infty.$$

Similar to the simplest Kermack-McKendrick model (4.1), this system has infinitely many disease-free equilibria. Hence, the next generation matrix method [13] fails to find the basic reproduction number, and the reactivity [31] or its generalization [27] can not be used in this model.

In the rest of this paper, we study the amplification rate  $\Gamma(t_0)$  where  $t_0$  can be any time during an epidemic. Thus, we are not restricted to the initial populations at an equilibrium. For simplification, we use the notation  $\Gamma_0$  instead of  $\Gamma(t_0)$  and call it the initial amplification rate. Focusing on the infected compartments, let  $\mathbf{x}(t) = [I_1(t), I_2(t)]$ . Given that

$$[S_1(0), S_2(0), I_1(0), I_2(0), R_1(0), R_2(0)] = [S_{10}, S_{20}, I_{10}, I_{20}, R_{10}, R_{20}] \in \mathbb{R}_{>0}, \quad (4.13)$$

the linearized system for  $\mathbf{x}(t)$  near the initial point is

$$\frac{d\mathbf{x}}{dt} = \mathbf{A}_0 \mathbf{x} \quad \text{with} \quad \mathbf{A}_0 = \begin{pmatrix} \beta_1 S_{10} - \gamma_1 - d_{12}^I & d_{21}^I \\ d_{12}^I & \beta_2 S_{20} - \gamma_2 - d_{21}^I \end{pmatrix}. \quad (4.14)$$

Substituting  $\mathbf{A}_0$  and initial condition (4.13) into (4.9) yields

$$\Gamma_0 = \frac{(\beta_1 S_{10} - \gamma_1 - d_{12}^I) I_{10}^2 + (\beta_2 S_{20} - \gamma_2 - d_{21}^I) I_{20}^2 + (d_{12}^I + d_{21}^I) I_{10} I_{20}}{I_{10}^2 + I_{20}^2}. \quad (4.15)$$

The initial amplification rate is linearly dependent on parameters  $d_{12}^I$ ,  $d_{21}^I$ ,  $\beta_1$ ,  $\beta_2$ ,  $\gamma_1$ , and  $\gamma_2$ . Moreover,  $\Gamma_0$  is increasing with respect to  $\beta_1$  and  $\beta_2$  since

$$\frac{\partial \Gamma_0}{\partial \beta_1} = \frac{S_{10} I_{10}^2}{I_{10}^2 + I_{20}^2} > 0 \quad \text{and} \quad \frac{\partial \Gamma_0}{\partial \beta_2} = \frac{S_{20} I_{20}^2}{I_{10}^2 + I_{20}^2} > 0,$$

and it is decreasing with respect to  $\gamma_1$  and  $\gamma_2$  since

$$\frac{\partial \Gamma_0}{\partial \gamma_1} = -\frac{I_{10}^2}{I_{10}^2 + I_{20}^2} < 0 \quad \text{and} \quad \frac{\partial \Gamma_0}{\partial \gamma_2} = -\frac{I_{20}^2}{I_{10}^2 + I_{20}^2} < 0.$$

Suppose that different interventions are implemented to control the spread of an infectious disease and therefore to mitigate the outbreak. Wearing a mask in public areas and practicing social distance, for instance, result in a lower transmission rate and thus a smaller initial amplification rate. Some numerical examples are provided in Figure 4.1. As we already known,  $\Gamma_0$  is a linear increasing function of  $\beta_1$ , the transmission rate in patch 1. Positive/negative  $\Gamma_0$  indicates an initial amplification/attenuation in the magnitude of solution  $\|\mathbf{x}(t)\|$ . A decrease in  $\beta_1$ , yielding a lower  $\Gamma_0$ , leads to a better control of the epidemic, as is shown in Figure 4.1(b).

Figure 4.1(c) gives an example when  $\| [I_1(t), I_2(t)] \|$  initially decreases but the outbreak will continue after a short period of time. In this case, the basic reproduction number in two patches without dispersal satisfying  $\mathfrak{R}_0^{(1)} > 1 > \mathfrak{R}_0^{(2)}$ .

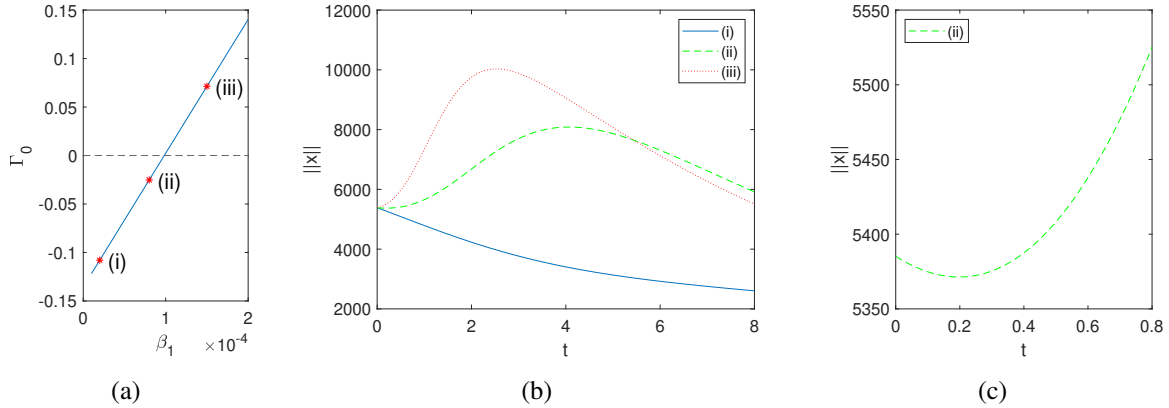


Figure 4.1: Three sample points of  $\beta_1$  are taken as: (i)  $0.2 \times 10^{-4}$ , (ii)  $0.8 \times 10^{-4}$ , and (iii)  $1.5 \times 10^{-4}$ . (a) The initial amplification rate  $\Gamma_0$  is negative for (i) and (ii), while it is positive for (iii). (b) The outbreak is mitigated with  $\beta_1$  decreasing from (iii) to (ii), and is completely under control when  $\beta_1$  further reduces to (i). (c) For the chosen value (ii), the magnitude of solution initially experiences a short-period reduction then grows to its maximal value. Set  $\beta_2 = 2 \times 10^{-5}$ ,  $\gamma_1 = 0.2$ ,  $\gamma_2 = 0.4$ ,  $d_{12}^S = 0.08$ ,  $d_{21}^S = 0.1$ ,  $d_{12}^I = 0.02$ ,  $d_{21}^I = 0.05$  and  $[S_{10}, S_{20}, I_{10}, I_{20}] = [10000, 15000, 2000, 5000]$ .

Vaccination, as the most effective method of preventing infectious diseases, can be simply considered as a reduction in susceptible populations, yielding a smaller  $\Gamma_0$  since

$$\frac{\partial \Gamma_0}{\partial S_{10}} = \frac{\beta_1 I_{10}^2}{I_{10}^2 + I_{20}^2} > 0 \quad \text{and} \quad \frac{\partial \Gamma_0}{\partial S_{20}} = \frac{\beta_2 I_{20}^2}{I_{10}^2 + I_{20}^2} > 0.$$

Assume that only the number of susceptible individuals in patch 2 changes while all other initial conditions and parameter values are fixed. The numerical examples given in Figure 4.2(b) show that the outbreak is better controlled with the decrease in  $S_{20}$ . The linear dynamics of solutions near the initial point, as is displayed in Figure 4.2(c), are consistent with the corresponding value of  $\Gamma_0$ .

Note that  $\Gamma_0^{(i)} = \beta_i S_{i0} - \gamma_i$  is the initial amplification rate of patch  $i \in \{1, 2\}$  in isolation (i.e.,

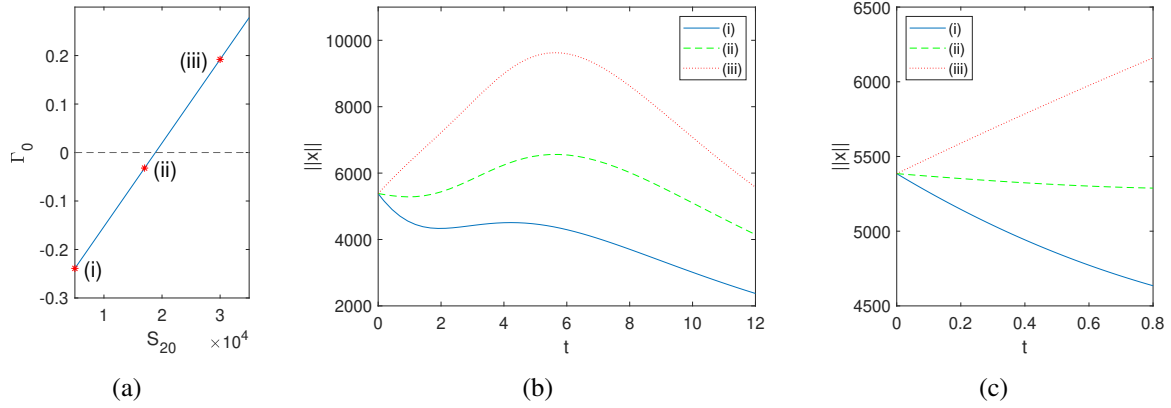


Figure 4.2: Three sample points of  $S_{20}$  are taken as: (i) 5000, (ii) 17000, and (iii) 30000. (a) The initial amplification rate  $\Gamma_0$  is a linear increasing function of  $S_{20}$ , whose value is negative for (i) and (ii) and is positive for (iii). (b) The dynamics of  $\|\mathbf{x}(t)\| = \|[I_1(t), I_2(t)]\|$  for different initial conditions. (c) The linear dynamics of  $\|\mathbf{x}(t)\|$  near the initial point. Set  $\beta_1 = 5 \times 10^{-5}$ ,  $\beta_2 = 2 \times 10^{-5}$ ,  $\gamma_1 = 0.2$ ,  $\gamma_2 = 0.4$ ,  $d_{12}^S = 0.08$ ,  $d_{21}^S = 0.1$ ,  $d_{12}^I = 0.02$ ,  $d_{21}^I = 0.05$  and  $[S_{10}, I_{10}, I_{20}] = [10000, 2000, 5000]$ .

no dispersals/travels are allowed as  $d_{ij} = 0$ ). Then  $\Gamma_0$  that given by (4.15) can be rewritten as

$$\Gamma_0 = \frac{\Gamma_0^{(1)} I_{10}^2 + \Gamma_0^{(2)} I_{20}^2 + (I_{10} - I_{20})(d_{21}^I I_{20} - d_{12}^I I_{10})}{I_{10}^2 + I_{20}^2}. \quad (4.16)$$

If  $I_{10} > I_{20}$ , then  $\Gamma_0$  is decreasing in  $d_{12}^I$  and increasing in  $d_{21}^I$ ; if  $I_{10} < I_{20}$ , then  $\Gamma_0$  is increasing in  $d_{12}^I$  and decreasing in  $d_{21}^I$ . Such dependence is illustrated by Figures 4.3(a) to 4.3(d). That is to say, if the infected population in one patch is larger than the other, then accumulating more infected individuals in that patch (lower leaving rate and higher entering rate) will make the global outbreak worse (larger  $\Gamma_0$ ). For the special case when  $I_{10} = I_{20}$  or  $d_{21}^I I_{20} = d_{12}^I I_{10}$ , that is the infected populations in two patches are of equal size or the net movement of infectives is zero, we can see that

$$\min_{i \in \{1,2\}} \Gamma_0^{(i)} \leq \Gamma_0 \leq \max_{i \in \{1,2\}} \Gamma_0^{(i)}.$$

Otherwise,  $\Gamma_0$  may exceed such bounds due to the population flow.

Comparing Figures 4.3(a) and 4.3(c), 4.3(b) and 4.3(d), the results demonstrate that a higher local (when isolated) initial amplification rate produces a greater  $\Gamma_0$ , which is consistent with expression (4.16). The dynamics of  $\|\mathbf{x}(t)\|$  for the sample sets of travel rates are shown in Figures 4.3(e) and 4.3(f), where the solutions (i)-1 and (iii)-1, (ii)-1 and (iv)-1, (i)-2 and (iii)-2,

(ii)-2 and (iv)-2 share the same  $\Gamma_0$ . We observe that the system presents various behaviours when different parameter values are chosen, even if the calculated  $\Gamma_0$  and initial conditions are the same. This is because such linear approximation is only valid in a small neighbourhood close to the initial point, then the effect of nonlinearities becomes dominant.

### 4.3.2 Estimate $\Gamma_0$ in early stage

In practice, the initial data is not always available. In the early stage of an outbreak, especially of a newly emerging infectious disease, it takes time to identify the patients and conduct large-scale tests. Let  $N_{10}$  and  $N_{20}$  denote the total population at  $t = 0$  in each of the two patches. Since the number of infection cases is relatively small during the initial phase, we can approximate the linearized system (4.14) by letting

$$S_{10} = N_{10} \quad \text{and} \quad S_{20} = N_{20}.$$

According to (4.10), we are able to predict the best and worst situations that the epidemic may develop by the upper and lower bounds of  $\Gamma_0$  which are the largest and smallest eigenvalues of  $H(\mathbf{A}_0)$ ,

$$\begin{aligned} \lambda_{max} &= \frac{1}{2} \left[ m_1 + m_2 + \sqrt{(m_1 - m_2)^2 + D^2} \right], \\ \lambda_{min} &= \frac{1}{2} \left[ m_1 + m_2 - \sqrt{(m_1 - m_2)^2 + D^2} \right], \end{aligned} \tag{4.17}$$

where

$$m_1 = \Gamma_0^{(1)} - d_{12}^l, \quad m_2 = \Gamma_0^{(2)} - d_{21}^l, \quad \text{and} \quad D = d_{12}^l + d_{21}^l. \tag{4.18}$$

Analysis on matrix  $H(\mathbf{A}_0)$  leads to the following results:

(S1) when  $4m_1m_2 - D^2 > 0$ , then

(S1-a) if  $m_1 + m_2 > 0$ , then  $\lambda_{min} > 0$  and hence,  $\Gamma_0 > 0$  for all  $\mathbf{x}_0 > 0$ ;

(S1-b) if  $m_1 + m_2 < 0$ , then  $\lambda_{max} < 0$  and hence,  $\Gamma_0 < 0$  for all  $\mathbf{x}_0 > 0$ ;

(S2) when  $4m_1m_2 - D^2 < 0$ , then  $\lambda_{min} < 0 < \lambda_{max}$  and hence, the sign of  $\Gamma_0$  depends on initial conditions.

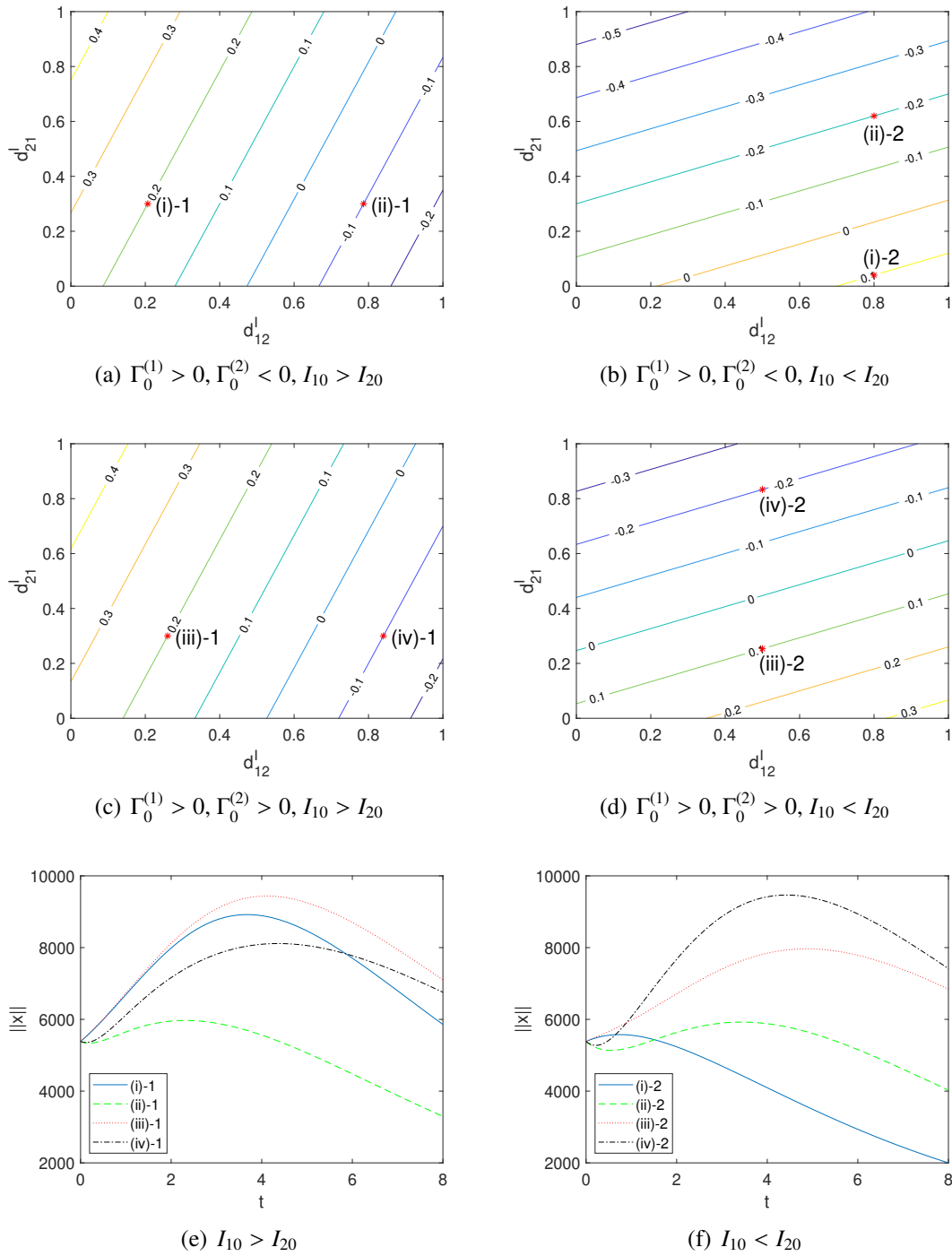


Figure 4.3: (a–d) The contour graphs of  $\Gamma_0$  for dispersal rates of infectives. (e, f) The dynamics of  $\|\mathbf{x}(t)\|$  for the sample sets. The choices, (i)-1 and (iii)-1, (ii)-1 and (iv)-1, (i)-2 and (iii)-2, (ii)-2 and (iv)-2, yield the same  $\Gamma_0$ . Set  $\beta_1 = 5 \times 10^{-5}$ ,  $\beta_2 = 2 \times 10^{-5}$ ,  $\gamma_1 = 0.2$ ,  $d_{12}^S = 0.4$ ,  $d_{21}^S = 0.6$ , and  $\gamma_2 =$  (a, b) 0.4; (c, d) 0.2. The initial conditions for  $[S_{10}, S_{20}, I_{10}, I_{20}]$  are: (a, c, e) [10000, 15000, 5000, 2000]; (b, d, f) [10000, 15000, 2000, 5000].

Moreover, if  $\Gamma_0^{(i)} > 2 \max\{d_{12}^l, d_{21}^l\}$  for  $i \in \{1, 2\}$ , then conditions for (S1-a) are satisfied and hence,  $\|\mathbf{x}(t)\|$  will always grow at the initial time; if  $\Gamma_0^{(i)} < \min\{d_{12}^l, d_{21}^l\} - \max\{d_{12}^l, d_{21}^l\}$  for  $i \in \{1, 2\}$ , then conditions for (S1-b) are satisfied and hence,  $\|\mathbf{x}(t)\|$  will never grow at the initial time.

In addition, the two bounds,  $\lambda_{max}$  and  $\lambda_{min}$ , are independent of initial infected populations, and their dependence on other parameter values are no longer linear like that of  $\Gamma_0$ . Analyzing the expressions given by (4.17), we obtain that (see Appendix A)

- $\lambda_{max}$  and  $\lambda_{min}$  are increasing with respect to  $\Gamma_0^{(i)}$  (hence, they are increasing in  $\beta_i$  and decreasing in  $\gamma_i$ ) for  $i \in \{1, 2\}$ ;
- $\lambda_{max}$  is decreasing in  $d_{12}^l$  and increasing in  $d_{21}^l$  if  $m_1 > m_2$ , while it is increasing in  $d_{12}^l$  and decreasing in  $d_{21}^l$  if  $m_1 < m_2$ ;
- $\lambda_{min}$  is always decreasing with respect to  $d_{12}^l$  and  $d_{21}^l$ .

### 4.3.3 $n$ patches

Now we consider the general model when the number of patches is  $n \geq 2$  which has been presented in the introduction as equation (4.5) with  $\Omega = \{1, \dots, n\}$ :

$$\left\{ \begin{array}{l} \frac{dS_i}{dt} = \sum_{j \in \Omega, j \neq i} d_{ji}^S S_j - \sum_{j \in \Omega, j \neq i} d_{ij}^S S_i - \beta_i S_i I_i, \\ \frac{dI_i}{dt} = \sum_{j \in \Omega, j \neq i} d_{ji}^I I_j - \sum_{j \in \Omega, j \neq i} d_{ij}^I I_i + \beta_i S_i I_i - \gamma_i I_i, \\ \frac{dR_i}{dt} = \sum_{j \in \Omega, j \neq i} d_{ji}^R R_j - \sum_{j \in \Omega, j \neq i} d_{ij}^R R_i + \gamma_i I_i, \end{array} \right. \quad \text{for } i \in \Omega. \quad (4.19)$$

Given that

$$[S_i(0), I_i(0), R_i(0)] = [S_{i0}, I_{i0}, R_{i0}] \in \mathbb{R}_{>0}, \quad i \in \Omega, \quad (4.20)$$

the dynamics of this system is of the same nature as that of the two-patch case. At the initial point, we obtain the linearized system for infected compartments,  $\mathbf{x}(t) = [I_1(t), \dots, I_n(t)]$ ,

where

$$\mathbf{A}_0 = [a_{ij}]_{n \times n} : \quad a_{ii} = \beta_i S_{i0} - \gamma_i - \sum_{j \in \Omega, j \neq i} d_{ij}^I, \quad i \in \Omega, \quad (4.21)$$

$$a_{ij} = d_{ji}^I, \quad i, j \in \Omega, \quad i \neq j.$$

Thus, the initial amplification rate is

$$\Gamma_0 = \frac{\sum_{i \in \Omega} (\beta_i S_{i0} - \gamma_i - \sum_{j \in \Omega, j \neq i} d_{ij}^I) I_{i0}^2 + \sum_{i, j \in \Omega, j > i} (d_{ij}^I + d_{ji}^I) I_{i0} I_{j0}}{\sum_{i \in \Omega} I_{i0}^2}, \quad (4.22)$$

which is linearly increasing with respect to transmission rates  $\beta_i$  and initial susceptible population sizes  $S_{i0}$ , and is linearly decreasing with respect to removal rates  $\gamma_i$ . Its dependence on travel rate  $d_{ij}^I$  is determined by the difference in infected populations between two patches,  $I_{i0}$  and  $I_{j0}$ ,

$$\frac{\partial \Gamma_0}{\partial d_{ij}^I} = I_{i0}(I_{j0} - I_{i0}). \quad (4.23)$$

Similarly, we can find the upper and lower bounds of  $\Gamma_0$  by calculating the largest and smallest eigenvalues of  $H(\mathbf{A}_0)$ . However, it is not always possible to obtain explicit expressions for the eigenvalues when matrix is of large size.

## 4.4 SIR endemic patch model

In this section, we incorporate a simple demographic structure into the SIR patch model (4.19). Let  $N_i(t) = S_i(t) + I_i(t) + R_i(t)$  for  $i \in \Omega$ . Assume that there are no deaths caused by the disease, and the birth rate and the natural death rate in each patch are set to be equal. Hence, the total population size of two patches,  $N = N_1(t) + N_2(t)$ , remains constant. The population dynamics in patch  $i$  now becomes

$$\begin{cases} \frac{dS_i}{dt} = \sum_{j \in \Omega, j \neq i} d_{ji}^S S_j - \sum_{j \in \Omega, j \neq i} d_{ij}^S S_i + b_i N_i - \beta_i S_i I_i - b_i S_i, \\ \frac{dI_i}{dt} = \sum_{j \in \Omega, j \neq i} d_{ji}^I I_j - \sum_{j \in \Omega, j \neq i} d_{ij}^I I_i + \beta_i S_i I_i - \gamma_i I_i - b_i I_i, \\ \frac{dR_i}{dt} = \sum_{j \in \Omega, j \neq i} d_{ji}^R R_j - \sum_{j \in \Omega, j \neq i} d_{ij}^R R_i + \gamma_i I_i - b_i R_i, \end{cases} \quad \text{for } i \in \Omega. \quad (4.24)$$

Using the same Proposition (1.1 in [11]) as to the epidemic patch model, one can easily verify that all solutions to the initial value problem remain non-negative for all  $t > 0$ . A disease-free equilibrium (DFE) for model (4.24) is given by

$$\mathbf{E}_0 = [S_1^{(0)}, \dots, S_n^{(0)}, 0, \dots, 0, R_1^{(0)}, \dots, R_n^{(0)}].$$

According to the  $R$ -equation in (4.24), we have  $R_i^{(0)} = 0$  for all  $i \in \Omega$ . Then,  $\mathbf{S}^{(0)} = [S_1^{(0)}, \dots, S_n^{(0)}]$  is a solution to the linear system,

$$\begin{cases} \sum_{j \in \Omega, j \neq i} d_{ji}^S S_j - \sum_{j \in \Omega, j \neq i} d_{ij}^S S_i = 0, & i \in \Omega, \\ \sum_{i \in \Omega} S_i = N. \end{cases} \quad (4.25)$$

#### 4.4.1 Measures of dynamics

**The basic reproduction number.** Based on the concept of next generation matrix presented in [13], we define

$$\mathbf{F} := \begin{bmatrix} \beta_1 S_1^{(0)} & 0 & \dots & 0 \\ 0 & \beta_2 S_2^{(0)} & \dots & 0 \\ \dots & \dots & \dots & \dots \\ 0 & 0 & \dots & \beta_n S_n^{(0)} \end{bmatrix}$$

and

$$\mathbf{V} := \begin{bmatrix} \gamma_1 + b_1 + \sum_{j \neq 1} d_{1j}^I & -d_{21}^I & \dots & -d_{n1}^I \\ -d_{12}^I & \gamma_2 + b_2 + \sum_{j \neq 2} d_{2j}^I & \dots & -d_{n2}^I \\ \dots & \dots & \dots & \dots \\ -d_{1n}^I & -d_{2n}^I & \dots & \gamma_n + b_n + \sum_{j \neq n} d_{nj}^I \end{bmatrix}.$$

Then, the next generation matrix is  $\mathbf{FV}^{-1}$  and the basic reproduction number is defined as its spectral radius,  $\mathfrak{R}_0 = \rho(\mathbf{FV}^{-1})$ . By Theorem 2 in [13], the DFE is locally asymptotically stable if  $\mathfrak{R}_0 < 1$  but is unstable if  $\mathfrak{R}_0 > 1$ .

**Reactivity.** Considering merely the infection-related variables (i.e.,  $I_1(t), \dots, I_n(t)$ ), the Jacobian matrix of model (4.24) is

$$\mathbf{J} = [J_{ij}]_{n \times n} : \quad J_{ii} = \beta_i S_i - \gamma_i - b_i - \sum_{j \neq i} d_{ij}^I, \quad i \in \Omega,$$

$$J_{ij} = d_{ji}^I, \quad i, j \in \Omega, i \neq j.$$

Evaluated at the DFE,  $\mathbf{E}_0$ , the Jacobian matrix becomes  $\mathbf{J}_0 = \mathbf{F} - \mathbf{V}$ . One can obtain the same linearization according to [27] by letting  $\mathbf{C} = [\mathbf{0} \ \mathbf{I} \ \mathbf{0}]$  (each block matrix is of the size  $n \times n$ ). Then, the generalized reactivity of  $\mathbf{E}_0$  is given by  $\Lambda_0 = \lambda_{\max}(H(\mathbf{J}_0))$ . The threshold index for epidemics as defined by Hosack et al. [23] is

$$\mathcal{E}_0 = \rho(H(\mathbf{F})H(\mathbf{V})^{-1}) = \rho(\mathbf{F} \cdot H(\mathbf{V})^{-1}), \quad (4.26)$$

since  $\mathbf{F}$  is diagonal. According to [23], if  $\mathcal{E}_0 < 1$ , then  $\Lambda_0 < 0$  and  $\mathbf{E}_0$  is non-reactive, and if  $\mathcal{E}_0 > 1$ , then  $\Lambda_0 > 0$  and  $\mathbf{E}_0$  is reactive.

**The initial amplification rate.** Evaluating the Jacobian matrix,  $\mathbf{J}$ , at the initial point, we acquire the expression of  $\Gamma_0$ ,

$$\Gamma_0 = \frac{\sum_{i \in \Omega} (\beta_i S_{i0} - \gamma_i - b_i - \sum_{j \in \Omega, j \neq i} d_{ij}^I) I_{i0}^2 + \sum_{i, j \in \Omega, j > i} (d_{ij}^I + d_{ji}^I) I_{i0} I_{j0}}{\sum_{i \in \Omega} I_{i0}^2}, \quad (4.27)$$

which is similar to that of the SIR epidemic patch model given by (4.22). Based on the definition of  $\Gamma_0$ , the size of solution,  $\| [I_1(t), \dots, I_n(t)] \|$ , will initially attenuate if  $\Gamma_0 < 0$ , while it will initially amplify if  $\Gamma_0 > 0$ .

### 4.4.2 Application to two patches

In the case where the patch number is  $n = 2$ , system (4.24) reduces to

$$\left\{ \begin{array}{l} \frac{dS_1}{dt} = d_{21}^S S_2 - d_{12}^S S_1 + b_1 N_1 - \beta_1 S_1 I_1 - b_1 S_1, \\ \frac{dS_2}{dt} = d_{12}^S S_1 - d_{21}^S S_2 + b_2 N_2 - \beta_2 S_2 I_2 - b_2 S_2, \\ \frac{dI_1}{dt} = d_{21}^I I_2 - d_{12}^I I_1 + \beta_1 S_1 I_1 - \gamma_1 I_1 - b_1 I_1, \\ \frac{dI_2}{dt} = d_{12}^I I_1 - d_{21}^I I_2 + \beta_2 S_2 I_2 - \gamma_2 I_2 - b_2 I_2, \\ \frac{dR_1}{dt} = d_{21}^R R_2 - d_{12}^R R_1 + \gamma_1 I_1 - b_1 R_1, \\ \frac{dR_2}{dt} = d_{12}^R R_1 - d_{21}^R R_2 + \gamma_2 I_2 - b_2 R_2, \end{array} \right. \quad (4.28)$$

which has a unique DFE,

$$\mathbf{E}_0 = \left[ \frac{d_{21}^S N}{d_{12}^S + d_{21}^S}, \frac{d_{12}^S N}{d_{12}^S + d_{21}^S}, 0, 0, 0, 0 \right]. \quad (4.29)$$

The basic reproduction number  $\mathfrak{R}_0$  is an index for long-term asymptotic behaviour and the initial amplification rate  $\Gamma_0$  is an index for short-term transitory behaviour. Figure 4.4 displays the two indices as functions of infection-related parameters, transmission rate  $\beta_i$  and recovery rate  $\gamma_i$  for  $i \in \{1, 2\}$ . Within the range of values presented, both of them are increasing in  $\beta_i$  and decreasing in  $\gamma_i$ . But the critical points at which  $\Gamma_0$  and  $\mathfrak{R}_0 - 1$  switch signs are different in values. Therefore, the dynamics of disease has four possibilities:

(II-1) when  $\mathfrak{R}_0 < 1$ ,

(II-1a) if  $\Gamma_0 > 0$ , then  $\| [I_1(t), I_2(t)] \|$  initially grows but eventually converges to zero;

(II-1b) if  $\Gamma_0 < 0$ , then  $\| [I_1(t), I_2(t)] \|$  initially decays and converges to zero in the long run;

(II-2) when  $\mathfrak{R}_0 > 1$ ,

(II-2a) if  $\Gamma_0 > 0$ , then  $\| [I_1(t), I_2(t)] \|$  initially grows and ultimately approaches a positive steady state;

(II-2b) if  $\Gamma_0 < 0$ , then  $\| [I_1(t), I_2(t)] \|$  initially decays before reaching a positive steady state.

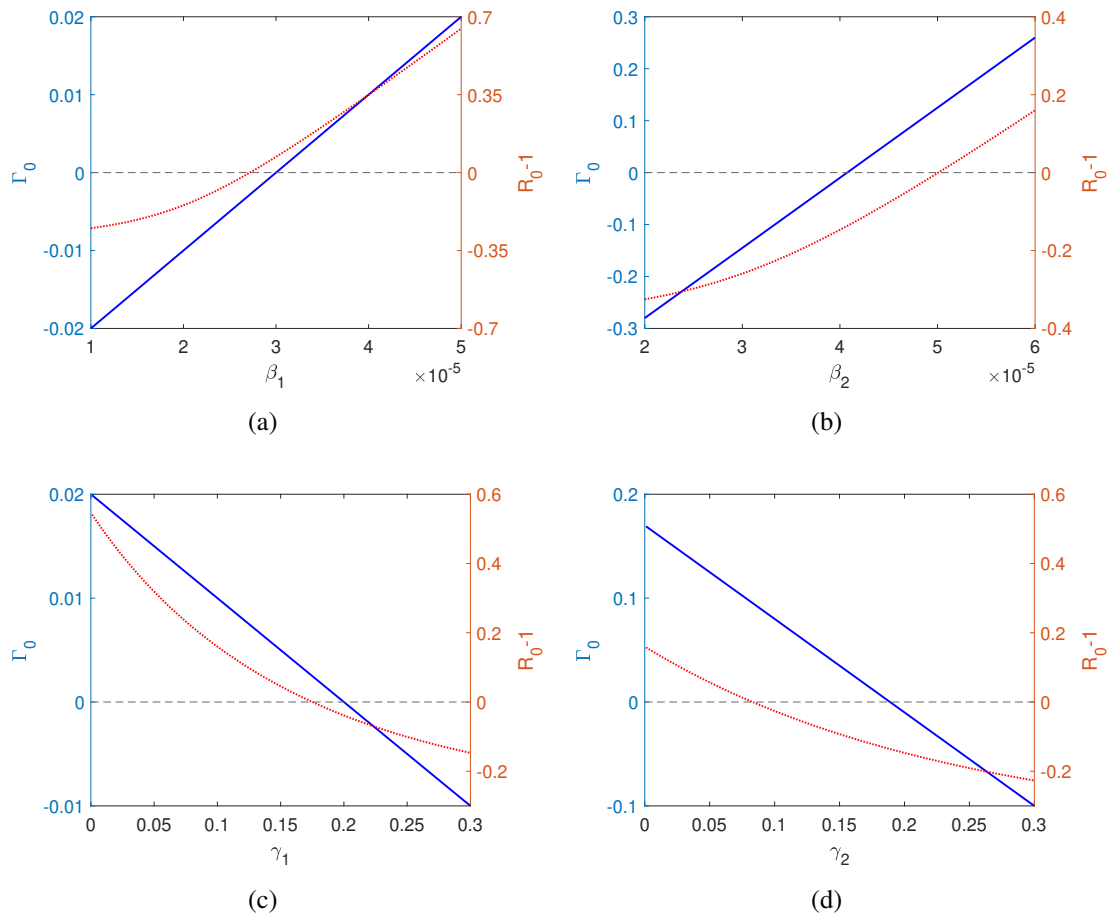


Figure 4.4: Indices  $\Gamma_0$  (solid line) and  $\mathfrak{R}_0$  (dotted line) as functions of infection-related parameters. Except chosen to be a variable, parameter values are  $b_1 = b_2 = 0.2$ ,  $\beta_1 = 2 \times 10^{-5}$ ,  $\beta_2 = 4 \times 10^{-5}$ ,  $\gamma_1 = 0.3$ ,  $\gamma_2 = 0.2$ ,  $d_{12}^S = 0.4$ ,  $d_{21}^S = 0.6$ ,  $d_{12}^I = 0.1$  and  $d_{21}^I = 0.3$ . Set  $[S_{10}, S_{20}, I_{10}, I_{20}] = [10000, 15000, 1000, 3000]$ .

We are interested in two scenarios: (II-1a) the disease dies out in the long run but there exists at least a transitory epidemic; (II-2b) the disease persists for all  $t > 0$  but initially the infection size drops. See the figures in Figure 4.5 for a demonstration. The two cases are of particular importance in disease controlling. The effect of a control measure may be misunderstood without knowing its effect on both long-term and short-term dynamical behaviours. If  $\mathfrak{R}_0$  is the only index to be examined, the unanticipated epidemic in (II-1a) may have very serious consequences. If (II-2b) happens, people may be misled by the initial decrease in the size of infections when the disease is indeed an endemic.

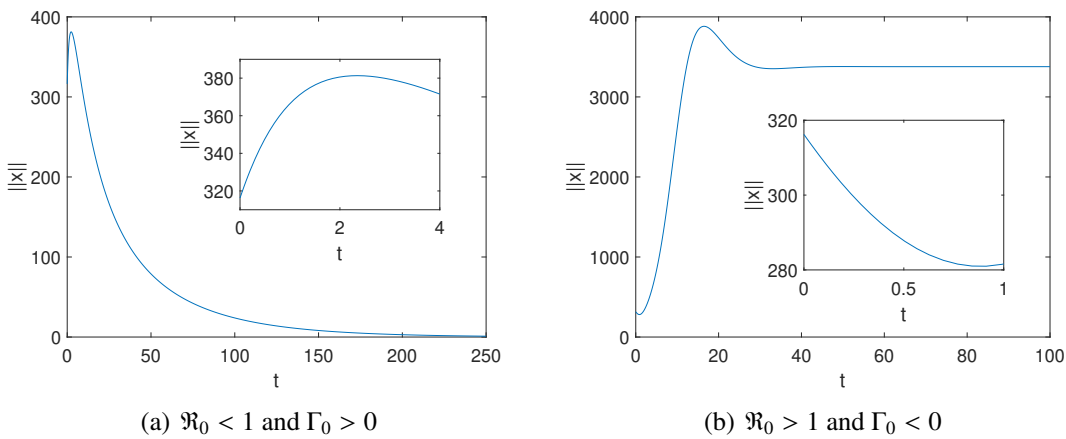


Figure 4.5: Long-term and short-term dynamics of  $\| [I_1(t), I_2(t)] \|$ . (a) is an example of (II-1a) with  $\beta_1 = 10^{-5}$  and  $\beta_2 = 6 \times 10^{-5}$ . (b) is an example of (II-2b) with  $\beta_1 = 6 \times 10^{-5}$  and  $\beta_2 = 2 \times 10^{-5}$ . Set  $d_{12}^R = 0.4$ ,  $d_{21}^R = 0.6$  and  $[S_{10}, S_{20}, I_{10}, I_{20}, R_{10}, R_{20}] = [10000, 15000, 100, 300, 0, 0]$ . Other parameter values are same as those used in Figure 4.4.

The impact of dispersal on long-term asymptotic dynamics and transitory amplification/attenuation in infection size is demonstrated by Figures 4.6 and 4.7. According to the definitions given in Section 4.1, both of  $\Gamma_0$  and  $\mathfrak{R}_0$  depend on the dispersal rates of infectives. An example is shown in Figure 4.6 where the contours give the values of  $\Gamma_0$  and  $\mathfrak{R}_0$  for combinations of  $d_{12}^I$  and  $d_{21}^I$ . With the chosen parameter values and initial conditions,  $\Gamma_0$  and  $\mathfrak{R}_0$  are increasing in  $d_{12}^I$  and decreasing in  $d_{21}^I$ . Besides, there exists an area on the  $d_{12}^I-d_{21}^I$  plane within which transitory epidemic is possible before the disease dying out ( $\Gamma_0 > 0$  but  $\mathfrak{R}_0 < 1$ ).

As for the dispersal rates of susceptibles, they have no effect on  $\Gamma_0$  but change the value of  $\mathfrak{R}_0$  via the population sizes in DFE. Figure 4.7 shows the contour graphs of  $\mathfrak{R}_0$  on the  $d_{12}^S-d_{21}^S$  plane, which includes the four possible combinations of short-term and long-term behaviours.

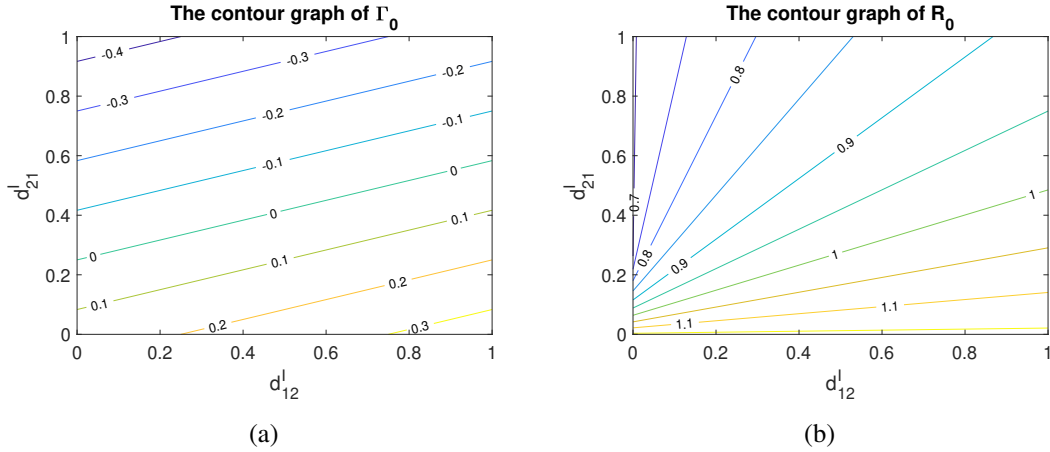


Figure 4.6: The contour graphs of  $\Gamma_0$  and  $\mathfrak{R}_0$  for dispersal rates of infectives. Other parameter values and initial conditions are same as those used in Figure 4.4.

It seems to suggest that a disease is more likely to develop an endemic when  $\Gamma_0 > 0$ . In addition, we point out that the dispersal of recovered individuals has no impact on  $\Gamma_0$  and  $\mathfrak{R}_0$ .

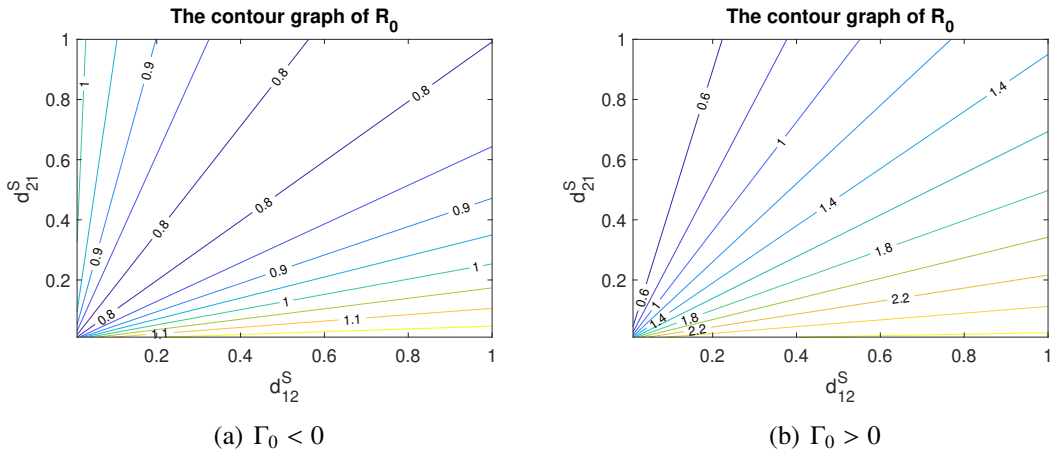


Figure 4.7: The contour graphs of  $\mathfrak{R}_0$  for dispersal rates of susceptibles. Set (a)  $d_{12}^I = 0.2$  and  $d_{21}^I = 0.8$  so that  $\Gamma_0 < 0$ ; (b)  $d_{12}^I = 0.9$  and  $d_{21}^I = 0.1$  so that  $\Gamma_0 > 0$ . Other parameter values and initial conditions are same as those used in Figure 4.4.

## 4.5 Conclusion and discussion

In this work, we studied the short term disease dynamics in addition to long term disease dynamics. We firstly reviewed some related notions in mathematical ecology, then employed the measurement of amplification rates which is closely related to reactivity [31]. The initial

amplification rate, denoted by  $\Gamma_0$ , is defined as the instant rate at which the initial size of infected population amplifies or attenuates. It is derived from the linearization of a nonlinear system at the initial point, as in a particular form known as the Rayleigh quotient. We point out that the initial time of our model ( $t = 0$ ) is not necessary to denote the beginning of an outbreak. Indeed, it can be set as any point of time during the course of a disease.

We firstly applied  $\Gamma_0$  to the SIR epidemic patch model, which was extended from the simplest Kermack-McKendrick model. We have assumed that the environment consists of discrete patches which are connected in the sense that individuals can travel or migrate from one patch to another. The local dynamics of each patch is coupled to that of other patches by the dispersal terms. We have shown that this extended system (4.12) also does not allow the disease to persist. The calculation of  $\Gamma_0$  helps us to explore the patterns by which the disease dies out. We have obtained an expression of  $\Gamma_0$  for a general  $n$ -patch model and analyzed its dependence on the involved parameter values and initial conditions. Numerical examples have been given for a special case of two patches. The results show how different interventions affect  $\Gamma_0$  and transient behaviours of the system. See more details in Section 3.1. Based on the upper and lower bounds of the Rayleigh quotient, we have also estimated  $\Gamma_0$  with  $t = 0$  indicating the onset of an epidemic when the system is at an (approximate) disease-free equilibrium.

We continued to study the SIR endemic patch model with a simple demographic structure (4.24). Unlike the above one, this system admits a locally asymptotically stable DFE. Therefore, we are able to obtain  $\mathfrak{R}_0$  by the next generation matrix method [13] and calculate the (generalized) reactivity according to [31, 27]. The expression for  $\Gamma_0$  is similar to that of the SIR epidemic patch model. While  $\mathfrak{R}_0$  determines the long-term asymptotic behaviour, both reactivity and  $\Gamma_0$  measure the short-term transitory dynamics. In addition,  $\Gamma_0$  is the instant amplification/attenuation rate evaluated at the initial point, meaning that it depends on the initial condition; reactivity, however, is defined as the maximal amplification rate over all possible (small) perturbations, corresponding to a particular equilibrium. We have further numerically compared  $\Gamma_0$  and  $\mathfrak{R}_0$  as functions of infection-related parameters and dispersal rates of different compartments. The results suggest four possible combinations of transitory and asymptotic behaviours. Two of the scenarios are of particular interests in disease controlling: (II-1a) the

disease eventually dies out but transitory epidemics are possible; (II-2b) the size of infected populations initially decreases but the disease will persist.

By the definition of  $\Gamma_0$ , we quantify the transitory behaviour for infected compartments as a whole instead of examining the specific dynamics in each patch. Euclidean norm has been used to measure the size of a vector. Thus, the value of  $\Gamma_0$  and its sign are not always consistent with  $I'_1(0)$ ,  $I'_2(0)$  or  $I'_1(0) + I'_2(0)$  (in the case of two patches for an example), and the results will be different if other norms are applied. Our idea that solely consider the infection-related variables is a special case of the generalization proposed by Mari et al. [27]. Indeed, the measure can be evaluated based on unequally weighted state variables. We refer to that paper for a detailed discussion.

We need to point out that the initial amplification rate merely characterizes the linear dynamics near a given point. Nonlinearities, however, can produce longer and more complex transients, as observed in Figures 4.1(c), 4.2(b) and 4(e, f). In addition to reactivity, amplification envelop has also been proposed by Neubert and Caswell [31] as another measure of transient dynamics, which is not included in this work. On the other hand, Hastings and Higgins [19] stressed the importance of transients in spatially structured ecological systems. For discrete-space models, there are some works that have explored the transient behaviours by numerical simulations. See, e.g., [33, 34] for one-species models and [16] for predator-prey systems. However, only a few studies have theoretically analyzed the effect of spatial heterogeneity on transient dynamics. The notions of reactivity and amplification envelop have been extended to advective systems by Anderson et al. [3] and to reaction-diffusion systems by Wang et al. [36]. As for the patch model, we will leave this for future works.

## 4.6 Appendix

### 4.6.1 The dependence of $\lambda_{max}$ and $\lambda_{min}$ for SIR epidemic patch model

Taking partial derivatives of (4.17) with respect to  $\Gamma_0^{(i)}$  for  $i \in \{1, 2\}$ , we have

$$\frac{\partial \lambda_{max}}{\partial \Gamma_0^{(1)}} = \frac{\partial \lambda_{min}}{\partial \Gamma_0^{(2)}} = \frac{M + \sqrt{M^2 + D^2}}{2\sqrt{M^2 + D^2}} \quad \text{and} \quad \frac{\partial \lambda_{max}}{\partial \Gamma_0^{(2)}} = \frac{\partial \lambda_{min}}{\partial \Gamma_0^{(1)}} = \frac{-M + \sqrt{M^2 + D^2}}{2\sqrt{M^2 + D^2}}$$

where  $M := m_1 - m_2 = \Gamma_0^{(1)} - d_{12}^l - \Gamma_0^{(2)} + d_{21}^l$  and  $D = d_{12}^l + d_{21}^l > 0$ . All of these partial derivatives are positive since

$$\sqrt{M^2 + D^2} > |M|. \quad (4.30)$$

With respect to travel rates, the partial derivative of  $\lambda_{max}$ ,

$$\frac{\partial \lambda_{max}}{\partial d_{12}^l} = \frac{D - M - \sqrt{M^2 + D^2}}{2\sqrt{M^2 + D^2}},$$

is positive if  $M < 0$  and is negative if  $M > 0$ , and,

$$\frac{\partial \lambda_{max}}{\partial d_{21}^l} = \frac{D + M - \sqrt{M^2 + D^2}}{2\sqrt{M^2 + D^2}},$$

is positive if  $M > 0$  and is negative if  $M < 0$ . As for  $\lambda_{min}$ , the partial derivatives are

$$\frac{\partial \lambda_{min}}{\partial d_{12}^l} = \frac{-D + M - \sqrt{M^2 + D^2}}{2\sqrt{M^2 + D^2}} \quad \text{and} \quad \frac{\partial \lambda_{min}}{\partial d_{21}^l} = \frac{-D - M - \sqrt{M^2 + D^2}}{2\sqrt{M^2 + D^2}},$$

which are both negative by the inequality (4.30).

# Bibliography

- [1] Allen, L. J., Bolker, B. M., Lou, Y., & Nevai, A. L. (2007). Asymptotic profiles of the steady states for an SIS epidemic patch model. *SIAM Journal on Applied Mathematics*, 67(5), 1283-1309.
- [2] Almarashi, R. M., & McCluskey, C. C. (2019). The effect of immigration of infectives on disease-free equilibria. *Journal of Mathematical Biology*, 79, 1015-1028.
- [3] Anderson, K. E., Nisbet, R. M., & McCauley, E. (2008). Transient responses to spatial perturbations in advective systems. *Bulletin of Mathematical Biology*, 70, 1480-1502.
- [4] Andreasen, V. (2011). The final size of an epidemic and its relation to the basic reproduction number. *Bulletin of Mathematical Biology*, 73, 2305-2321.
- [5] Arino, J., & Van den Driessche, P. (2003). A multi-city epidemic model. *Mathematical Population Studies*, 10(3), 175-193.
- [6] Arino, J., & Van Den Driessche, P. (2003). The basic reproduction number in a multi-city compartmental epidemic model. In *Positive Systems* (pp. 135-142). Springer, Berlin, Heidelberg.
- [7] Arino, J., & Van den Driessche, P. (2006). Disease spread in metapopulations. *Fields Institute Communications*, 48, 1-12.
- [8] Arino, J., Brauer, F., van den Driessche, P., Watmough, J., & Wu, J. (2007). A final size relation for epidemic models. *Mathematical Biosciences And Engineering*, 4(2), 159-175.

- [9] Arino, J., Brauer, F., Van Den Driessche, P., Watmough, J., & Wu, J. (2008). A model for influenza with vaccination and antiviral treatment. *Journal of Theoretical Biology*, 253(1), 118-130.
- [10] Chen, S., Shi, J., Shuai, Z., & Wu, Y. (2020). Asymptotic profiles of the steady states for an SIS epidemic patch model with asymmetric connectivity matrix. *Journal of Mathematical Biology*, 80, 2327-2361.
- [11] Chepyzhov, V. V., & Vishik, M. I. (2002). *Attractors for equations of mathematical physics*. American Mathematical Society.
- [12] Diekmann, O., Heesterbeek, J. A. P., & Metz, J. A. (1990). On the definition and the computation of the basic reproduction ratio  $R_0$  in models for infectious diseases in heterogeneous populations. *Journal of Mathematical Biology*, 28, 365-382.
- [13] van den Driessche, P., & Watmough, J. (2002). Reproduction numbers and sub-threshold endemic equilibria for compartmental models of disease transmission. *Mathematical Biosciences*, 180, 29-48.
- [14] Eisenberg, M. C., Shuai, Z., Tien, J. H., & Van den Driessche, P. (2013). A cholera model in a patchy environment with water and human movement. *Mathematical Biosciences*, 246, 105-112.
- [15] Kermack, W. O., & McKendrick, A. G. (1927). A contribution to the mathematical theory of epidemics. *Proceedings of the Royal Society of London. Series A*, 115(772), 700-721.
- [16] Hastings, A. (2001). Transient dynamics and persistence of ecological systems. *Ecology Letters*, 4, 215-220.
- [17] Hastings, A. (2004). Transients: the key to long-term ecological understanding?. *Trends in Ecology and Evolution*, 19(1), 39-45.
- [18] Hastings, A. (2010). Timescales, dynamics, and ecological understanding. *Ecology*, 91(12), 3471-3480.

- [19] Hastings, A., & Higgins, K. (1994). Persistence of transients in spatially structured ecological models. *Science*, 263, 1133-1136.
- [20] Horn, R. A., & Johnson, C. R. (1985). *Matrix analysis*. Cambridge university press.
- [21] Hsieh, Y. H., Van den Driessche, P., & Wang, L. (2007). Impact of travel between patches for spatial spread of disease. *Bulletin of Mathematical Biology*, 69, 1355-1375.
- [22] Hethcote, H. W. (1976). Qualitative analyses of communicable disease models. *Mathematical Biosciences*, 28(3-4), 335-356.
- [23] Hosack, G. R., Rossignol, P. A., & Van Den Driessche, P. (2008). The control of vector-borne disease epidemics. *Journal of Theoretical Biology*, 255, 16-25.
- [24] Lutscher, F., & Wang, J. (2020). Reactivity of communities at equilibrium and periodic orbits. *Journal of Theoretical Biology*, 493: 110240.
- [25] Ma, J., & Earn, D. J.D. (2006). Generality of the final size formula for an epidemic of a newly invading infectious disease. *Bulletin of Mathematical Biology*, 68, 679-702.
- [26] Magal, P., Seydi, O., & Webb, G. (2016). Final size of an epidemic for a two-group SIR model. *SIAM Journal on Applied Mathematics*, 76(5), 2042-2059.
- [27] Mari, L., Casagrandi, R., Rinaldo, A., & Gatto, M. (2017). A generalized definition of reactivity for ecological systems and the problem of transient species dynamics. *Methods in Ecology and Evolution*, 8, 1574-1584.
- [28] Mari, L., Casagrandi, R., Rinaldo, A., & Gatto, M. (2018). Epidemicity thresholds for water-borne and water-related diseases. *Journal of Theoretical Biology*, 447, 126-138.
- [29] Mari, L., Casagrandi, R., Bertuzzo, E., Rinaldo, A., & Gatto, M. (2019). Conditions for transient epidemics of waterborne disease in spatially explicit systems. *Royal Society Open Science*, 6, 181517.
- [30] Mari, L., Casagrandi, R., Bertuzzo, E., Pasetto, D., Miccoli, S., Rinaldo, A., & Gatto, M. (2021). The epidemicity index of recurrent SARS-CoV-2 infections. *Nature communications*, 12, 2752.

- [31] Neubert, M. G., & Caswell, H. (1997). Alternatives to resilience for measuring the responses of ecological systems to perturbations. *Ecology*, 78(3), 653-665.
- [32] O'Regan, S. M., O'Dea, E. B., Rohani, P., & Drake, J. M. (2020). Transient indicators of tipping points in infectious diseases. *Journal of the Royal Society Interface*, 17, 20200094.
- [33] Ruxton, G. D., & Doebeli, M. (1996). Spatial self-organization and persistence of transients in a metapopulation model. *Proceedings of the Royal Society of London. Series B: Biological Sciences*, 263, 1153-1158.
- [34] Saravia, L. A., Ruxton, G. D., & Coviella, C. E. (2000). The importance of transient's dynamics in spatially extended populations. *Proceedings of the Royal Society of London. Series B: Biological Sciences*, 267, 1781-1785.
- [35] Wang, W., & Zhao, X. Q. (2004). An epidemic model in a patchy environment. *Mathematical Biosciences*, 190, 97-112.
- [36] Wang, X., Efendiev, M., & Lutscher, F. (2019). How spatial heterogeneity affects transient behavior in reaction–diffusion systems for ecological interactions? *Bulletin of Mathematical Biology*, 81, 3889-3917.
- [37] Woodall, H., Bullock, J. M., & White, S. M. (2014). Modelling the harvest of an insect pathogen. *Ecological Modelling*, 287, 16-26.

# Chapter 5

## Conclusions and Future Work

### 5.1 Conclusion

In this thesis, we incorporated spatial structure into different ecological systems in a discrete way by using patch models. Consider an environment consisting of spatially isolated habitats. The populations on different patches are functionally separate yet connected through between-patch dispersal. The coupled local dynamics yields a large system of differential equations. This model allows spatial heterogeneity, that is, the equations for local population dynamics can be patch-specific. For simplicity, they are same in forms but different in parameter values.

The simplest case of dispersal is passive diffusion, as introduced in Chapter 1, which however, is not realistic. In Chapter 2, we considered two specific costs associated with dispersal: (i) the period of time spent for migration; (ii) deaths during dispersal process. A two-patch model was proposed with the assumptions that individuals moving from one patch to the other need a fixed period of time  $\tau_2$  and the per capita dispersal-related mortality rate is a positive constant. Together with another time lag  $\tau_1$  in the logistic growth, this model is given by a system of delay differential equations with two constant delays. The associated ODE system without time delays has a unique positive equilibrium which is globally asymptotically stable. By letting  $\tau_1 = 0$ , only the delay due to dispersal is considered, in which case no oscillations occur. The loss by dispersal only affects the population size at equilibrium and may even drive the populations to extinction. As is known, the delayed logistic growth generates periodic

orbits. We numerically explored the impact of dispersal costs on the oscillations.

In Chapter 3, we studied a predator-prey system in a two-patch environment with indirect effect (fear) considered. The anti-predation strategies adopted by the prey lead to a higher chance of survival from predation at the cost of reduced reproduction rate. Both the cost and benefit functions depend on the anti-predation response level and the local population of predator. To make it simple, we assumed a generalist predator that has a constant population on each patch. We started from the local dynamics of prey without dispersal. Applying adaptive dynamics with time scale separation, the results show that the existence of an optimal anti-predation strategy  $\alpha^* > 0$ , which is a convergence stable ESS, depends on its relative strength on reducing the predation to that on reducing the reproduction. When two patches are connected by dispersal which is also mediated by fear (to be specific, the dispersal rate becomes lower due to predation risk), we investigated how anti-predation strategy  $\alpha$  affects the persistence of prey on both patches. We also numerically explored the evolution of trait  $\alpha$  in two ways: (i) with time scale separation by presenting the pairwise invasibility plot; (ii) without time scale separation by adopting two biologically meaningful fitness functions. The results of two approaches both indicate the existence of an optimal anti-predation response level.

In Chapter 4, our interest shifted to epidemiological models. We first extended the simplest Kermack-McKendrick SIR epidemic model to patchy environment and showed that the coupled system still does not allow the disease to persist. To explore the patterns by which the disease dies out, we employed the measurement of amplification rates previously used in ecology which captures the short term dynamics. Denote by  $\Gamma_0$  the initial amplification rate. According to the definition, the infection size (measured by the Euclidean norm as a whole) initially amplifies if  $\Gamma_0 > 0$ , while it initially attenuates if  $\Gamma_0 < 0$ . We obtained an explicit expression of  $\Gamma_0$  for a general  $n$ -patch model and analyzed its dependence on the involved parameter values and initial conditions. Numerical examples were given for a special case of two patches illustrating the effects of different public health interventions on transient dynamics. We continued to study the SIR endemic patch model with vital dynamics (births and disease-unrelated deaths). This system admits a locally asymptotically stable disease-free equilibrium so that we are able to calculate the basic reproduction number  $\mathfrak{R}_0$  by the next generation ma-

trix [1]. We numerically compared  $\Gamma_0$  and  $\mathfrak{R}_0$  as functions of infection-related parameters and dispersal rates of different compartments. The results suggest four possible combinations of short-term response and long-term asymptotic behaviour. Two of the scenarios are of particular interests in disease controlling: (i) the disease eventually dies out but transitory epidemics are possible; (ii) the infection size initially decreases but the disease will persist.

## 5.2 Future work

A possible extension of the model studied in Chapter 3 is to consider a predator whose population also changes with time. This introduces richer dynamics and makes it more difficult for mathematical analysis due to the increased dimension of the system. The example given at the end of Chapter 2 presents dimorphism that prey with different trait values can co-exist. Hence, evolutionary branching is possible.

As we pointed out in Chapter 3, the choice of fitness function plays a decisive role in adaptive dynamics without time scale separation. On the other hand, there are many fitness functions presented in the extensive literatures. Usually, the function is chosen based on the main biological feature(s) and mathematical convenience. We tried two fitness functions in this work, but their results do not quantitatively match that obtained from the method assuming time scale separation. It is an interesting future work to compare different fitness functions in details and find the particular one which links the two approaches.

The initial amplification rate presented in Chapter 4 merely characterizes the linear dynamics near the initial point. Nonlinearities, however, can produce longer and more complex transients. Thus, other measures are needed to complete the picture. Besides, the results of numerical experiments displayed in [3, 5, 6, 2] and the theoretical analysis given by Wang et al. [7] for reaction-diffusion systems all suggest the significant impact of spatial structure on the transient dynamics. We leave these as our future directions of work.

# Bibliography

- [1] van den Driessche, P., & Watmough, J. (2002). Reproduction numbers and sub-threshold endemic equilibria for compartmental models of disease transmission. *Mathematical Biosciences*, 180, 29-48.
- [2] Hastings, A. (2001). Transient dynamics and persistence of ecological systems. *Ecology Letters*, 4, 215-220.
- [3] Hastings, A., & Higgins, K. (1994). Persistence of transients in spatially structured ecological models. *Science*, 263, 1133-1136.
- [4] Neubert, M. G., & Caswell, H. (1997). Alternatives to resilience for measuring the responses of ecological systems to perturbations. *Ecology*, 78(3), 653-665.
- [5] Ruxton, G. D., & Doebeli, M. (1996). Spatial self-organization and persistence of transients in a metapopulation model. *Proceedings of the Royal Society of London. Series B: Biological Sciences*, 263, 1153-1158.
- [6] Saravia, L. A., Ruxton, G. D., & Coviella, C. E. (2000). The importance of transient's dynamics in spatially extended populations. *Proceedings of the Royal Society of London. Series B: Biological Sciences*, 267, 1781-1785.
- [7] Wang, X., Efendiev, M., & Lutscher, F. (2019). How Spatial Heterogeneity Affects Transient Behavior in Reaction–Diffusion Systems for Ecological Interactions? *Bulletin of Mathematical Biology*, 81, 3889-3917.

# Curriculum Vitae

**Name:** Ao Li

**Post-Secondary Education and Degrees:** University of Western Ontario  
London, ON, Canada  
2015 - Present Ph.D. Candidate

University of Western Ontario  
London, ON, Canada  
2013 - 2014 M.Sc.

Shanghai Jiaotong University  
Shanghai, China  
2009 - 2013 B.Sc.

**Honours and Awards:** Graduate Student Teaching Award (2021)  
Western Graduate Research Scholarships (2015-2021)  
Excellent Undergraduate Student Scholarship (2009-2012)

**Related Work Experience:** Teaching Assistant, University of Western Ontario (2015-2021)  
Research Assistant, University of Western Ontario (2015-2021)

## Publications:

1. Li, A., & Zou, X. (2021). Evolution and adaption of anti-predation response of prey in a two-patchy environment. *Bulletin of Mathematical Biology*, 83, 59.
2. Cao, H., Yan, D., & Li, A. (2019). Dynamic analysis of the recurrent epidemic model. *Mathematical Biosciences and Engineering*, 16(5), 5972-5990.
3. Li, A., & Corless, R. M. (2019) Revisiting Gillbert Strang's "A chaotic search for  $i$ ". *ACM Communications in Computer Algebra*, 53(1), 1-22.
4. Li, A., Wang, Y., Cong, P., & Zou, X. Re-examination of the impact of non-pharmaceutical interventions and media coverage on the COVID-19 outbreak in Wuhan. *Infectious Disease Modelling*, in press.

5. Li, A., & Zou, X. A single species model with delay and dispersal, in preparation.
6. Li, A., & Zou, X. Transient dynamics of SIR models over patchy environment, in preparation.
7. Li, A., & Zou, X. Modelling the intraseasonal waning of vaccine-induced immunity over a two-patch environment, in preparation.